Development of an Inspection Platform and a Suite of Sensors for Assessing Corrosion and Mechanical Damage on Unpiggable Transmission Mains

Final Report

October 2002 – March 2004

Dr. George C. Vradis
Consultant to the RD&D Director
NYSEARCH / Northeast Gas Association

William Leary
Project Manager
Foster-Miller, Inc.

March 2004

DOE Award Number: DE-FC26-02NT41645

Northeast Gas Association
1515 Broadway, 43rd Floor
New York, NY 10036

Foster-Miller, Inc.
350 Second Ave.
Waltham, MA 02451-1196

DISCLAIMER

"This report was prepared as an account of work sponsored by an agency of the United States Government. Neither the United States Government nor any agency thereof, nor any of their employees, makes any warranty, express or implied, or assumes any legal liability or responsibility for the accuracy, completeness, or usefulness of any information, apparatus, product, or process disclosed, or represents that its use would not infringe privately owned rights. Reference herein to any specific commercial product, process, or service by trade name, trademark, manufacturer, or otherwise does not necessarily constitute or imply its endorsement, recommendation, or favoring by he United States Government or any agency thereof. The views and opinions of the authors expressed herein do not necessarily state or reflect those of the Unites States Government or any agency thereof."

EXECUTIVE SUMMARY

Summary

The National Energy Technology Laboratory of the US Department of Energy (under Award DE-FC26-02NT41645) and the NYSEARCH Committee of the Northeast Gas Association (previous the New York Gas Group), have sponsored research to develop a robotic pipeline inspection system capable of navigation through the typical physical and operational obstacles that make transmission and distribution pipelines unpiggable. The research contractors, Foster-Miller and GE Oil & Gas (PII North America) have performed an engineering study and developed a conceptual design that meets all the requirements for navigating and inspecting unpiggable transmission pipelines. Based on Foster-Miller's previous efforts developing the Pipe Mouse robot, the RoboScan inspection robot (Figure ES-1) meets the navigational and physical challenges of unpiggable pipelines through an innovative modular platform design, segmented MFL inspection modules and improvements to the inter-module coupling design.

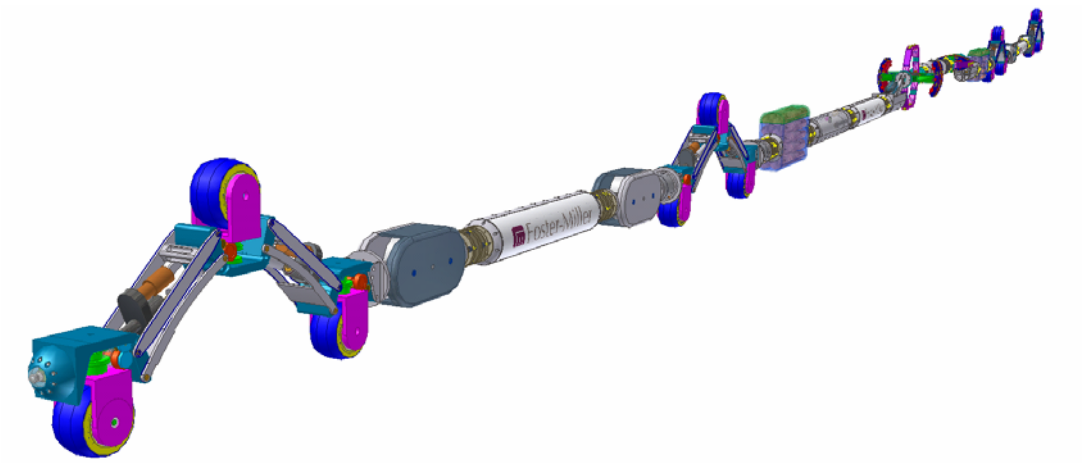

Figure ES-1. RoboScan Inspection Robot for unpiggable pipelines

Description of Problem

North America is crisscrossed with an extensive system of gas transmission and distribution infrastructure including underground pipelines. There are hundreds of thousands of miles of high-pressure gas transmission lines that cross the country and are owned and operated by a large number of interstate pipeline operators. There are millions of miles of low-pressure distribution piping that are owned and operated by hundreds of local gas distribution companies. The safe and efficient function of this infrastructure is vital to the Nation's energy security, the commercial operations of many industries and the continuous delivery of fuel to millions of

residential customers. Inspection, maintenance and repair of these pipelines are necessary elements of a pipeline integrity program. When access is practical, internal pipe inspection, maintenance and repair can offer a cost-effective approach to providing the services needed to ensure the safe and efficient operation of the infrastructure. However, difficulties in gaining physical access to and through these pipelines can present a potentially staggering economic burden on the owners/operators.

Unpiggable Pipelines

Physical Obstacles: There are many physical "obstacles" in the piping network that makes pigging impossible. The most intractable of these obstacles include:

- Bends/elbows (90 degree) with bend radius less than 1.0 D.
- Mitered joints/elbows greater than 10 degrees.
- Back to back combinations of bends/joints.
- Reduced port valves, including valves with full ports but smaller in diameter than the pipeline and/or plug valves that have neither full diameter ports nor circular openings.
- Reduction/expansion in pipe diameter greater than 50 mm (2 in.).
- Unbarred branch connections.

The elimination of one or more of these physical obstacles is required to make an unpiggable pipeline into one that can use a Smart pig. The Gas Research Institute in a report issued in 1995 entitled "In-Line Inspection of Unpiggable Natural Gas Pipelines" noted that the cost to replace just two of the most common obstacles would be substantial. The cost to replace unpiggable valves and sharp bends was estimated at approximately $1.5 billion. In addition, another $1.5 billion would be needed to install the necessary launch and retrieval stations used to insert and recover the pig from the pipeline. These costs do not include the operating problems associated with the loss of service while these repairs are undertaken.

Flow "Obstacles": The use of pigs is totally dependent on the availability of pressure to "push" the pig through the pipeline. The pressure level must be sufficiently great to accommodate the additional pressure drop across the pig along with the expected pressure drop needed to maintain the flow capacity and its associated pipe friction loss. Typically, this requires very high pressure given the enormous weight of the pig hardware and the large pressure drop required across the elastomeric cups used to seal the pig against the pipe wall. Unfortunately, the operation of many utility owned transmission pipelines is at a pressure too low to support the operation of a conventional pipe pig.

Other Considerations: The cost of pipeline inspection is expensive and assumes that the launch and retrieval traps are already installed and available to the inspection contractor. Although most interstate pipelines are many miles long, transmission pipelines owned and operated by the local distribution company are usually extremely short by comparison. Some of these pipelines are only one to two miles in length, and essentially none have traps installed.

Regulatory Requirements

The U.S. Department of Transportation through its Office of Pipeline Safety (OPS) has long held the position that all transmission lines must be inspected on a regular basis to ensure the safety of the public. In the past, this requirement was only applied to liquid pipelines, but not to the unpiggable portions of those pipelines. However, with the advances in robotics and sensor technology, OPS has recently endorsed the concept that all transmission pipelines (both liquid and natural gas) should ultimately be capable of 100 percent inspection. This can be accomplished through the elimination of pipeline obstacles for pigging, through the development of innovative inspection technologies, hydrostatic testing, or using a direct assessment technique.

Congress recently passed legislation (Pipeline Safety Improvement Act 2002) to require that the Department of Transportation's Office of Pipeline Safety institute new rulemaking on a testing program for natural gas pipelines in high consequence areas. The rulemaking includes a 10-year baseline inspection of all piping in high consequence areas followed by a seven-year re-inspection period. This applies to the use of hydrostatic testing, direct assessment or an in-line inspection robot. The adaptation of current pigging technology may not be viable given the geometric challenges, flow restrictions and economic drivers of utility owned transmission lines especially in high consequence areas. The external direct assessment technique has not been shown to be sufficiently reliable/accurate or cost-effective under typical field conditions. Hydrostatic testing, although physically possible, is very expensive and time-consuming with little or no useful pipeline condition data generated after completion of the testing. The application of an innovative robotic approach to the inspection of unpiggable pipelines may be the most viable approach.

RoboScan Inspection Platform

The RoboScan ™ robot is based on Foster-Miller's previous efforts developing the Pipe Mouse robot. The original Pipe Mouse robot was designed for use in gas distribution lines ranging in diameter from 100 to 150 mm (4 to 6 in.). This robot was designed to operate in both forward and reverse directions, as well as navigate through gentle bends (1.5D), mitered bends and tees (both main and branch lines). The RoboScan robot receives its locomotive force from two tractors (front and rear), with each tractor comprised of two 'triads' and an electronics module. The front and rear tractors provide the necessary pushing and pulling force to transport the platform through the piping system. Figure ES-2 is a conceptual representation of the RoboScan triad/tractor arrangement.

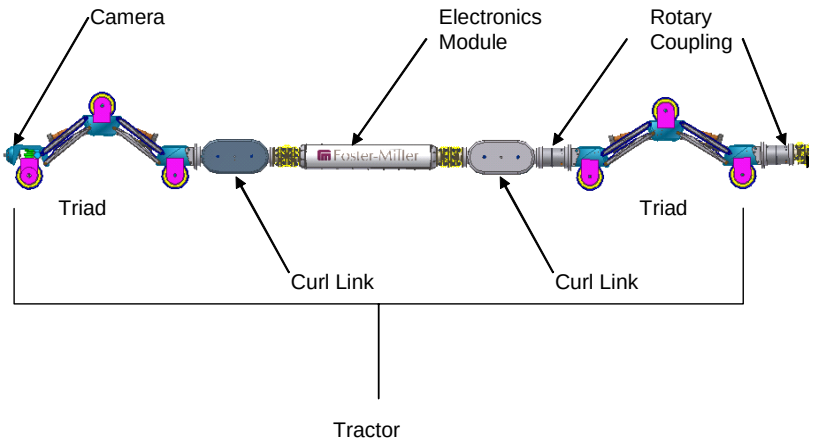

Figure ES-2 RoboScan triad/tractor arrangement (located at front and rear of train)

A fundamental feature of each triad is the ability to contract and extend within the pipe. Onboard drive motors actuate four bar linkages causing each triad to independently contract or extent by shortening the triad wheelbase. This motion is controlled via a force feedback loop based on load cells located in each of the three wheels on each triad. The feedback loop measures the force that the pipe wall exerts on each of the three wheels, and then either contracts or extends the linkages to maintain a preset force level. This control system provides each triad with the capability to autonomously expand or contract upon the encounter of a change in pipe diameter (either larger or smaller). This capability is also particularly useful when the robot encounters small obstacles such as weld beads, displaced joints or debris. The robot can easily change shape to accommodate these types of obstacles and continue its passage through the piping system.

Another key feature of the triad design is the curling link. The curling link connects each triad to its corresponding electronics module, and exerts a curling force that assists the robot when it enters and exits a bend or the branch line of a tee. Each curling link is designed to exert a downward force on either a module or triad creating a tendency for the robot to curl inward upon itself (referred to as preferential curl).

Tractor steering is accomplished by rotating the drive wheels on each triad such that the robot may roll (in either direction) along the pipe wall. The preferential direction of curl can be aligned with the oncoming bend by rotating and aligning the centerline of the robot within the pipe. This orientation process will allow the robot to automatically enter any bend or tee that intersects the pipe.

Inter-module couplings play a critical role in the RoboScan systems negotiation of the pipeline, keeping the train intact while transferring axial forces (tension and compression) and torsion, and performing supplemental control functions to get the platform through each obstacle. Electrical, sensor, and signal wires must be routed across the modules without risk of damage or impeding coupling function. Throughout the majority of the mission, the front and rear tractors will assume the same orientation in the pipe (typically 12:00 to 6:00). When negotiating obstacles, the tractors will perform choreographed movements (through onboard control algorithms) to assure that all modules move through the pipeline with minimal drag. A steady-

state speed of 30 ft/min (9 m/min) will be maintained.

Bend sensors are integrated into each bend link, and sense the degree of coupling bend so that the tractor drive control system can vary speed between the front and rear tractors to eliminate buckling. Supplemental control is provided through other inter-module components for lifting the triads into a bend (curl), allowing relative twist between sections of the train (rotation), and lifting and centralization of the MFL modules for proper engagement of the pipe wall (centralization). When traversing obstacles, the front and rear tractors, in conjunction with the inter-module couples, will perform independent sequences of motion to move the train through the various twists and turns of the pipeline. During the negotiation of certain pipe configurations, portions of the inspection platform must twist (and sometimes lock and transmit torque) relative to the other sections of the train.

Platform Kinematics

Bi-Directional Motion. The platform can travel within the pipe in both the forward and reverse directions. This motion is achieved by the use of bi-directional drive motors at each wheel on the four triads. Through constant engagement of the triads with the pipe wall and through use of the force feedback loop, the platform is capable of traveling both the downstream and upstream directions (as well as vertically upwards and downwards) regardless of the flow velocity.

Pipe Ingress/Egress. The RoboScan platform will be capable of entering and exiting pipelines at a 90 deg angle utilizing a field-installed hot tap fitting. By orienting the robot such that the direction of curl is aligned with the desired direction of travel, the constant curling force exerted by the curling links will direct the robot towards the chosen path.

Smooth Bends (<1.0 D). A typical bend installed in a transmission line can have a tight bend radius less than 1.0 times that of the pipe diameter. This type of obstacle is easily traversed using the basic functionality of the RoboScan platform. When the robot is properly aligned with the orientation of the bend, the curling force provided by the curling links will self-direct the platform through the bend. During all maneuvers, any one of the four triads can provide all of the necessary locomotion force should any of the other triad wheels lose contact with the pipe wall.

Plug Valves. A substantial obstacle for any pipe inspection robot is the plug valve. In most cases, the plug valve restricts approximately 70 percent of the available pipe width and 20 percent of the available height. The plug valve presents multiple obstacles to overcome. Beyond the severe restriction in available cross-sectional area, any reduction in height will create a ‘step’ for the robot to roll over. Based on the particular severity of this step, a combination of large diameter wheels and the autonomous contraction and expansion of the triad allow each tractor to pass through the valve. Clearly, both the tractors and the modules must maintain a slim aspect ratio or profile in order to pass through the narrow confines of the plug valve. Since the valve significantly reduces the working cross-sectional area of the pipe, and is a severe deviation from the standard geometry of a pipe wall, NDE sensing capabilities are curtailed during passage through plug valves.

Defect Detection: Magnetic Flux Leakage (MFL)

The principles of magnetic flux leakage are well established and the technique has been used for the detection of defects in ferritic components for a number of years. The basic technique relies on applying a magnetic field across the pipe wall, and mapping the flux density at the surface. The presence of a defect (internal or surface breaking) essentially changes the cross section of the pipe wall under examination. This causes a redistribution of the magnetic flux and localized changes in the magnetic permeability of the material. As a result, some of the magnetic flux leaks out of the surface and the presence of the defect is detected by hall-effect sensors. Even defects on the far side of the pipe wall can be detected. The technique is robust, fairly insensitive to dirt and pipe surface condition, and particularly suited to those defects that constitute a loss in volume of ferritic material.

A practical solution for the inspection module of the RoboScan platform utilizing a segmented MFL module and deployment mechanism was developed based on operational and geometrical requirements. The sensor platform consists of two segmented modules (90 degrees out of phase) that will inspect half the pipe circumference going away from the launch tube, and the remaining half during the return to the launch tube. Although the current emphasis has been on MFL inspection technology, the platform could just as easily be used with any inspection technology that is currently available or developed in the future. Magnetic methods invariably result in strong attractive forces, thus increasing drag and locomotion power requirements. By performing experiments to determine the field sensitivity, and to confirm rolling friction, it has been possible to optimize the design to provide inspection to a GE PII 30/50 specification while keeping power requirements to a manageable level. By utilizing novel shunting mechanisms, it will be possible to reduce the field and attractive power, making it easier to retract the sensor platform from the pipe wall, and also minimize the risk of accidental clamping onto other ferrous surfaces.

The data collection, storage and power modules will utilize current or future GE PII systems, and draw upon 30 years of experience. This includes electronics that can be mounted in pressure vessels or externally in the pressurized environment. The sensing electronics will also be based on current GE PII developments, providing high resolution mapping of the MFL distribution.

Command, Control, and Communication

The control architecture of the RoboScan system will be based on a network of micro-controllers. Each module in the overall platform will contain its own micro-controller. The couplings between the modules will function as physical, power and communications connectors. When a module is physically coupled to the system, that module will also be powered and its micro-controller becomes part of the overall control network. In an emergency, any module (micro-controller) can become master of the network, directing the other system functions. This aspect of the system serves two purposes. First, sensor or task modules can take control of the operation of the RoboScan, dictating speed, position and direction as needed by that particular task. Second, each controller can monitor the functional "health" of the other controllers. If a problem is diagnosed in part of the control network, the problem can be isolated. Once identified, another controller can assume the operation of the problem controller in the system.

A commercially available single-mode fiber optic cable (tether) that will provide the communication link between RoboScan and the base station has been identified. Although the command and control system focused on the use of a fiber optic tether for real-time communication between the operator and the robot, the proposed system architecture of the RoboScan platform incorporates numerous features that will facilitate both supervised and autonomous inspection. Throughout the development of the RoboScan platform, the need and inclusion of sensors and control surfaces became apparent and have been integrated into the control system design. The first generation RoboScan platform is geared towards supervised (tele-operated) control via a fiber-optic cable with autonomous control planned for later inclusion.

Battery Technologies

To power the computer, sensors, data acquisition and the drive wheels, some form of energy storage and electrical power supply is required. Of all the various possibilities (e.g., batteries, heat engines, fuel cells, ultra-capacitors, etc.), the battery approach is clearly the simplest, safest and most reliable. To minimize the number of launch and retrieval stations on long duration missions, the batteries should have maximum energy density. The modular platform approach has the advantage that battery "cars" may be added as needed, up to the length of the launch tube. However, certain obstacles (e.g., mitered corners) also impose a length constraint that must also be taken into consideration.

A power analysis was conducted based on a 2.5 mile mission (inspect out and inspect back for 360 degrees of coverage) that takes into account the resulting drag of the sensor modules, and the route through a "typical" pipeline. Using commercially available Lithium-ion technology, four battery modules of secondary (rechargeable) cells would be required to complete a mission. Discussions were conducted with a battery manufacturer who claimed that a Lithium-polymer battery could be developed with twice the power density, thus reducing the battery modules from four to two. Of the two choices of module shape (dictated by plug valve geometry), the asymmetric shape (over the symmetrical sausage shape) was chosen based on greater battery cell packing density. If not the for the plug valve, the modules (whether battery or any other supporting system) could utilize the full diameter of the pipe, providing more volume (battery energy) in a much shorter package.

Connection ports for in-situ battery charging and battery diagnostics will be provided in the launch tube. Automatic connection will be achieved either through the motions of the platform (battery module engages a connector) or a mechanism built into the launch station that connects battery power and signal wires.

Platform Operations: Launch and Retrieval

The RoboScan platform has several advantages that simplify the launch and retrieval hardware compared to conventional pigging. First, the robot can be "driven" into the main line rather than having to be pressurized and "blown" in from behind. This greatly reduces the complexity of the plumbing and operation of the launch and retrieval traps. Second, RoboScan

can be launch in its smallest configuration and can (depending on the pipeline size) result in a launch station that is half the diameter of the receiving pipeline. This advantage will result in significantly lower capital and construction cost for the launch and retrieval traps.

Unlike conventional pigs, the RoboScan can be launched (and retrieved) in a variety of positions. Smart pigs need the in-line launch and retrieval tube orientation to be horizontal which necessitates a major reconfiguration of the existing pipeline. In contrast, the RoboScan launch tube can be installed at a right angle (either vertically or horizontally) to the pipeline through a hot-tap saddle arrangement. This permits the launch station to be located almost anywhere along the pipeline. Because the RoboScan can be inserted vertically into the pipeline, many of the construction and pipeline reorientation problems and cost associated with conventional pigging traps are eliminated. The retrieval station is also greatly simplified. Instead of having to catch the pig, slow it down and divert the flow, RoboScan can be programmed to stop and crawl into a simple 90 degree branch-line. In fact, the launch tube can also act as a retrieval tube should the RoboScan platform return to the launch location at the end of the pipeline survey.

Summary

Based on the research efforts completed (to date) by Foster-Miller and GE/PII, the team members have the confidence to bring the RoboScan design concept into a detailed design phase, and believe that the fully-developed system will achieve these anticipated benefits:

- Ability to inspect otherwise inaccessible pipelines (transmission and distribution).
- Cost savings from not having to remove pipeline obstacles for conventional pigs.
- Inspection cost lower ($/mile) than direct assessment or hydro testing.
- A more versatile platform capable of performing a variety of inspection services.

ABSTRACT

The present project focuses on the development of an inspection platform and a sensor suite for the detection of corrosion and mechanical damage in unpiggable pipelines. Much of the existing natural gas infrastructure was designed and built without inspection or pigging as an operational consideration. There are many physical obstacles in the piping system that makes the passage of conventional and SMART pigs impossible. The inspection of unpiggable gas mains (both transmission and distribution) will require the marriage of a highly adaptable/agile robotic platform with advanced sensor technologies operating as a semi-autonomous inspection system. The integration and adaptation of an existing pipeline inspection robot as the underlying platform allows us to springboard over many of the expensive and speculative research activities associated with the development of an entirely new robotic system. In addition, the integration of proven sensor technology significantly reduces the uncertainty and total cost of the proposed research.

The concept developed under this project was that of a robotic platform that is train-like in nature. Both front and rear tractors propel the train in either the downstream or upstream directions inside the pipeline. Like a train, the platform includes additional "cars" to carry the required payloads. The cars are used for various purposes including the sensor modules, the power supply, data storage and location/position devices. The on-board intelligence gives the platform the benefit of an engineer steering the train through the complex (yet well defined) pipe geometry.

The Pipeline Inspection Robot (RoboScan) is expected to overcome all of the current shortcomings of transmission pigs and has the following performance targets:

- Capable of bringing a full suite of NDE sensors into transmission and distribution networks
- Self-powered and capable of traveling long distances from the entry point
- Negotiate mitered (zero degrees) elbows and tees as well as back to back out-of-plane bends
- Navigate in both the horizontal and vertical planes in both directions
- Not dependent on pressure drop to "push" the robot
- Passable through partially ported plug valves
- Automatically adaptable, by a factor of two, to changes in pipe diameter

The project was funded by the National Energy Technology Laboratory of the US Department of Energy under Award DE-FC26-02NT41645, the NYSEARCH Committee of the Northeast Gas Association (previous the New York Gas Group). The research contractors were Foster Miller and GE Oil & Gas (PII North America).

CONTENTS

Section **Page**

ILLUSTRATIONS

Figure **Page**

Figure **Page**

Figure **Page**

TABLES

THIS PAGE INTENTIONALLY LEFT BLANK

1. INTRODUCTION

1.1 Description of Problem

The United States is crisscrossed with an extensive system of gas transmission and distribution infrastructure including pipelines. There are hundreds of thousands of miles of high-pressure gas transmission lines that cross the country and are owned and operated by a large number of inter-state pipeline operators. There are millions of miles of low-pressure distribution piping that are owned and operated by hundreds of local gas distribution companies. The safe and efficient function of this infrastructure is vital to the Nation's energy security, the commercial operations of many industries and the continuous delivery of fuel to millions of residential customers. Inspection, maintenance and repair of these pipelines are necessary elements of a pipeline integrity program. When access is practical, internal pipe inspection, maintenance and repair can offer a cost-effective approach to providing the services needed to insure the safe and efficient operation of the infrastructure. However, difficulties in gaining physical access to and through these pipelines can present staggering economic burdens on the owners/operators.

The use of in-line inspection robots, the so-called Smart pigs, is a well-established method for the evaluation of high-pressure transmission mains. The pigs carry a wide variety of non-destructive examination sensors into these pipelines to inspect for defects in the pipe wall. The NDE techniques employed (e.g. magnetic flux leakage, acoustics and ultrasonics) that can identify such faults as cracks, wall thinning, pitting, corrosion, weld inclusions and changes in pipe geometry caused by denting, gouging and crushing. These pigs have traditionally been used on long distance, large diameter pipelines that contain essentially no obstacles to these fixed-diameter machines. In an effort to expand the market for these devices/services, the pigging industry has re-engineered the pigs and sensors to work in a more diversified environment. Today pigs can negotiate sharper bends (radius of curvature around 1.5 D), travel through a 2-inch diameter reduction in cross-section, and pass through certain types of valves. The pigs are now capable of operating in smaller pipe diameters that are more typical of distribution networks. However, there remain many physical limitations within the pipeline environment that prevent the use of these Smart pigs.

1.2 Non-Piggable Pipelines

Physical Obstacles

Problems arise when the piping network is older and constructed without pigging as a design consideration. This is the situation with countless miles of interstate pipelines, transmission piping owned and operated by local gas distribution companies, and essentially all low-pressure distribution piping. There are many physical “obstacles” in the piping network that makes pigging impossible. The most intractable of these obstacles include:

- Bends/elbows (90-deg) with bend radius less than 1.5 D: This is by far the most common obstruction.

- Mitered joints/elbows greater than 10-deg: This is a common obstacle found in older systems. Mitered elbows are typical found in many New York state pipelines.

- Back to back combinations of bends/joints: Commonly found in tightly spaced locales where pipeline layouts were restricted. These combinations can be further classified either in plane or out-of-plane (comparing the orientation of the second elbow compared with the first elbow).

- Reduced port valves: This includes valves with ports smaller in diameter than the pipeline and/or plug valves that do not have a full diameter port opening.

- Reduction/expansion in pipe diameter greater than 2-inch: These changes can either be diametrically concentric or eccentric. Changes in section diameter also commonly occur in the lateral branch line of a tee.

- Unbarred branch connections: Pigs are not designed to turn down branch lines, and therefore, branch lines must be barred to prevent the nose of the pig from crashing into the lateral and jamming itself in place.

The elimination of one or more of these physical obstacles is required to make an unpiggable pipeline into one that can use a Smart pig. The Gas Research Institute in a report issued in 1995 (entitled "In-Line Inspection of Unpiggable Natural Gas Pipelines") noted that the cost to replace just two of the most common obstacles would be substantial. The cost to replace nonpiggable valves and sharp bends was estimated at approximately $1.5 billion. In addition, another $1.5 billion would be needed to install the necessary launch and retrieval stations used to insert and recovery the pig from the pipeline. These costs do not include the operating problems associated with the loss of service while these repairs are undertaken.

Flow "Obstacles"

The use of pigs is totally dependent on the availability of pressure to "push" the pig through the pipeline. The pressure level must be sufficiently great to accommodate the additional pressure drop across the pig along with the expected pressure drop needed to maintain the flow capacity and its associated pipe friction loss. Typically, this requires several hundred PSI line pressure given the enormous weight of the pig hardware and the large pressure drop required across the elastomeric cups used to seal the pig against the pipe wall. Unfortunately, the operation of many utility owned transmission pipelines is at a pressure too low to support the operation of a conventional pipe pig. In some cases, the seasonal variation in demand results in a situation where there is very little flow for extended periods of time. Furthermore, in some limited situations, the flow can actually reverse direction. Therefore, any internal inspection technology must be self-powered to insure its ability to travel within the piping network under all flow conditions throughout the year.

Other Considerations: The cost of pipeline inspection is expensive and is usually quoted on a per mile basis. The cost assumes that the launch and retrieval traps are already installed and available to the inspection contractor. Although most interstate pipelines are many miles long,

transmission pipelines owned and operated by the local distribution company are usually extremely short by comparison. Some of these pipelines are only one to two miles in length, and essentially none have traps installed. Furthermore, there have been no regulations mandating inspection of these types of pipelines. Therefore, the traditional pigging operation is impractical and too expensive for these types of application.

The gas industry is now facing increasing demands by the Federal Government to insure the integrity of the Nation's gas transmission infrastructure. Recent terrorist events against the United States, combined with several high-profile pipeline accidents, have prompted Congress to act on this issue. It now appears assured that the inspection of some portion of the Nation's gas transmission system will be required.

It has been estimated by OPS that there are approximately 292,000 miles of regulated natural gas transmission pipelines in the United States. Taking into consideration that the regulations will only apply to high consequence areas, the total length of transmission pipeline affected by the proposed rulemaking has been estimated to be 24,500 miles. However, much of the Nation's gas transmission system is not currently piggable. The Interstate Natural Gas Association (INGAA), the American Gas Association (AGA) and the American Public Gas Association (APGA) each has developed an estimate of the percentage of transmission mileage operated by their members in both Class 3 and 4 areas that are considered to be either piggable or unpiggable. Their reported values (to OPS) are shown in Table 1. Although the number varies between these organizations, there is no doubt that a large percent of the current population is unpiggable based on commercially available technology.

Table 1 Piggable Status of Natural Gas Transmission Pipelines

Pipeline Status	**INGAA**	**AGA**	**APGA**
Easily piggable	24.4	12	13
Easily made piggable	25.3	10	no report
Piggable with extensive retrofit	45.9	43	41
Not piggable	4.4	35	46

It is clear that the ability to inspect non-piggable transmission pipelines presents a significant need and challenge to the gas industry. The adaptation of current pigging technology may not be viable given the geometric challenges and flow restrictions of the utility owned transmission line population. The external direct assessment technique has not been shown to be sufficiently reliable/accurate or cost-effective under all field conditions. Hydrostatic testing, although physically possible, is too expensive and time consuming with little or no useful pipeline condition data generated after completion of the testing. The application of an innovative robotic approach to the inspection of unpiggable pipelines may be the most viable approach

1.3 Regulatory Requirements

1.3.1 Federal/State Codes

With the recent advances in robotics and sensor technology, and the occurrence a few unfortunate pipeline accidents, the Office of Pipeline Safety (OPS) of the US Department of Transportation has endorsed the concept that all oil and gas transmission pipelines should be capable of 100 percent inspection. This can be accomplished through the elimination of pipeline obstacles that would allow for pigging, or through the development of innovative inspection technologies, hydro testing, or use of direct assessment techniques. Problems arise when the piping network is older and/or constructed without pigging as a design consideration. This is the situation with countless miles of transmission pipelines owned and operated by local gas distribution utilities.

1.4 Research Objectives

The Gas Research Institute in a report issued in 1995 (entitled "In-Line Inspection of Un-piggable Natural Gas Pipelines") noted that the cost to replace just two of the most common obstacles would be substantial, costing over $3 billion. Therefore, the development of tools to inspect un-piggable transmission and/or distribution pipelines presents both a formidable technical challenge as well as a significant financial incentive to the gas industry. The adaptation of current pigging technology may not be viable given the geometric challenges of existing interstate and utility owned pipelines. External direct assessment techniques have not been shown to be universally adequate, accurate or cost-effective. Use of an innovative robotic approach would apparently be dictated.

The inspection of un-piggable gas transmission and distribution pipelines requires the innovative marriage of a highly adaptable/agile robotic platform with advanced sensor technologies operating as an autonomous or semi-autonomous inspection system. The work conducted under this program is based on a robotic platform that is train-like in nature and is based on Foster-Miller's Pipeline Inspection System (PipeMouse) developed in early to mid 1990's. Both front and rear tractors propel the train in the forward and reverse directions inside the pipeline. Like a train, the platform includes additional "cars" to carry the required payloads. The cars are used for various purposes including the installation and positioning of sensor modules, the power supply, data acquisition/storage, location/position devices and onboard micro-processors/electronics. The onboard intelligence gives the platform the benefit of an engineer steering the train through complicated pipe geometry. The system includes launching and retrieval stations that are similar to that used for conventional pigging systems, but much simpler in design and operation.

The Pipe Mouse was built to a strict set of performance criteria appropriate for low-pressure gas distribution networks. The Mouse was designed to be highly mobile and agile, had the ability to travel long distances from the entry point and steer down branch line of pipe tees, negotiate mitered (zero degrees) elbows, navigate in both the horizontal and vertical planes, pass through partial section valves, and adapt, by a factor of two, to changes in pipe diameter. These same types of obstacles create problems for inspecting un-piggable transmission mains.

General Electric Power Systems (previously PII North America; a subcontractor for this project) has extensive experience designing and working with sensors based on ultrasonics, electromagnetism, eddy-currents and optical methods. For this program, sensor development was considerably more challenging than for conventional pigging due to the greater variance of pipe diameter and the more difficult obstacles encountered in un-piggable pipelines. The ability to actively expand and retract the onboard sensor was required for obstacle avoidance.

The robot is controlled via a fiberoptic tether system, which was analyzed, designed, and tested as part of this project. The tether is expected to provide sufficient range for the robot to inspect a substantial length of the pipe without the need of many expensive tappings of the pipeline

To power the computer, sensors, data acquisition, drive wheels and sensors, some form of energy storage and electrical power supply is required. Of all the various possibilities (e.g., batteries, fuel cells, ultra-capacitors, flywheels, etc.), the battery approach is clearly the simplest, safest and most reliable. To minimize the number of launch and retrieval stations, the batteries should have maximum energy density. The modular platform concept has an advantage in that battery "cars" can be added as needed, up to the length of the launch tube. Certain obstacles (e.g., mitered corners) also impose a length constraint. Different battery and charging modules may also be swapped in and out based on the range requirement, power and availability of recharging stations.

Preliminary mechanical, electrical and controls engineering was performed in this study for the purpose of developing a new robotic platform and sensor module capable of navigating through all known physical obstacles found in non-piggable transmission gas pipelines (12" to 24" range, 18" nominal) while performing a reliable inspection of the pipe wall. Engineering calculations and 3-D CAD models were produced to substantiate the design approach.

The anticipated benefits derived from the use of this platform include the following:

- Ability to inspect otherwise inaccessible pipelines (transmission and distribution).
- Cost savings from not having to remove pipeline obstacles for conventional pigs.
- Inspection cost much lower ($/mile) than direct assessment or hydro testing.
- A more versatile platform capable of performing a variety of inspection services.

2.0 ROBOSCAN INSPECTION PLATFORM

2.1 System Overview

The RoboScan system presented in Figure 1 represents the latest incarnation of the Pipe Mouse platform. The system addresses all the design requirements summarized in Table 1 through the incorporation of additional degrees-of-freedom in maneuverability of the triad-based locomotion platform along with a deployable segmented MFL sensor for detecting and measuring internal and external pipe corrosion. A fiber optic tether with winder integral to the robot is used to facilitate platform control and real-time inspection video viewing. MFL inspection data is stored onboard for later retrieval. A concept for a non-contacting ovality sensor is also incorporated into the design.

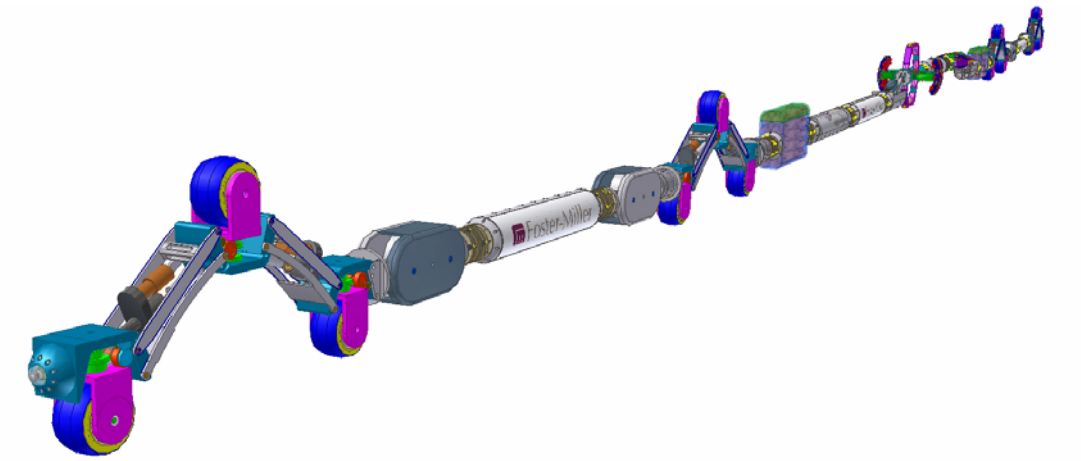

Figure 1 RoboScan Inspection Robot for unpiggable pipelines

Table 1-A. RoboScan primary and secondary design criteria

Criteria	Primary Criteria	Secondary Criteria
Pipe Size Range	12 to 24-in (18" nominal)	
Pipe Wall (in.)	Up to .50-in	
Inspection Distance (miles)	5 (target), ±2.5 each direction	
Pipeline Velocity (fps) & Pressure (psig)	Nominal: 20 fps & 350 psig	Min: 10 fps & 250 psig Max: 75 fps & 1000 psig
Obstacles to Negotiate	• Plug Valves (Nordstrom drawing no. C-50710) • Min Bend R<1.5D (miter bend worst case) • Compound 90° bends (in & out of plane) • Diameter Reduction (2 pipe sizes up or down)	
Defects to be Detected	External Corrosion	Ovality, Gouges, Internal Corrosion
Contaminants	Loose debris on invert Sludge deposits, oil, water Corrosion deposits	
Pipeline Corrosives	Mercaptan	
Platform Launch Capabilities	Live launch	
Pipeline Cleaning Requirements	None	Investigate Further
Nominal Inspection Velocity (ft/min)	30	55 platform speed (no inspection)
Drive System	• Bi-directional • Battery-Powered	
Platform Size (cross-section)	• Maximum allowable pressure drop in smallest diameter within range (needs to be defined)	Maximum allowable pressure drop in pipeline obstacles (valves, bends, etc) - needs to be defined
Communications	• Bi-directional data link (tether) – control and inspection data • Camera • Electromagnetic sonde (emergency location)	
Control	• Remote control (tether) through base station (base station design not included) • Semi-autonomous (tether break return)	Full autonomous in future – "learn" with tether
Modular Design	Expandable and repairable by modular changeout	

The RoboScan platform consists of front and rear locomotion tractors each comprised of 2 triads that drive the various platform modules through the pipe. These modules, illustrated in Figure 2 and discussed in the following sections of the report, are summarized below:

- Tractor/Triad systems - provides platform locomotion.
- Curling links – provides lifting moment to assists triad through bends.
- Electronics modules – packages electronics for various systems.
- Rotary couplings – provides relative rotation capability between triads for back-back out-of-plane bends.
- Flexible couplings – allows modules to bend in all planes relative to each other while providing sufficient axial and torsional rigidity, and wire passing.
- Battery modules – provide power, power management and remote charging interface.

- Winder module – houses fiber optic tether, contains communications interface and manages tether payout and take-up.
- Centering coupling – positions MFL sensor/ovality modules on the pipe centerline.
- MFL sensors – records and maps internal and external pipe wall corrosion
- Ovality sensor – measures and maps pipeline ovality

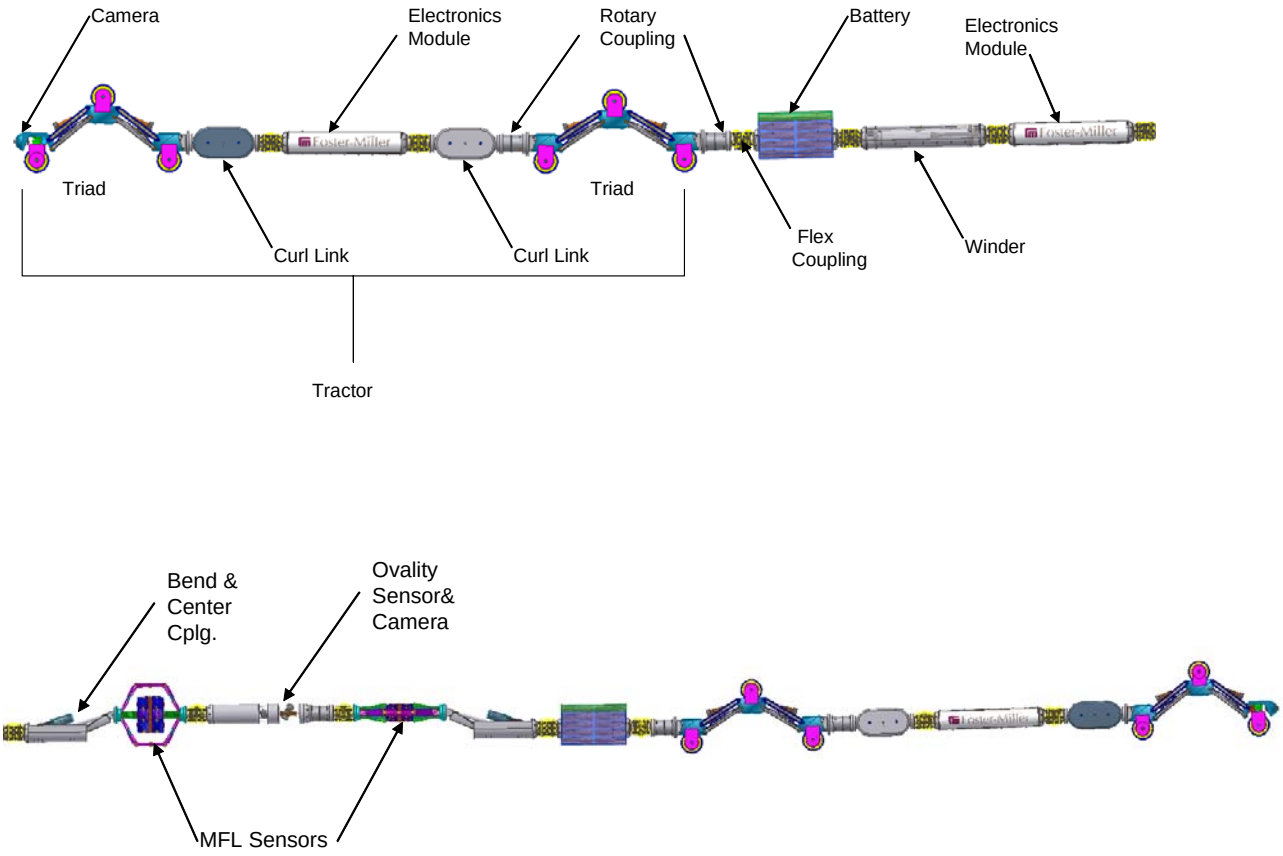

Figure 2. Detail of RoboScan Modules

The conceptual design of the RoboScan system was based on the requirement for a platform capable of inspecting a range of 16 inch to 20 inch pipe (18 in nominal). Due to the design requirement for passing plug valves (smallest in 16 inch pipe), a slim "sausage" shaped module of circular cross-section was required. This slim profile results in a platform length of approximately 40 feet (for 16 inch to 20 inch pipelines) due to the fact that only 10% of the pipe's cross-sectional area is being utilized because of the presence of plug valves. The length of the module was limited by the geometry of a 16 inch mitered bend as determined in the module volume study summarized below. Note that the available volume will increase with the cube of

the diameter, so packaging is less onerous in larger pipes. Positioned at the bottom of the pipe, the symmetric module will clear the plug valve regardless of train orientation.

An asymmetric module shape was chosen for battery storage. While the symmetric "sausage" shape simplifies control, the oval shaped module can pack more battery cells, reducing the total number of battery modules (for the prescribed 5 mile mission) from 4 to 2. The battery module must be correctly oriented by the leading tractor. The system will be designed with a focus on modularity to facilitate simple exchange of modules in the field. The following sections of this report will discuss the details of each of the RoboScan's sub-systems and the requirements for a Phase II prototype.

2.2 Geometric Constraints on Module Sizing

2.2.1 Module Volume Optimization

The proposed robotic platform consists of a train of payload modules with a tractor at either end. The degree of "packing efficiency" of the platform is dependent on the range of pipe sizes inspected by a given platform (its portability) and the types of pipeline obstacles encountered. The purpose of the module volume optimization study (conducted during the earlier NYGAS program) was to determine the optimum size (shape and length) of the payload modules for a given range of pipe sizes, with module size dictated by the smallest pipe diameter. The RoboScan platform developed in this study is close to 40 feet long because of the plug-passing requirement (long and slender modules) and the need to negotiate back-back out-of-plane bends (need for four rotary joints adjacent to triads).

Ideally, the payload modules should be as large as possible without compromising the mobility of the robot, or excessively blocking the flow. Use of fewer, larger modules makes for a shorter train which allows a shorter launch tube and shorter transport equipment. Large modules also make it easier to package batteries, sensors and other components, and allow the inspection sensors to adapt to a wider range of pipe size. A summary of relevant module sizing formulas from the Module Volume Maximization Study are shown in Figure 3. The battery modules were sized based on the "plug and miter passing oval module", while the other modules were based on the plug and miter passing circular module.

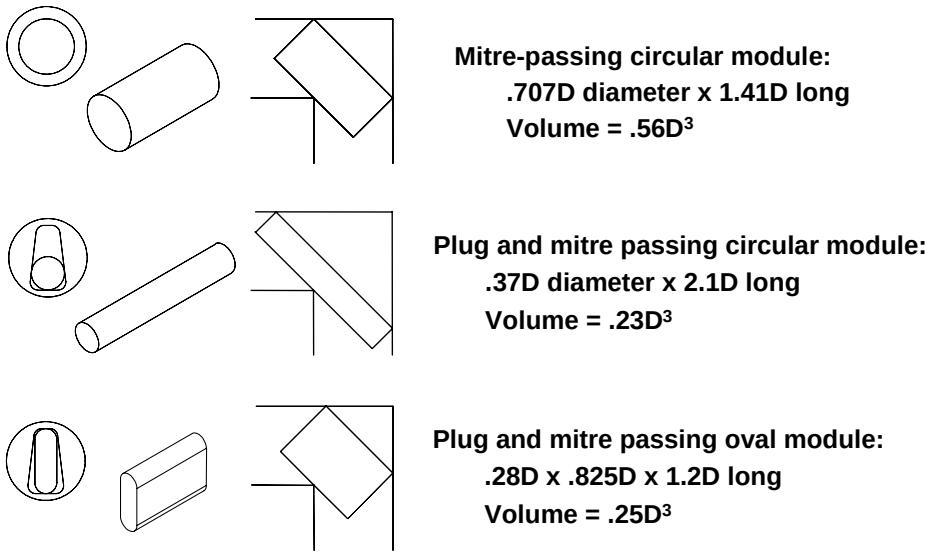

Figure 3. Module size limits as function of pipeline obstacles

2.2.2 Kinematics Analysis

A kinematics analysis was conducted to determine the degrees of freedom required for the robotic platform to negotiate the obstacles as stated in the requirements of this program and based on the constraints dictated by the Module Volume Maximization Study. In order to pass through these obstacles, complex articulations, beyond the capabilities of the previously developed Pipe Mouse, are required. Foster-Miller's approach was to augment the functionality developed for Pipe Mouse to address the additional maneuverability requirements. Various techniques were employed, including software modeling, pencil and paper analysis, and the development of a physical model. For this study, models were designed around a nominal pipe size of 18" diameter, with the capability to expand/contract to +/- 1 pipe size.

Before modeling could begin, a rough size envelope was established based on all the obstacles that need to be traversed. Considering these obstacles and the +/- 1 pipe size requirement, the following tractor design drivers were established:

Table 2 Tractor design drivers

Design Variable	Design Driver	Value
Triad Max. Width	Plug Valve Orifice	5.25"
Triad Max. Length	Geometric Limitations of Mitered Bend	Approx. 1.5D*
Triad Max. Height	Triad Max. Length	<1.5D
Wheel Diameter	Maximum Plug Valve Step	>5"
Module Size	Clearance Through Bends/Plug Valves	.37D x 2.1D

*This length may be accomplished provided that the linkage geometry is optimized for cornering clearance.

The maximum width of the triad is limited by the narrow opening of the plug valve. For the 18 inch nominal case, the maximum width allowable (without a safety margin) is 5.25 inches (16 inch pipe). Maximum triad height is related to maximum allowable length, and was determined by establishing a maximum length that would allow passage around the sharp cornered mitered bend. The mitered bend is the worst case obstacle in terms of two dimensions, and will limit the length due to its unfavorable geometry. Based on our analysis, a triad length of approximately 1.5 times the pipe diameter may be achievable with the proper linkage design. Maximum triad height is directly related to the maximum length of the triad. Once the maximum length is established, we can consider the robot in its 'tallest' state (fully contracted), and call this the maximum height. The triad wheels were sized such that the axle placement is sufficiently above the tallest step of the plug valve, allowing the wheel to easily roll over the step. A minimum diameter of 5 inches was recommended. Lastly, the module size was determined by the Module Volume Maximization Study of Phase I that considered the passage of modules through all obstacles. The module diameter is related to pipe diameter, and can be determined by the expression "Max. Diameter = .37*D". Module length is also associated with pipe diameter, and can be calculated with the expression "Max. Length = 2.1*D".

Software Modeling

Kinematic analysis through software modeling was initiated with the construction of a 2 dimensional model of a single triad. Rough dimensions for the triad were chosen based on the results of the analysis described above. This analysis provided a size envelope to work within, that would theoretically allow passage through all 2-D obstacles. The next step was to constrain the 2-D model to renderings of the various obstacles. Once the proper relationship was established between the triad model and the obstacle model, we were able to 'drive' the triad through the obstacle, observing the motions required to pass through it completely. This was a simplified case, and used a simplified model of the triad for all cases. Using this technique, we were able to observe the triad through 1.5D bends, back to back 1.5D bends, pipe diameter expansions and reductions, and to a point, mitered joints and pipe ingress/egress. The 2-D model verified that nearly all of the capabilities of the Pipe Mouse robot could be directly transferred to a next generation robot to service larger pipes.

Following the 2 dimensional model design and analysis, a second model was created. The second model, created in 3D, was developed with the intentions of defining the requirements for the robot to travel in 3 dimensions, particularly back-to-back, out of plane bends (the most difficult to model). During the modeling process for this portion of the analysis, we reached the limits of the 3D modeling software, and realized that accurate conclusions could not be drawn from this type of modeling for the 3D case.

Physical Modeling

The goal of the kinematics/mockup testing is to establish the design requirements for the platform. These include:

- Triad link lengths, shapes, and mechanical means for active adjustment

- Triad max and min wheelbases
- Linkage/joint configuration and placement, force requirements (tension, compression, torque), and active or passive control requirements
- Required motions and timing to clear obstacles
- Load sharing requirements between front and rear tractor
- Overall volume requirements (platform and modules)
- Control sensor requirements

To clearly understand the mechanical/control requirements of the robot for passage through out-of-plane, back-to-back bends, it was determined that a physical model should be constructed. The physical model included a tractor (two triads and a center module) and a means for attaching a train of additional modules. From previous studies in the Pipe Mouse development program, the required degrees of freedom of coupling modules, and their approximate locations on the platform, were determined for the back-to-back out-of-plane case. The physical model was designed with this information, and provided for a degree of adjustability so that the exact size envelope, and locations of DOF's within the pipe could be determined. A mockup consisting of several obstacles, including back-to-back in and out-of-plane bends and mitered bends was constructed using the 16" steel pipe provided by KeySpan. Testing commenced with the goal of establishing the controlled motions and degrees of freedom (linkage/coupling designs) required to move the platform, sensor and associated modules through the pipeline.

Simple physical tests with the Pipe Mouse Robot (3"-6") were performed to better understand some of the kinematics of the larger robotic system under study. The goal of this testing was to simulate plug valve passage, and observe how the robot reacted to the vertical climb required to move into the body of the plug valve. Each possible plug valve geometry configuration was considered (based on the Nordstrom drawing no. C-50710), and the worst case (largest step) was chosen for testing. A scaled version of the 'step' was created and fixed into the pipe for the 3"-6" robot to operate in. This procedure was performed for both the 3" (lower height limit) case and the 6" (upper height limit) case. After installation of the step, the robot was run through the pipe, and its reaction to the step was observed. It was noted that using a finely tuned force feedback loop, the triad could sense the step when engaged, and resize itself accordingly to pass over it. Other observations included the necessity for a smooth 'robot underbody' to avoid snagging the step, as well as the need for sufficient traction between the tire and step materials to ensure a positive engagement.

A mockup of the tractor (with intermediate module) was fabricated. Adjustable link arms (each arm of 4-bar linkage) were incorporated in anticipation of this expanded (but more complex) control function to traverse back-back out-of-plane bends. Timing gears were incorporated between the each set of link arms to maintain the correct relative orientation as the triad changed in height. To facilitate the manual movement of the mocked-up tractor through the pipe, access holes were placed in strategic locations to facilitate the movement of the mocked-up platform through each obstacle in the pipeline.

The required motions of the tractor (2 triads and intermediate module) were simulated by moving the kinematics model by hand through 16" pipe. The tractor model was designed and built as a

highly adjustable scaled model with equivalent degrees-of-freedom. Sections of straight pipe, mitered bend, and back-back in and out-of-plane pipe sections were assembled (Figure 4). The triad/tractor and module section was incrementally moved by hand through each obstacle while the position and relative sequencing of each degree-of-freedom was recorded. Simulated tractor components (motor drive, steering, and clamp mechanism) were attached to the triad skeleton to verify that the system could physically fit through the pipe obstacles.

Figure 4. Mockup tests

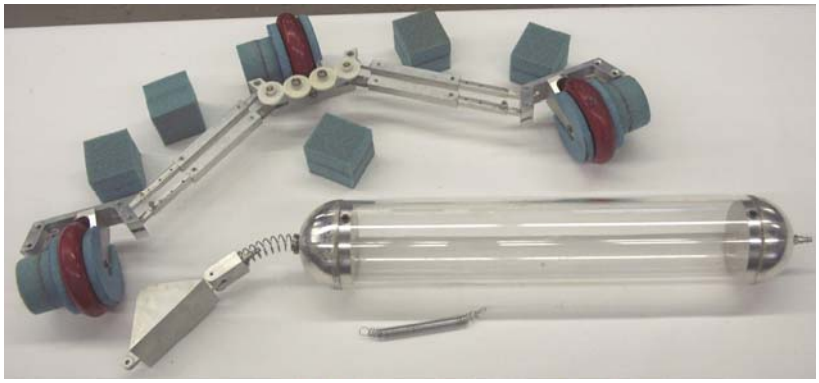

Figure 5. Model of triad drive components and intermediate module

The "limiting" obstacles in the design process are the back-back out-of-plane bends and the mitered bend. Since the triads are sized to fit through a plug valve, and the fact that the required control sequence has been verified with the Pipe Mouse, it was decided that further verification

of plug valve passing was not required. The results of the back-back out-of-plane bends and the mitered bend passing tests are detailed below.

Back-Back Out-of-Plane-Bends

The control sequence for moving a triad through a back-back out-of-plane bend is shown in Figure 6 (Appendix F). A single triad is shown, but the actual system will consist of 2 triads separated by an intermediate module. Mockup tests verified that the tractor unit (2 triads and module) could pass through with the appropriate couplings. The intermediate module, like all modules on the inspection platform, will be optimized in shape to pass through all obstacles, and because of its symmetric cross-section will be position-independent (see Figure 5). A swivel joint, positioned on one end of the module, will allow the triads to rotate independent of each other. Thus the limiting factor in back-back out-of-plane passing involves fitting each triad through in succession. As illustrated in Step 3 of Figure 6, each triad must stop between bends (and reposition) when the middle wheel is centered between the two bends (positioned on the weld seam). Proper positioning within the bend is key to optimization of platform portability.

The back-back out-of-plane bend was identified early in the program as the limiting factor in platform portability (number of pipe sizes a given platform could negotiate). Portability of the platform is determined by the maximum pipe size (at minimum wheel base) and minimum pipe size (at maximum wheel base) that a tractor can negotiate. In large pipe the wheel base must be long enough to remain stable, while in short pipe the wheel base must not be so long as to limit bend passing (Step 3 of Figure 6).

Figure 7 (Appendix F) illustrates the physical limitation of triad length when passing a back-back out-of-plane bend. The figure shows the triad centered within the two bends prior to re-alignment, and illustrates the situation where the triad contacts the pipe wall of the second bend. In this case the triad is too long to complete the bend-passing sequence. The triad must be capable of rotating 180 degrees as shown without making contact. Based on our mockup testing, in 16” pipe, the longest possible link length to achieve bend passing will net a 24” triad height (smallest wheel base where triad remains stabile). Preliminary indications are that with optimization, a range of 16”-24” may be possible with a single platform.

Mitered Bends

The control sequence for moving a triad through a mitered bend is shown in Figure 8 (Appendix F). Control of this motion is fairly straight-forward, and has been verified with the Pipe Mouse. Using the same criteria as applied to the back-back out-of-plane situation, it was found that the maximum link lengths for a mitered bend yields a 27.5” total triad height. This suggests that for the mitered bend case, with optimization, a single platform may cover 14”-24”. Since the mitered bend is less limiting than the back-back out-of-plane situation, our best estimate of total system portability at this time, and as dictated by the back-back out-of-plane obstacle, is 16”-24” with a single platform.

2.3 Tractor Locomotion System

The kinematics testing defined the functional requirements of the system in terms of the inter-module coupling requirements (functions and degrees-of-freedom), the module volume constraints, and the control motions required to get through the pipeline. Upon completion of the kinematics testing, the next step in the design process was to design the tractor locomotion system which consists of the wheel drive system, wheel steering system, and wheel clamp system. The first step in the design of the tractor locomotion system was to establish the power required to pull the system through the pipeline based on the number and weight of modules, and the static and rolling friction coefficients involved.

Assumptions for the drive power calculations presented here were based upon estimates made during the NYGAS study. As PII progressed in their design for the MFL inspection modules and better understood how a segmented magnetizer could be deployed, advances were made to reduce drag and thus reduce power requirements. We decided to stay with the conservative power requirements as a basis for the design of the locomotion system to provide a factor of safety to protect against any unforeseen power requirements. The following discussion summarizes the design process and system specs for the wheel drive, steering, and clamping components of the robotic platform based on the updated power requirements.

Locomotion Power Requirements

A complete analysis of the drive power requirements is included in Appendix A. Power requirements of the triad/tractor drive system were calculated on two levels:

- Steady-state inspection in level pipe where any 1 triad (3 wheels) would handle the load.
- Peak load condition where 2 triads (6 wheels) would share the load.

The total drive force required will be equal to the sum of the steady-state drive force and the peak drive force. The system will be designed such that a single triad can pull the train under steady-state conditions. Motor sizing was determined by the worst case condition where a tractor (2 triads, 6 wheels) would pull the train under peak load conditions. Highlights of this analysis are included below.

Steady State Driving Force:

$$F_{d\_steady} = F_{elec\_modules} + F_{bat\_modules} + F_{sensor} + F_{shear\_drag} + F_{pressure\_drag} + F_{triads} + F_{mag}$$

Where:

$F_{elec\_modules} = 55\ lb_f$	Frictional drag of payload modules to pipe wall
$F_{bat\_modules} = 142\ lb_f$	Frictional drag of battery modules to pipe wall
$F_{sensor} = 108\ lb_f$	Rolling friction, total for 4 MFL magnetizers
$F_{shear\_drag} = 0.5\ lb_f$	Shear drag on eight modules in straight pipe
$F_{pressure\_drag} = 0.4\ lb_f$	Pressure drag on leading module
$F_{triads} = 72\ lb_f$	Rolling friction of all 12 driven triad wheels
$F_{mag} = 20\ lb_f$	Magnetic eddy current forces

$F_{d\_steady} = 398\ lb_f$

Peak Driving Forces

$F_{d\_peak} = F_{step} + F_{climb} + F_{valve\_pressure\_drag}$

Where:

$F_{step} = 132\ lb_f$	Force of driving wheel over plug valve step
$F_{climb} = 1280\ lb_f$	Force to pull train through 20 ft elevation
$F_{valve\_pressure\_drag} = 6\ lb_f$	Pressure drag upon entering plug valve

Since it is highly unlikely that a plug valve will be positioned in a vertical section of pipe, and the fact that the force to pull the train through a 20 ft elevation (F_{climb}) is the highest peak force encountered, the peak power was calculated solely on F_{climb}.

Total Drive Force

$F_d = F_{d\_steady} + F_{d\_peak} = 398\ lb_f + 1280\ lb_f = 1{,}678\ lb_f$

Total Drive Power

$P_{total} = F_d \times V_{pig} = 1.53$ hp (where Vpig = 30 ft/min)

It should be noted here that this level of drive force is a peak condition, corresponding only to the vertical climb. With six of the 12 wheels supplying peak power, and based on a 75% drive train efficiency, the output requirements for the wheel drives is as follows:

Wheel Speed = 19 rpm
Wheel Torque = 839 in-lb_f
Wheel Power output = 0.25 hp
Drive Train Efficiency = .75

Motor Power = 0.34 hp

Wheel Drive:

Based on requirements that were established through kinematics experiments, a wheel diameter of 6 inches was chosen. It was also determined that significant advantages were to be realized by maximizing exposure of the wheel circumference. Constraints on overall width that are required in order to pass through plug valves severely limited choices in drive components. The resulting tractor wheel drive design provides a very compact package owing to the use of both a frameless motor and a frameless reducer that are packaged inside the wheel hub. Further compactness is achieved by keeping bearings common between the motor shaft and the reducer input stage as

well as between the gearbox output stage and the wheel itself. The wheel bearing arrangement is such that the reducer does not transmit the wheel clamping loads.

Figure 9 (Appendix F) illustrates the wheel drive layout and identifies the main components that have been selected. The split housing feature is required in order to facilitate assembly. Both the selected motor and reducer have ample torque speed and power ratings for this application. The limiting design case of only 3 wheels driving occurs infrequently only when navigating obstacles, yet the components can easily run continuously under these conditions. The package size of these components (Figure 9) is well within the width constraints of a plug valve for a 16-inch pipe which limits max width to 5.25 inches.

The design specifications for the wheel drive are as follows:

Peak power required = .25 hp (Motor rated at .48 hp)
*Peak torque required at wheel = 839 in*lb (Reducer rated at 1478 in*lb peak)*
*Steady state torque required at wheel = 398 in*lb (Reducer rated at 593 in*lb cont.)*

Wheel Steering Drive

Given the triangular triad geometry, wheel clamping loads are not the same for all three wheels. The clamping force on the middle wheel is actually the sum of the clamping forces on the two outside wheels. The wheel steering drive has been selected based upon the "middle wheel" clamping force that results when only three wheels must drive the RoboScan. Given that the middle wheel endures twice the clamping load of the outside wheels it will always require twice the torque to steer. This worst case design case conservatively assumes steering actuation without forward movement under peak drive load conditions (vertical climb). The required steering torque will be much lower under conditions when the wheel is rolling.

Since the wheel steering duty cycle is relatively small as compared to the other control axis, it was decided that a cycle time of 10 seconds (1.5 rpm) to turn 90° was reasonable. This reduced the power requirements and facilitated a smaller motor package. The resulting wheel steering drive design consists of a worm and gear coupled to a compact gear motor through a set of spur gears. Overall reduction from motor shaft to steering pivot shaft is approximately 44000:1. The wheel pivot shaft is supported by a pair of tapered roller bearings. Figure 10 (Appendix F) illustrates the steering drive design and identifies the primary components.

Design specifications for the steering drive are as follows:

*Required peak steering torque = 280 in*lb.*
*Worm and Gear rated at 360 in*lb continuous.*
*Worm input requires 7 in*lb peak, spur gears rated at 41 in*lb continuous.*
Motor rated at 18 W, required peak power = 5 W
Bearing rated at 1600 lb static axial load, worst case axial load = 932 lb.

Wheel Clamping Actuator

The wheel clamping actuator mechanism consists of a machine screw jack type actuator that is driven by a gear motor which is coupled to the screw through a set of spur gears. A machine screw form was chosen in order to prevent back-driving so as to minimize power consumption. The design case used for sizing the components of the wheel clamping drive mechanism is conservative. It is based on the worst case wheel clamping force that is required under peak driving conditions (vertical climb) while the four bar linkage in the position with the least mechanical advantage (roughly a 2:1 mechanical disadvantage).

Actuator speed is based on the ability to responds to a single pipe diameter reduction (assuming 1D transition length) at one half of normal inspection speed. Figure 11 (Appendix F) illustrates the clamping drive design and identifies the main components that have been selected. Design specifications for the wheel clamping drive are as follows:

Screw form: Grade 5 lubricated 5/16-18 UNC
- *Can torque to 130 in-lb for an 80% of yield strength condition.*
- *Required torque = 38 in*lb*
- *Required load = 800 lb, buckling load at max extension = 10,000 lb.*

Bearing Set: Same as wheel steering pivot for commonality (tapered roller type)
- *Bearing rated at 1600 lb static axial load*
- *worst case axial load = 800 lb*

*Spur Gears: Rated at 59 in*lb, 38 in*lb required*
Motor: Rated at 70 W, predicted peak power = 57 W

A fully assembled triad showing the relationship of the wheel drive, wheel steering, and clamping system is detailed in Figure 12 (appendix F).

2.4 Fiber Optic Spooler

2.4.1 Fiber Optic Tether Analysis

An overview of the optical fiber industry, along with preliminary calculations and lab tests were performed in this task to:

- Gain an understanding of the forces and stresses imposed on a fiber optic tether when wound within the winder module and exposed to a pressurized gas environment.
- Assess commercially available fibers in terms of robustness and signal transmission performance while operating in the pressurized gas environment.
- Provide estimates of the limits of operation for commercially available fiber optic tethers based on the preliminary analysis.
- Provide recommendations for Phase II development.

Fiber Optic Tether Characteristics

An investigation of the strength and critical characteristics of optic fiber for use as a tether for the RoboScan platform is explored here. Size constraints on the original Pipe Mouse robot required the use of bare optical fiber to spool a sufficient tether length. The larger dimensions of the RoboScan robot for 18 inch pipelines make the use of jacketed fiber more feasible in spite of the requirement to negotiate the reduced port size of plug valves.

The strength of optical fiber is a subject of ongoing research. Pristine fiber strength (High Strength Mode) is determined by the theoretical strength of the glass.[1] However, a surface defect caused by factors such as abrasion or foreign particles on the surface may drastically lower the fiber strength (Low Strength Mode). The probability of failure relative to applied stress for 1 km lengths of fiber is illustrated in Figure 13. While such surface defects are rare, as the fiber length increases the probability of their occurrence becomes significant.

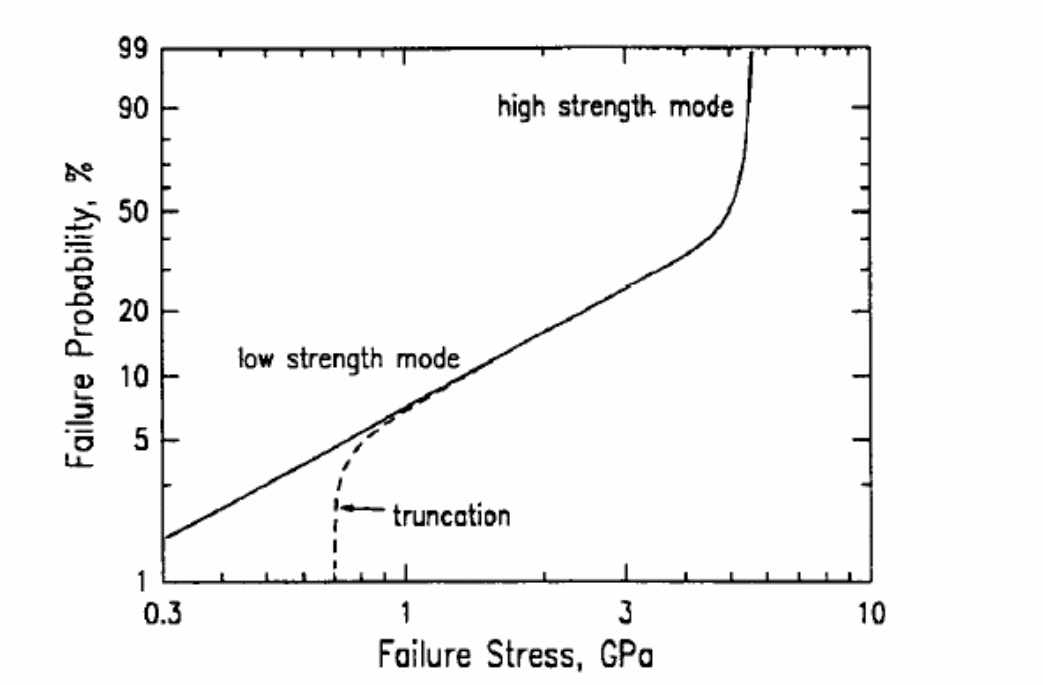

Figure 13. From Reference 1, Typical Weibull plot for ~1 km lengths of fiber.

Crack growth in optical fibers under stress is known to be accelerated by species in the environment, particularly water. The current practice of most manufacturers is to provide a proof test for optical fibers, generally at a 100 kpsi (0.689 GPa) stress level. This is designed to eliminate any weakened sections of fiber. For long-term installations, models indicate that stress levels of 1/4 to 1/2 of proof strength are acceptable. Most sections of fiber will withstand much

[1] M. John Matthewson, "Optical Fiber Reliability Models", SPIE **Critical Reviews of Optical Science: Fiber Optics Reliability and Testing**, CR50, 1994.

higher stresses with an inert strength on the order of 580 to 860 kpsi (4 to 6 GPa). For example, the typical stresses required when mechanically stripping the polymer coating off a fiber to make a splice is 290 to 430 kpsi (2 to 3 GPa). To obtain higher cable strengths, strength layers such a fiberglass or Kevlar are added to the cabling as shown in Figure 14. The strength element must have a lower stretch than the optical fiber to provide protection. As a point of reference, electrical wiring typically relies on the inherent strength of the conductors and the insulation provides little additional strength.

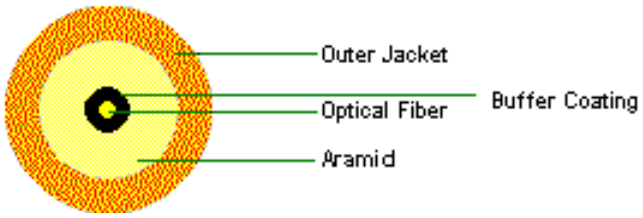

Figure 14. Cable cross-section showing Aramid strength element and tight buffer around the optical fiber

Both optical fiber and electrical cable will be subject to signal degradation caused by cable motion. Motion causes time varying changes in bending losses in optical fiber, which will contribute to the noise level of the signal transmission (attenuation). There are two types of optical fiber in common use for communications applications, multi-mode and single mode. These bending losses will be much larger in multimode optical fiber. Using single mode optical fiber will minimize the bending losses and preserve signal integrity, and is the choice for the RoboScan system.

Tether Evaluation

The following steps were taken during the tether analysis process and are discussed in the following sections:

- Obtained samples of commercially available fiber for evaluation.
- Performed analysis of fluid dynamics to characterized forces
- Performed simple lab flow tests to verify calculations and characterization tether oscillation events.
- Identified bend-insensitive fiber (Stocker-Yale) that was more amenable to tight winding requirements of winder module.
- Performed attenuation tests under wound condition and while oscillating in most extreme situation.

A variety of commercially available fibers were tested (listed in Appendix B). The majority of these fibers are intended for the wiring of communication systems within buildings, and cannot sustain a radius of bend less than 2 inches or an application (such as RoboScan) that requires multiple miles of fiber wound on a mandrel without undue signal attenuation. There was only one fiber identified that could achieve the requirements of this system. Produced by Stocker Yale of Salem, NH, the fiber can survive bends down to 0.75 inches and can be packaged in the

winder module with minimal signal loss (results presented below). A review of commercially available coatings revealed that a Hytrel/Aramid jacket would provide the best strength and abrasion resistance properties. Tether wall friction values were calculated based on a Hytrel/Aramid jacket (see Friction Coefficient Determination section below). While the tether tension tests were performed on all the initial fiber candidates (listed in Appendix B), it was decided prior to the mitered corner tests that the Stocker Yale fiber 0.9mm with Hytrel/Aramid jacket was the only viable candidate for Phase II development.

The choice of tether sizes for testing was based on packaging considerations for the RoboScan platform (see Table 3, Appendix F). The capacities (miles) listed in Table 3 are dictated by the length and diameter of the module (determined from the Module Volume Analysis) and the diameter of the mandrel core. A core size of 2.5 inches was chosen for the 16 to 20 inch platform that this study was based on. The mission length of the smaller sizes can be increased by going with a smaller mandrel core diameter, or with a fiber smaller than those listed. One caveat to using a smaller fiber diameter is the fact that the influence of flow drag (vs. friction drag of tether) increases as tether diameter decreases, thus limiting the flow regimes the system can operate in. The Stocker-Yale fiber can theoretically handle a 1 inch bend radius, but testing would be required to verify that attenuation was not beyond acceptable thresholds. It should be noted that the mission length would increase approximately 3 times if there were no plug valves to contend with.

Analysis Approach

An analysis of the fluid dynamics of the tether (of various diameters) under the minimum, nominal, and maximum pipeline gas flow conditions was conducted. Single mode fibers of 0.2, 0.9, 1.2, 1.8, and 2.9 mm were evaluated. Lab tests were performed to identify any unusual dynamics in the tether when routed through a scaled section of pipeline (including bends and straight sections). Communication tests were conducted to measure the signal degradation of each tether fiber when exposed to the worst case pipeline flutter situation which occurs when the tether crosses the flow stream between two back-back bends. A second tether communication test, representing the worst case scenario of a tether under a tensile load (flow induced) being pulled over a mitered corner was conducted. A varying tensile load was introduced (externally applied under no-flow conditions), with signal loss recorded for each load.

Gas flow through a pipeline is governed by the standard pipe flow equations. Shear stress at the wall (τ_w) is correlated with the flow parameters using the friction factor f defined as $f= 2\ \tau_w/\rho V2$ or $\tau_w = f\ \rho V^2/2$. Values of f are determined experimentally as a function of pipe Reynolds number ($\rho VD/\mu$) and pipe roughness. The tether will primarily lie along the bottom of the pipe and will be subjected to the same fluid shear stress as the fluid-pipe wall interface. Fluid drag force along the tether may be stated as drag / length = $\pi\ \tau_w\ d$, where d is equal to the diameter of the tether. The crux of the analysis was the assertion that for tensile stress to occur in the tether, the flow drag must be greater than the frictional drag (friction coefficient times weight) of the tether. The affect of stresses induced by oscillation of the tether were determined empirically.

The conditions chosen for investigation of the fluid dynamic effects on the tether in a gas pipeline were Methane at T = 77 °F and a viscosity of 2.3 x 10^{-7} lb_f sec/ft^2 in a pipe diameter of 18inches. The three flow conditions as stated in the design requirements and used to evaluate tether performance along with the important flow properties at each condition are summarized in Table 4.

Table 4. Pipeline flow conditions

Flow Rate	Velocity (ft/sec)	Pressure (psig)	Density (ρ) (slugs / ft^3)	Pipe Reynolds	$\rho V^2/2$ ($lb_f/ft^{2)}$	τ_w (lb_f/ft^2)
Nominal	20	350	0.0316	4.1 x 10^6	6.32	0.0221
Max	75	1000	0.0878	42.9 x 10^6	247	0.864
Min	10	250	0.0229	1.5 x 10^6	1.15	0.0040

Determination of Friction Coefficient

A friction coefficient for the Hytrel/Aramid jacketed fiber against the steel pipe was required to calculate the tether wall friction (weight of tether times friction coefficient). The test setup for measuring the friction coefficient is shown in Figure 15. The friction coefficient tests were conducted by looping a section of the Hytrel/Aramid jacketed fiber though 180 degrees of 16 inch steel pipe (same pipe as used in mockup tests), and securing each end of the tether to a plastic cup for accepting weights. Clearance holes were cut in the table under each end of the pipe to allow the tether to pass through freely. A series of measurements were made to determine a coefficient of sliding friction by filling one of the cups with a predetermined amount of weight (W_1), and then adding weight to the other cup (W_2) until sliding occurred. The coefficient of sliding friction was equal to W_1 / W_2. The results are shown below in Table 5.

Figure 15. Friction coefficient test setup

Table 5. Coefficient of sliding friction

W1 (grams)	W2 (grams)	μ
14.8	38.7	0.382
27.5	71.8	0.383
40.1	104.9	0.382
53.1	141.2	0.376
65.3	179.4	0.364
76.8	210.9	0.364

A somewhat conservative value of 0.37 was chosen, and is reflected in the revised tether flow drag results of Table 6. Table 7 presents the critical values for $\rho V^2/2$ where flow drag and friction drag are equal. Foster-Miller recommends that a given tether diameter be used under pipeline conditions only if the tether wall friction is greater than the flow drag (until pipeline tests can be performed in later phases of development).

Analytical Results for Flow Drag

Appendix F

Table 6. Flow drag results (Appendix F)

Table 7. Critical Values for $\rho V^2/2$ Where Tether Wall Friction is Equal to Fluid Drag (Appendix F)

Drag Verification Tests

Simple experiments were conducted to verify the analytical flow drag results and to better understand how the tether behaves under flow conditions and varying pipeline geometry. A short section of 2" Plexiglas pipe (6 feet in length) was connected to a 175 cfm blower (see Figure 16). Sufficient $\rho V^2/2$ was produced with air under atmospheric conditions to duplicate the nominal case of 20 ft/sec and 350 psig. The analysis was verified, demonstrating that the resulting drag force on the tether under these flow conditions was smaller than the retarding friction force, thus the tether remained on the bottom of the pipe.

Figure 16 Tether test setup

A higher capacity blower, shown in Figure 17, was procured and installed in series with the original blower, increasing the air flow to achieve $\rho V^2/2 = 20$ lb_f/ft^2. This setup produced flow conditions beyond that of the nominal case, but well short of the maximum pipeline condition ($\rho V^2/2 = 247$ $lb_f/ft^{2)}$. To go any higher would have required equipment beyond the scope of this Phase I analysis. The lack of higher flow capability proved to be a moot point due to the fact that the critical values for $\rho V^2/2$ (point where potential damage to a fiber could occur) were all under the attainable value of 20 (explained below). The primary reason for increasing the flow to the maximum practically achievable was for simulating tether vibration events in the pipeline to determine if degradation to the tether or signal strength occurred. From these simple tests, we learned that flow drag in straight pipe sections under nominal flow conditions was not a concern, but that situations where the tether enters the flow stream (going around bends) may induce local stresses.

Figure 17 Test setup with increased flow capacity

Tether Oscillation Tests

The tether will lie on the bottom of the pipe except when routed vertically through a bend. In this situation, the tether is exposed to the maximum gas velocity (and higher localized drag) as it crosses the flow. So that the actions of the tether could be observed under these conditions, a section of 2 inch plastic pipeline was assembled that consisted of two 90 degree elbows, with a 3 foot long piece of pipe between them, and a 6 foot section of straight pipe continuing from the second elbow (see Figure 18). This setup was used in both the tether oscillation and tether tension tests (discussed below). It is important to point out that although the 90 degree elbows appear to be swept bends, the inside corner actually comes together at a right angle. This is an important consideration to the tether tension tests (discussed below) which determined the effect of pulling a tether around the most extreme bend (a right angle) while attenuation was being monitored.

Figure 18. Tether routed through elbow of test pipeline (get picture of 2 elbows)

These tests were of short duration (approximately 5 minutes) to determine if the degree (mode) of oscillation was sufficient enough to reduce signal quantity. An endurance test was not necessary as any degradation due to oscillation of the tether under flow conditions would be immediately apparent. The mitered corner abrasion test (discussed below), which will test the tether in a worst case wear environment while oscillating will provide an endurance test for the tether. The tether was routed through the section of pipe. Fiber optic splice connectors were assembled on each end of the tether so that any attenuation in the signal due to potential fiber damage could be quantified. A baseline power loss reading was established using a 1310nm laser source and optical power meter. The maximum flow achievable in the lab was produced, resulting in $\rho V^2/2 = 20\ lb_f/ft^2$. Of concern was the potential for oscillation of the tether when going around the bend (flow turbulence and vortex shedding), adversely affecting signal quantity.

The results for the tether oscillation tests are included in Appendix B. In all cases, oscillation of the tether under these conditions did not contribute to any significant degradation. As would be expected, the smaller and less rigid fiber (0.9mm) exhibited much more movement than the larger (and stiffer) 2.9 mm fiber. Tension played a part in the degree of oscillation. Under low tension, the amplitude of the oscillation is large. As tension is increased (1 to 2 lbs), the amplitude of the oscillation decreased. Note that the low amount of force required to tension the tether is within the range of the winder car payout system, and below the threshold for attenuation increase due to tension discussed in the tension test. It should also be noted that the lengths of fiber exposed to these cross-flow conditions is relatively short and will not contribute much to total drag force (vast majority of tether will sit on bottom of pipe).

Attenuation Tests on Wound Fiber (Appendix F)

Figure 19. Attenuation spectra prior to upjacketing (Appendix F)

Figure 20. Attenuation spectra after upjacketing, 150 mm mandrel (Appendix F)

Table 8. Fiber attenuation (db) as a function of wavelength (Appendix F)

Mitered Corner Abrasion Test

The mitered corner abrasion test was performed to verify the durability and signal performance of the Stocker Yale 0.9mm BIF-1310-L2 bend-insensitive fiber tether (Hytrel/Aramid jacket) while exposed to the maximum laboratory flow conditions ($\rho V^2/2 = 20$ lb_f/ft^2). The mitered elbow was manufactured at Foster-Miller out of 2 inch steel pipe, with the joint left in the "as manufactured" conditions (sharp edges and weld debris maintained). While the earlier test measured the attenuation of the fiber while oscillating in a bend (plastic) over a short period of time to identify losses due to bending modes of the fiber, this test was more of an endurance test which was intended to reveal potential long term effects (fatigue, jacket wear, etc.) in a high-wear situation. A photograph of the mitered corner abrasion test is shown in Figure 21.

Figure 21. Tether abrasion test in mitered corner

In order that we could quantify any attenuation in the signal due to potential fiber damage, fiber optic splice connectors were assemble on each end. A baseline power loss reading of -14 dBm was established using a 1310nm laser source and optical power meter. The goal of the test was to determine if there was any damage to the fiber after 8 hours of exposure to these conditions. An attenuation of -13.6 dBm was observed at the 4 hour point of the test. The post-test attenuation reading was -13.7 dBm. Similar to an earlier test on a non-bend insensitive fiber with the same Hytrel/Aramid jacket, a "flattening" of the tether occurred in the area where it contacted the corner of pipe, but no abrasions or cuts in the jacketing were evident. It can be concluded after this test that the ribbon-like shape that the fiber assumes after oscillating in the mitered corner after 8 hours of testing under flow conditions ($\rho V^2/2$ (lb_f/ft^2) = 20) more adverse than normal conditions ($\rho V^2/2$ (lb_f/ft^2) = 6) does not adversely affect signal quality or tether integrity. The small dBm aberrations in the readings were due to misalignments in the splice connectors between the different sized fibers.

As a first step in determining potential long-term wear issues for the tether, the test was repeated for a 40 hour time period. The test data sheet is included as Appendix B. Baseline fiber dBm source readings were taken at the start of each test day, with subsequent readings recorded hourly. The average source reading did not vary significantly during the test process. Minor fluctuations were seen during the test due to movement of the connectors causing fiber alignment mismatch (normal with untuned fiber connections). Indications are that the optical fiber remained completely intact. The outer jacket of the fiber was worn completely through exposing the buffering aramid fibers which were beginning to fray. The wear area was approximately 1/4 inch long and was limited to the contact area at the sharp interior welded joint intersection of the mitered bend. The picture in Figure 22 (need clearer picture) shows the area of jacket wear and the fraying that occurred in the Aramid. Black marks were intentionally added to mark wear area. The Hytrel jacket is a clear over the Aramid fiber (strength) member. Whether or not the fiber will experience this kind of oscillation around as sharp a joint as was fabricated remains to

be seen. Overall the test results were encouraging due to the fact that the signal did not degrade over the test period. Tasks for Phase II development should include testing of the fiber in full size pipe consisting of commercial components. A parallel search for materials that are more wear-resistant than the hytrel jackets should be conducted.

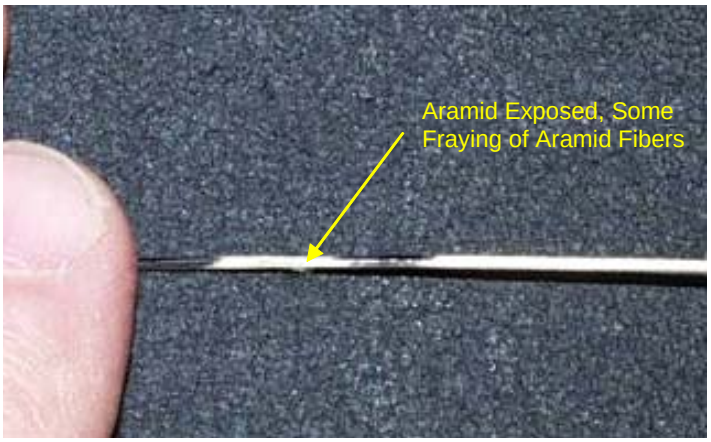

Figure 22. Tether jacket wear after 40 hr mitered corner test

Tether Test Conclusions

Foster-Miller has identified the situation of the tether being pulled tight around a zero degree bend (mitered corner) as the limiting factor when specifying a tether for a particular pipeline flow condition. When exposed to a flow-induced tensile load while spanning a mitered bend, the tether is forced to exceed its minimum bend requirement (introducing macro bend losses) and ultimately experiencing micro bend losses if the loads get high enough, reducing signal loss to unworkable levels and possibly failing the tether. It should be noted here that the tensile load required to break the fiber will probably be 2-3 times that which is experienced by the tether when signal loss occurs. Based on this initial assessment, it appears that signal loss will drive the design of a tether for a given set of pipeline conditions, not the tensile strength of the fiber. One caveat to this assertion is the influence of abrasion (potential for stress risers) on the cable. The glass fiber has a high modulus and is strong in tension, however surface defects caused by abrasion or foreign particles on the surface may drastically lower the fiber strength.

To avoid tensioning the tether across a mitered bend, tether wall friction must be greater than the fluid drag. Both of these values are a function of gas velocity and pressure, and tether diameter. Unfortunately, as a tether gets smaller (as needed in smaller pipes to maximize winder volume) the tether wall friction gain (friction coefficient times weight) reduces by D^2, while the fluid drag on the tether reduces by D (drag force wins out). Thus it is our conservative recommendation at this early point in the program to keep the $\rho V^2/2$ value of the gas flow below the point where tension is introduced into the tether. Of course, the total length of pipe under inspection will determine if a dangerous tensile load is produced. If only short sections (with tensile forces below the dangerous level) are being inspected, then this requirement may be adjusted. The bottom line is that tether tests under actual flow conditions in a test pipeline should be performed in Phase II to verify these initial results.

2.4.2 Fiber Optic Tether Module (Appendix F)

Figure 23. Winder Module - internal mechanisms (Appendix F)

Figure 24. Tether wiper concept (Appendix F)

Tether Winder Module (Appendix F)

Figure 25. Winder Module packaged in housing (Appendix F)

2.5 MFL Sensor Module

The work at PII has concentrated on devising and developing top-level schemes for the sensor module. Concentrating in this phase, on providing a Magnetic Flux Leakage (MFL) based technique, the work has proceeded essentially on four fronts:

1. Design of the deployment/retraction mechanism for the sensor head platform
2. Laboratory measurements to confirm the magnetization levels required to meet inspection requirements
3. Optimization of the size and strength of the magnetizer unit to provide adequate field to meet inspection requirements
4. Integration of the sensor module into the rest of the train.

2.5.1 Design of the deployment/retraction mechanism

The mechanism for deployment and retraction of the inspection platform or sensor head has evolved to its current state as a result of several iterations. The latest design embodiment (Deployment scheme 7) is considered to fulfill the project requirements for deploying and retracting the sensor platform, enabling it to navigate plug valves and mitered bends.

Results of a brain storming exercise and trade off analysis, at the start of the project, identified three concepts for further analysis and development. These were the single axial field magnetizer, the helical scan transverse field magnetizer, and the helical scan axial field magnetizer (figures 26 to 28) identified in the previous conceptual study.

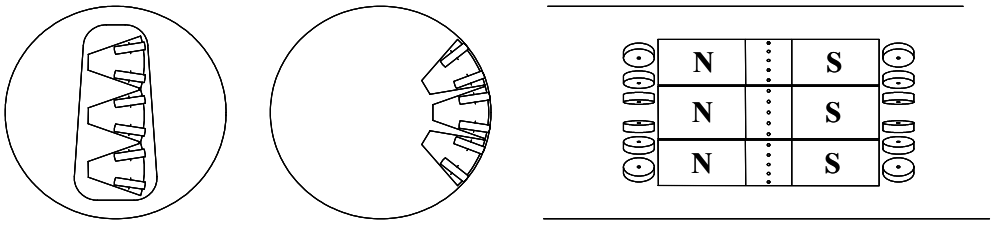

Figure 26. Concept 1, single-hinged sensor, axial field MFL

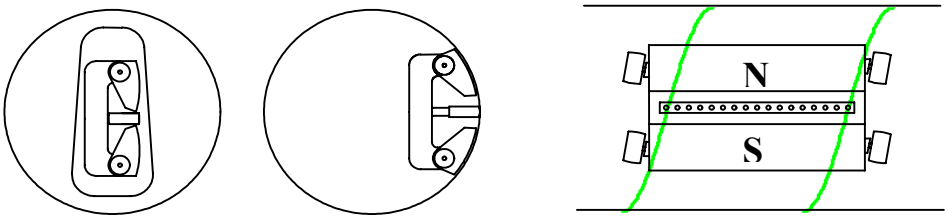

Figure 27. Concept 4, single module, helical scan, transverse field MFL

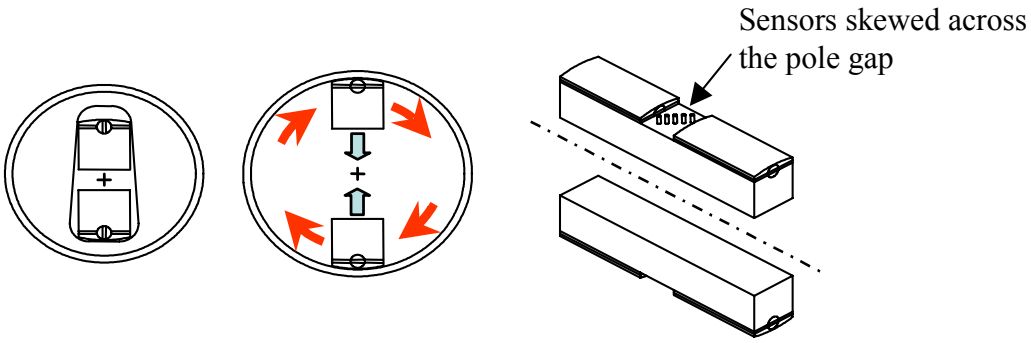

Figure 28: Concept 6, single module, plug-passing, helical sweep, axial field MFL

The essential requirement was that all schemes should be able to navigate plug valves and mitered bends and, for this phase, cover the range 16 to 20-inch. In additional they should be bi-directional. All the schemes would provide partial sensor coverage of the pipe wall. Complete coverage could be achieved with all schemes, but the process of achieving this differed between schemes.

By advancing on a very tight helix, the helical sweep schemes were intended to cover the whole pipe with just one module and one pass. A number of mechanical layouts were produced based on these schemes (Figures 29 and 30).

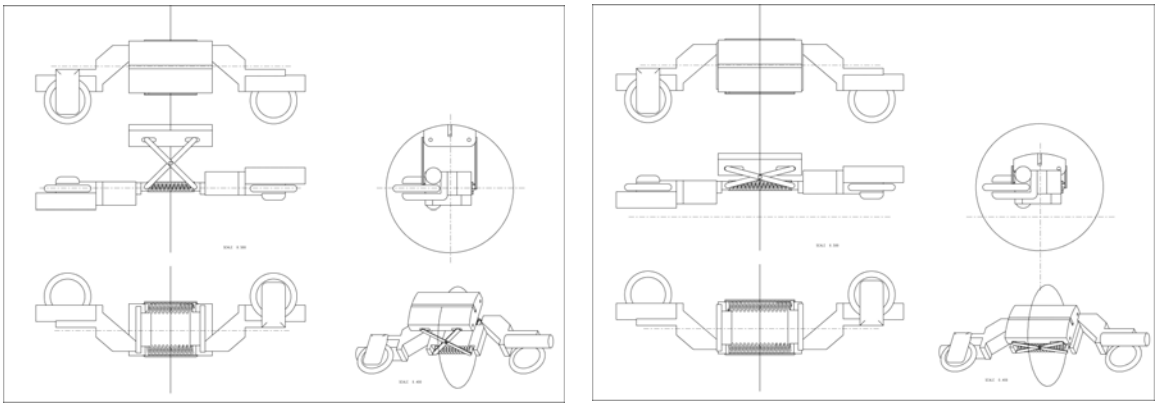

Figure 29. Helical scan, transverse field magnetizer, shown deployed (left) and retracted (right)

The helical scan, axial field magnetizer was schemed up with an "S" spring mechanism (Figure 30). The scheme on the left uses a flexible "S" spring, that on the right a hoop of spring material (the "bear trap" scheme). Two diametrically opposite, out of plane sensor platforms were used. The feasibility of the scheme to traverse plug valves was tested by constructing a simple 2D bench top mock-up (Figure 31). The red blocks represent the magnetizer/sensor platforms. These images show the passage of the magnetizer through the plug valve. It was initially

believed that the lead in/out of the plug valve was tapered, and advantage could be made of this to facilitate the entry of the mechanism. The client subsequently advised that the entrance to the plug valve was not tapered but a flat face.

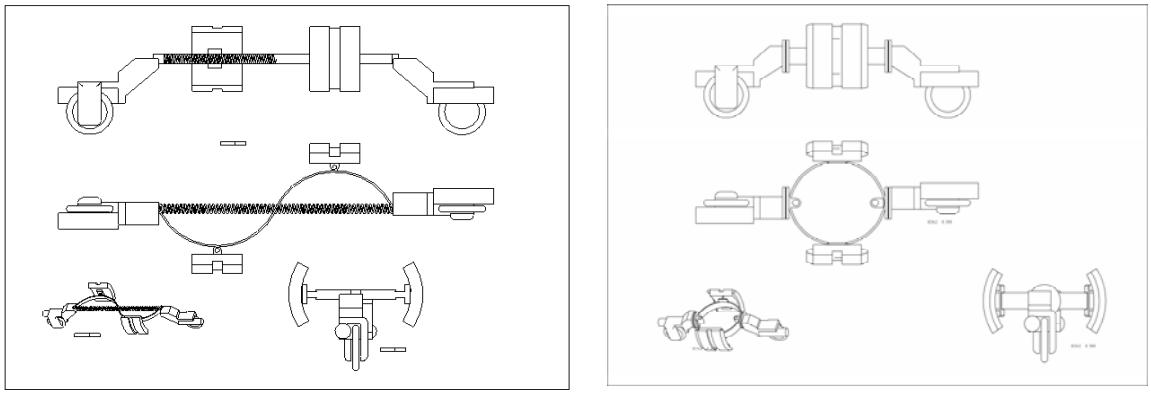

Figure 30. Mechanical schemes for the deployment of a single module, plug-passing, helical sweep, axial field MFL

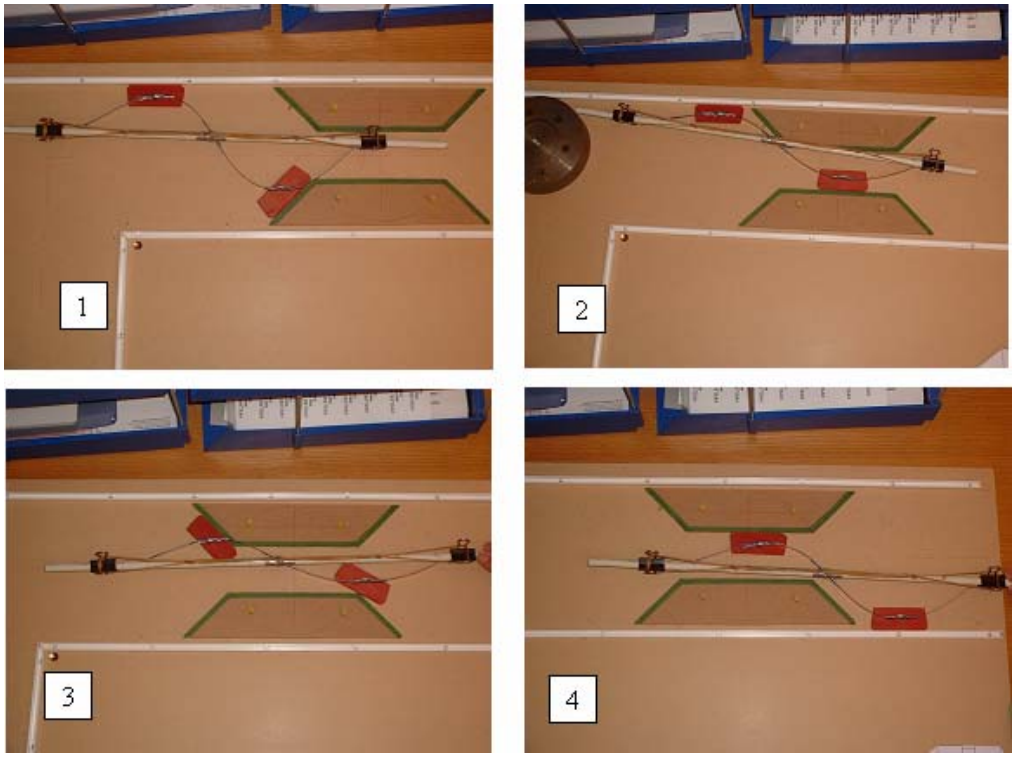

Figure 31. The bench top mock-up of the "S" spring mechanism as it passes through the plug valve

Moreover, additional analysis of all these helical schemes showed that the ratio of the rotational speed to forward speed had to be of the order of between 5 and 10 to 1. On this basis forward

speeds of even 1m/s become unrealistic. Multiple modules, a longer pitch helix and multiple passes would reduce this ratio, however the aligning and stitching of the spiraling data to provide a complete inspection map would be an extremely complex process, and would not display the data in a form compatible with existing MFL data. Effort therefore concentrated on developing ideas based on the single axial field magnetizer.

In its basic form there would be multiple, offset modules in a train. This would have the ability to rotate by some angle θ, so that half of the pipe could be inspected on the outward journey and half on the return. Aligning and merging the two data sets would then generate a full inspection map. This sort of data merge is very similar to what is already performed on the GEPII TranScan data, and considered more readily achievable than for the helical schemes.

Deployment Scheme 1: These initial schemes stuck to the original concept of a single segment magnetizer (see Figure 32). The scheme on the left utilize a solid central bar, off which the magnetizer re-acts for deployment. That on the right uses a central spring, the tension of which thrusts the magnetizer head against the pipe wall. Retraction relies on auxiliary tractor units stretching the spring and pulling the head off the pipe wall.

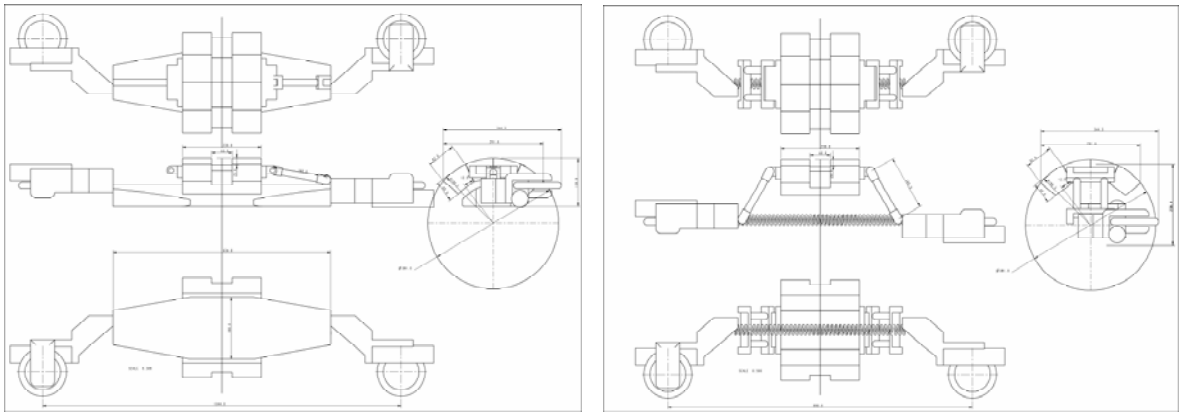

Figure 32. Single segment, plug-passing, axial field magnetizer

There was some concern over the mechanical stability with these schemes. Magnetic modeling had suggested that the magnetic attraction of an MFL sensor head to the pipe wall could run into thousands of Newtons (around 1000lb_f). This, combined with the single sidedness of the concepts, suggested that it may not be possible to generate enough reaction, or that the pull off from the pipe wall would not be smooth. This could cause a shock load, twist or vibration through the rest of the system, which would disturb the positional accuracy of the data collection.

Deployment scheme 2: The hoop spring concept, associated with the helical sweep axial field of Figure 30, appeared to offer a more balanced and stable design. This would inspect two diametrically opposite stripes of the pipe wall, and if the sector arc could be made wide enough, there was the potential for having two modules, offset by 90°, inspecting the line in a single pass, or a single module inspecting in two passes.

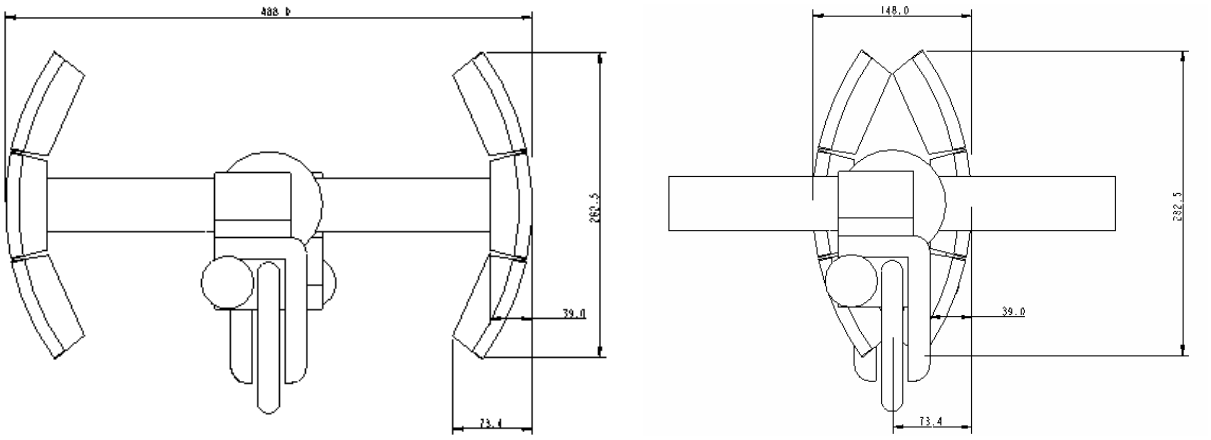

Figure 33. The "bear trap" concept, in the deployed or expanded state (left) for 20" pipe, and the retracted state (right) for plug valve and mitered bend passing.

This scheme was analyzed in greater detail using FEM, hand calculations and bench top mock-ups. Whilst it was clear which way the unit would have to traverse the plug valve it was not initially clear whether there would be a preferred orientation for miter bend passing and whether this would affect the development of the design concept.

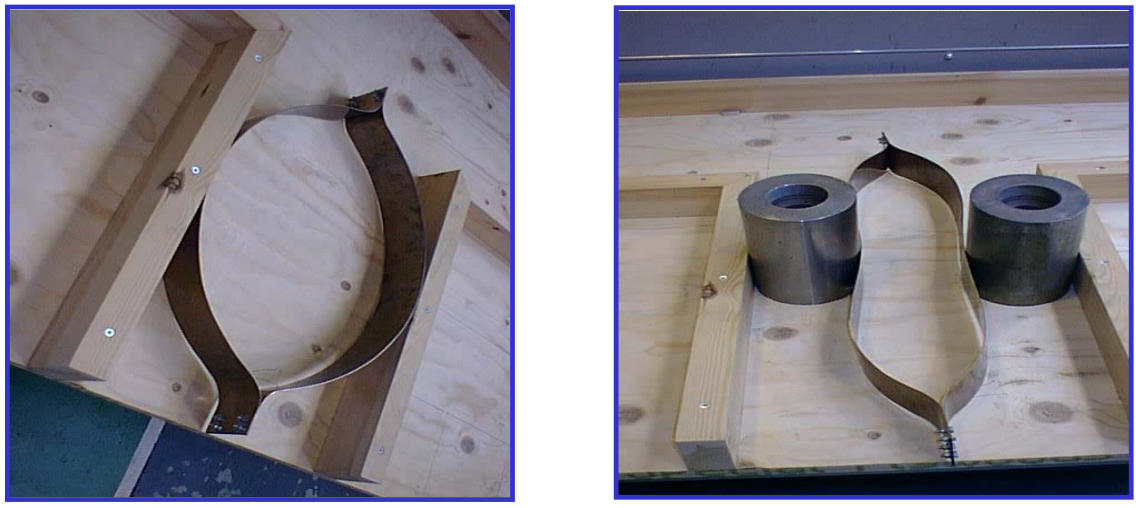

Figure 34. Bench top mock-up with beryllium copper spring material to simulate the "bear trap" concept

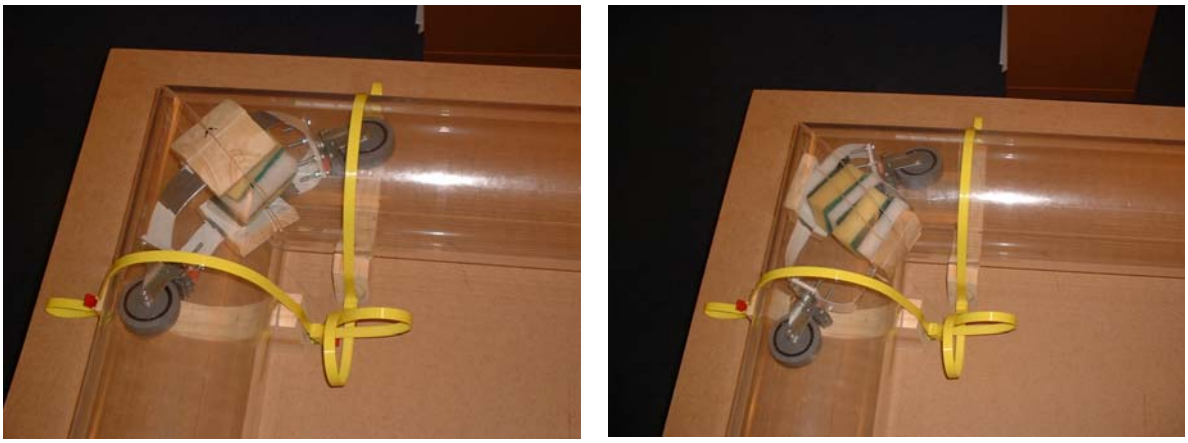

Figure 35. Bench top mock-up in Perspex tube to simulate two orientations for traversing the miter bend

It was clear from the mock-ups that it would be better to traverse the bends with the sensor platform taking the symmetrical track as shown in the left hand image of Figure 35. The alternative would mean the inner platform chafing the sharp corner of the intrados of the bend, possibly resulting in damage to the sensors. In any event, for an MFL based scheme there would be unbalanced attractive forces, being higher at the sharp corner.

Overall, the analysis indicated that the use of a hoop spring resulted in a prohibitive length to permit miter bend passing, and that the forces which could be applied to the spring were not great enough to overcome the magnetic attraction to the pipe wall. However it was believed that if some other mechanism could be devised, the concept of two diametrically opposed magnetizers, or more generally inspection platforms, was the best way forward. The mechanical layout work had broadly identified the space envelope in terms of how small the cross sectional profile should be to allow plug valve passing.

Deployment Scheme 3: (Appendix F)

Figure 36. Scheme3, Passive deployment mechanism (Appendix F)

Figure 37. Scheme3, Passive deployment mechanism retracted for mitered bend and plug valve passing (Appendix F)

Deployment scheme 4: Appendix F.

Figure 38: Scheme4, Deployment mechanism with centralization (Appendix F)

Figure 39. Scheme4, Retracted state of the basic centralizing scheme to allow plug valve passing (Appendix F)

Deployment scheme 5: Appendix F

Figure 40. Scheme5, First generation with active deployment, using a central worm screw drive (Appendix F)

Figure 41. Scheme5, Active deployment scheme for largest diameter inspection (Appendix F)

Figure 42. Scheme5, Active deployment scheme for plug valve passing (Appendix F)

Figure 43. Scheme5, Line drawing of the active deployment scheme in a 16" plug valve (Appendix F)

Figure 44. Scheme5, Active deployment scheme in a 16-inch bend (Appendix F)

Deployment scheme 6: Appendix F

Figure 45. Scheme6, Active deployment with centralization (Appendix F)

Figure 46. Scheme6 in its retracted state for plug valve passing (Appendix F)

Figure 47. Scheme6, in its retracted state (Appendix F)

Figure 48. Scheme6 with one unit deployed and the other retracted (Appendix F)

Deployment scheme 7: Appendix F

Figure 49. Scheme7 shown deployed at its shortest limit for maximum diameter (Appendix F)

Figure 50. Scheme7 at maximum extension to retract the sensor platform and allow plug valve and miter bend passing (Appendix F)

2.5.2 Confirmation of Magnetizer Levels – MFL Sensor Head

Concurrent with the development of the various deployment schemes, theoretical and experimental work was undertaken to address issues associated with an MFL sensor head. Experimentally, confirmation was obtained of the field magnitude for inspection, and also evidence to support the rolling coefficient of friction of the wheel units. 3D finite element modeling allowed optimization of the MFL sensor head in terms of coverage and field for minimum size, whilst allowing a prediction of the magnetic forces, which had to be overcome. The computer simulation also enabled various shunting schemes (the ability to turn off or counter the field so as to reduce magnetic strength/forces) to be modeled. Although this phase has concentrated on producing an MFL solution, the sensor platform could easily be deployed with some other sensor, which may be developed in the future.

Scanner rig work

GEPII qualify the inspection performance of the MFL tool in terms of an x/y specification. The x/y may be 10/20, 20/40 or 30/50, where 10/20 is best. These numbers refer to the ability of the tool to detect and size defects of a particular size. Corrosion defects can be simply graded into isolated pits or general corrosion. The demarcation between the two is when the surface extent exceeds three times the wall thickness (t). When the defect can be contained in a box less than 3t x 3t, it is classed as a pit, and if it exceeds this size it is general corrosion. The x/y notation means that general corrosion greater than x% of wall thickness, and pits greater than y% of wall thickness will be detected. Moreover 80% will be sized to within ±0.01t. The specifications were first defined in the early days of PII and were based on the failure probability curve derived from fracture mechanics. The above description defines a pair of stepped lines above which all defects will be detected. (see Figure 51). In reality the detection capability follows a curve which includes the simple linear definition described above. There is also a minimum width due to the sensor spacing.

The ability to meet a particular specification depends on a number of factors including pipe wall field, sensor pitch and sampling distance. Previous work at PII showed that to achieve reliable and accurate inspection to a 10/20 specification required a minimum pipe wall field of around 35 Oe (2800A/m). This ensured that the pipe wall could be magnetized up to at least the “knee” of the BH curve. Inspection could still be achieved at lower fields, but to a lesser specification. This is due to the pipe wall magnetization being on the maximum gradient of the BH curve, and any variation in magnetic properties or field has a much greater effect on the flux density in the pipe wall. This in effect introduces a source of magnetic noise, and also introduces variability into any defect flux leakage signal.

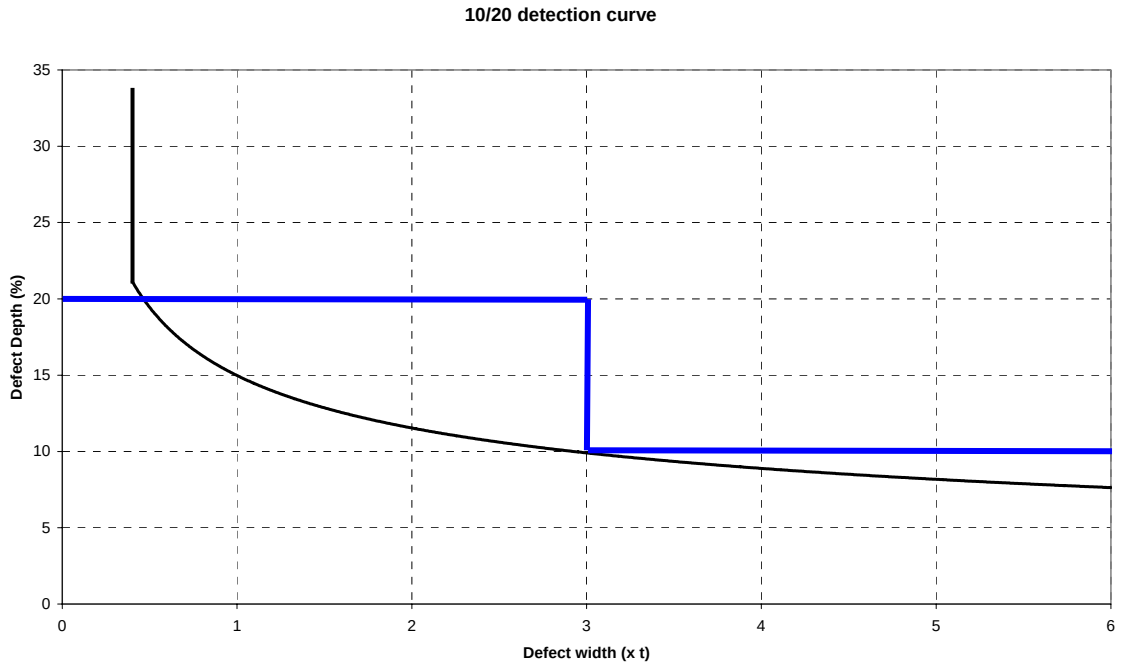

Figure 51. 10/20 detection curve showing the traditional stepped specification (in blue) and the more realistic curve (in black)

Given the space constraints for the unpiggable inspection tool, it was realized that it may not be possible to achieve the 35 Oe level required to meet the 10/20 specification. A number of experiments were performed at the GE Global Research Center (GRC) and at GEPII in Cramlington, to determine what sort of specification could be offered at lower field. In fact there were distinct advantages in running at lower field, even if it meant lowering the inspection performance. In particular, lower fields would mean smaller, lighter magnetizing units, resulting in less drag, less load on support wheels, lighter weight actuators and mechanisms, and less power to activate the mechanisms. In addition any specification would be better than what is currently available.

The work at GRC investigated the effect of field strength on the signal to noise of MFL signals produced by a series of external flat bottomed defects. The field was generated using a mild steel yoke wound with a solenoid coil. Results are shown in Figure 52. The noise is taken to be the standard deviation of the background signal, reliable detectability can be assumed if the signal to noise exceeds 10. The individual defects are expressed in terms of their size, e.g. 4T25 ≡ 25% deep defect, 4x the wall thickness in diameter, 1.5T10 ≡ 10% deep defect, 1.5x the wall thickness in diameter.

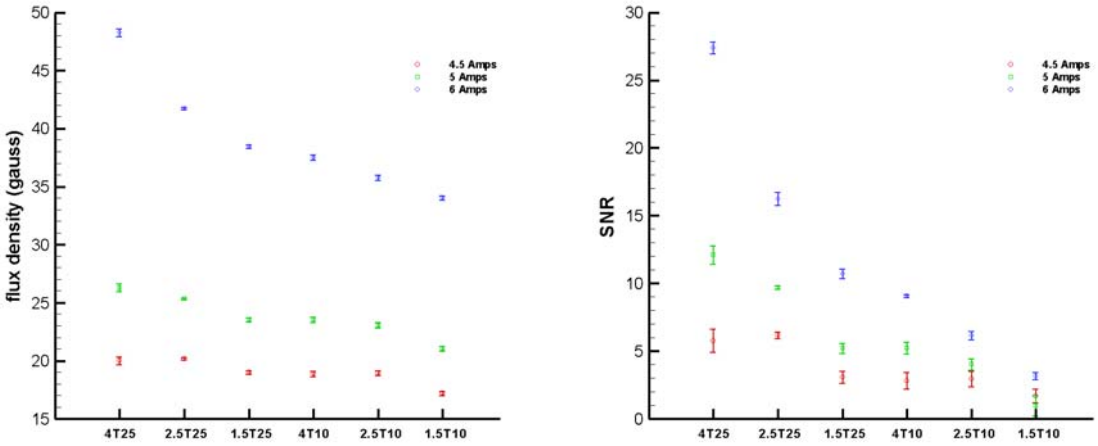

Figure 52. Results of MFL experiments at GE GRC. The graph to the left shows the total MFL signal from the defect, and that on the right the signal to noise for the defect. (A current of 4.5 Amps gives 18 Oe, 5 Amps gives 21 Oe and 6 Amps gives 31 Oe.)

Based on previous GE PII experience, the results indicate a field of at least 20 Oe is required to achieve a 30/50 specification, and at least 25 Oe for 20/40. On this basis the objective of the magnetizer design is to achieve a pipe wall field of at least 20 Oe across the whole sensor arc. Experimental work at Cramlington used a PC to control a three axis scanner bed, and record MFL data from a Hall probe as it traversed over the surface of a magnetized pipe coupon. The field in the coupon could be varied by changing the current through a pair of electromagnets.

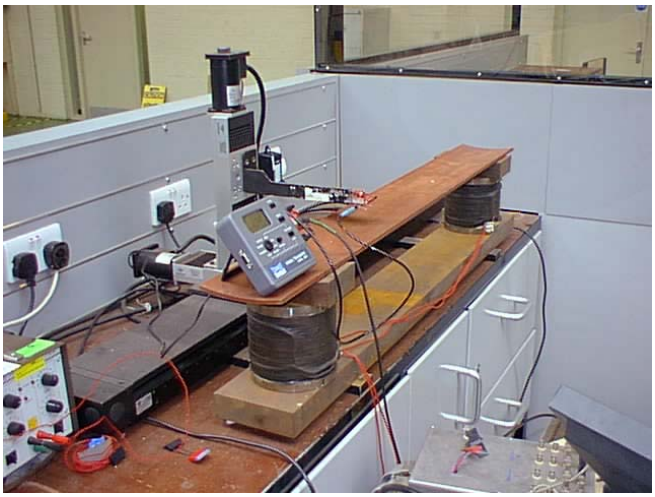

Figure 53. Three axis scanner rig used to collect MFL data at Cramlington

The data was sampled every millimeter along and across the coupon. MFL signals were collected for a far side 50% x 2.7T defect machined with a hemispherical cutter, and a 70% x 1.4T "V"-pit for a range of applied fields. A typical data plot is shown in Figure 54. The noise was

estimated from 500 points (100 points on each of 5 traverses) taken between the two defect signals. The effects of magnetic cycling were also investigated.

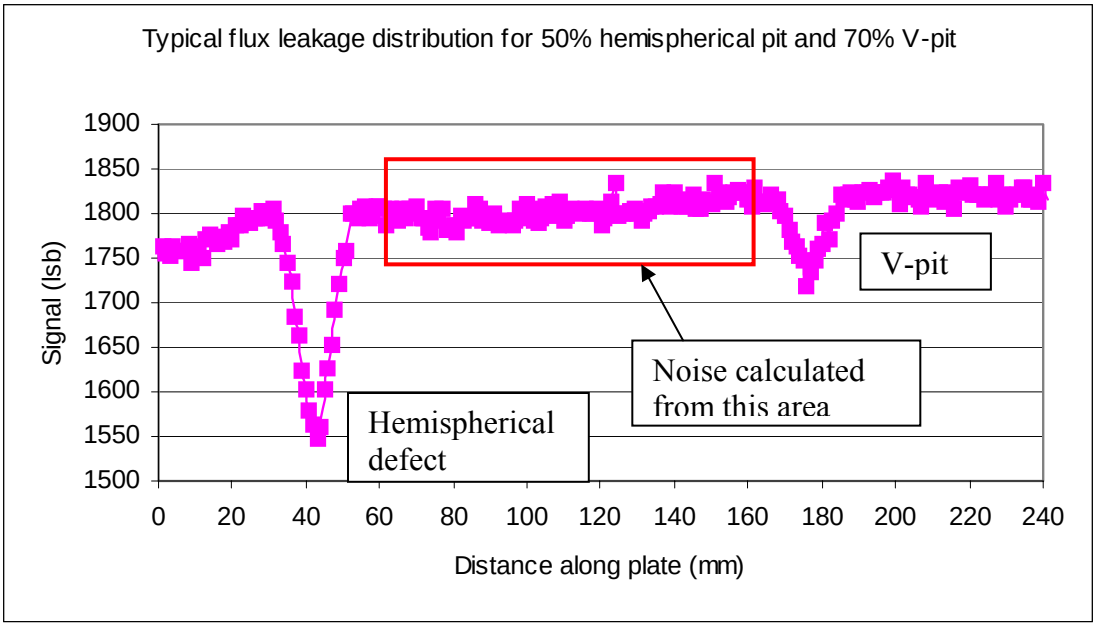

Figure 54. Typical MFL data obtained on the GE PII scanner rig

A wide shallow defect can give an MFL signal with similar amplitude to one which is deeper and narrower. The inspection profile of the V-pit is slightly worse than that of the equivalent 3t defect at 30%, and has a signal to noise of around 8 at 20 Oe. The inspection profile of the hemispherical defect is around 50% greater than that of the equivalent 3t defect at 30%, and has a signal to noise of around 18 at 20 Oe.

PROPRIETARY INFORMATION FOLLOWS – APPENDIX F

Overall the results from Cramlington are consistent with those obtained at GRC, and the design objective is to achieve a pipe wall field of at least 20 Oe, enabling a 30/50 specification to be met.

2.5.3 Magnetizer Design Optimization

The dimension of the plug valve physically constrains the size of the magnetizer unit in the collapsed state. The magnetizer must be able to collapse down and pass through the worst case situation, i.e. minimum aperture in a 16-inch plug valve. This not only defines the limits of the magnetizer but also the cross sectional area of the electronics pressure vessel. This is equivalent to a cylinder with an outer diameter of 5¾ - inches – commensurate with the existing PII 6” electronics package.

With the earlier decision to develop the single, plug passing axial field MFL design, it was clear that it would be impossible to inspect the whole pipe in a single pass. The initial concept was to use two diametrically opposed magnetizer platforms or shells, which are in evidence on the later

deployment schemes. It was assumed that two or more passes would be required to collect all the data. The question was what was the optimum configuration. The solution should generate enough field for reliable inspection, inspect as much pipe in one pass, and provide full coverage from as few modules or passes as possible. More modules mean fewer passes, but increase the train length. Fewer modules reduce the train length but increase the number of passes. It was also realized that if the pipe could be inspected on the outward and return legs of the mission then this would have an important effect on the system design.

PROPRIETARY INFORMATION FOLLOWS – APPENDIX F

Figure 55. Three segment magnetizer shell (Appendix F)

Detailed modeling has confirmed that it will be possible to design and operate a pair of MFL modules which will inspect the whole pipe by collecting data on the outward and return journeys. The drag from two modules will be greater than for a single module. This will have an effect on the battery capacity for the tractors to overcome the additional drag. However, using a pair overcomes the need for multiple passes with a single module.

Force Predictions

A major concern in the design of the MFL sensor platform was with the attractive forces between the magnetizing shells and the pipe wall. The units will be mounted on low friction ball race wheels, and expected to roll readily down the pipe during normal operation. However, during times of retraction for plug valve passing the force to physically pull the inspection shell off the pipe wall is expected to be high.

In addition it was believed there would be high repulsive forces between the shells in the collapsed state as like poles are adjacent to each other. Further FEM simulation was therefore undertaken to determine the magnetic forces as the two shells collapsed inwards. The initial modeling was revisited, to estimate first the maximum clamping force, which had to be overcome, with the magnetizer shells deployed in the inspection position, i.e. with a 2mm lift off. This was estimated from the FE model by integrating the square of the flux density over a surface surrounding the shell, and applying standard formulae (force = $B^2A/2\mu_0$). This gave an estimate for the pull off force of 205kg_f per shell.

The shells were then moved successively inwards from the pipe wall, and the forces re-estimated (see Figure 56). Figure 57 shows the variation in force as a function of shell separation. At 369mm, (maximum separation across the tips), the shells are deployed in inspection mode, whilst at 11mm, (minimum separation between the tips), they are in the retracted state. The graph shows that at minimum separation the resultant force, which is mainly repulsive, is only a fraction of a Newton. This is a lot lower than expected and is believed to be due to most of the flux still being constrained to the return path and exiting through the faces of the pole pieces, rather than leaking around the back of the return path.

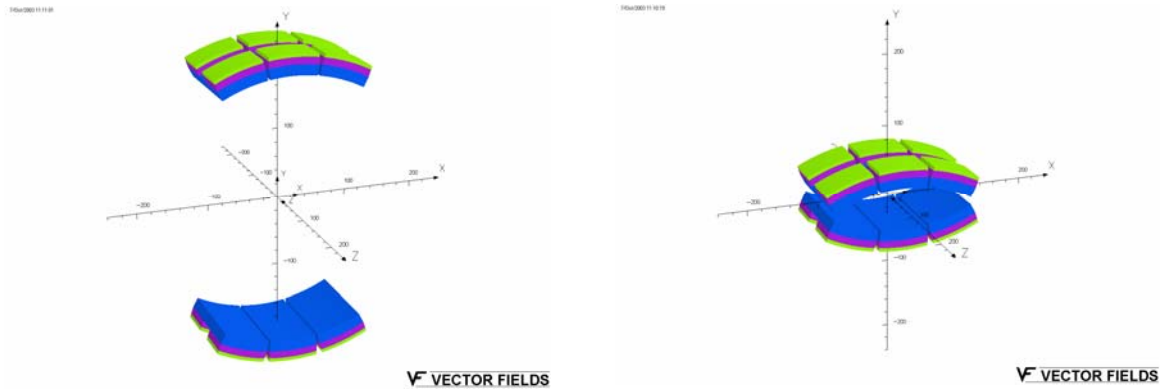

Figure 56. Magnetizer shells in the outer or deployed position (left), and in the retracted position for plug valve and miter bend passing (right). Magnetic forces have been calculated for various stages of deployment.

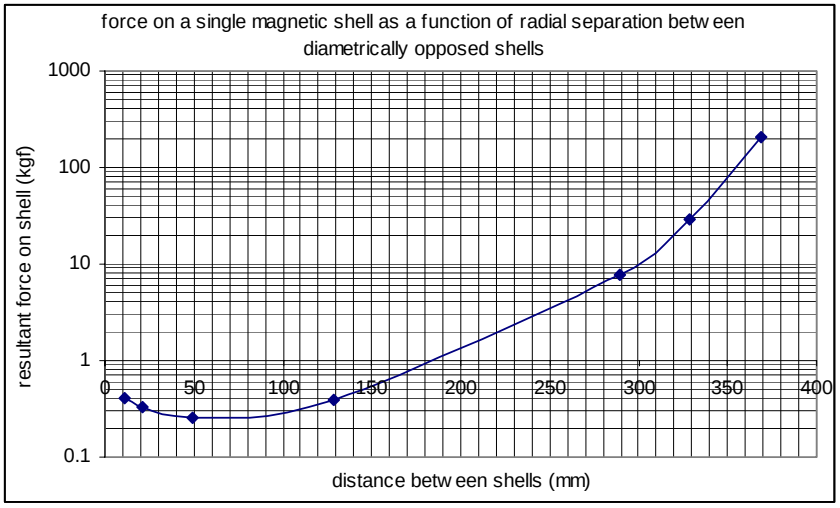

Figure 57. Graph showing the predicted force on a single magnetizer shell as the shells are retracted from the pipe wall.

Although the repulsive forces in the collapsed state have been shown to be small, this is an unstable arrangement and there could still be a significant torque trying to twist one shell with respect to the other. The magnitude of this torque is difficult to estimate theoretically, and will be investigated more fully in a later phase, during prototyping.

Another concern over forces was if the inspection module could not be kept central in the plug valve, or as it rounded the mitered bend. There would then be a distinct probability that it would "grab" to the nearest steel surface. In this situation there is no guarantee that the wheels would provide standoff, and the problem is then one of overcoming the magnetic forces of a metal-to-metal contact, which could be significantly higher than the non-contacting pull-off force

discussed above. To get a feel for these worst-case forces, a number of laboratory experiments were undertaken with a small magnetic trolley.

Magnet Trolley Tests (pull-off force tests)

The magnetic trolley comprised a small permanent magnet assembly mounted off a bridging bar and fitted with a set of wheels. The whole assembly was suspended from the overhead crane as shown in Figure 58. Low friction ball race wheels similar to those used elsewhere by PII were fitted so as to provide an air gap between the pole and pipe wall of around 2mm. The forces required to generate and maintain rolling motion were measured with a spring balance, and the lift off force measured with a peak reading load cell attached to the workshop crane (Figure 59).

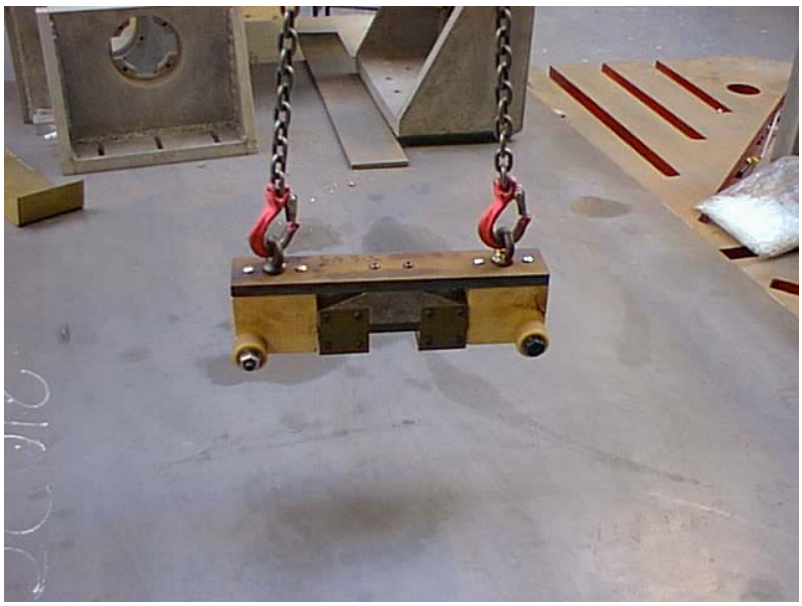

Figure 58. Permanent magnet yoke assembly used in the magnet trolley tests

The mean force required to sustain rolling motion was around 1.25kgf, and for a vertical lift-off, 90kgf. (For confirmation, the flux in the air gap was measured and the magnetic force estimated from $B^2A/2\mu_0$. This gave a magnetic attractive force of 83kgf. With the weight of the trolley at 5.5kgf gives a predicted pull off force of 88.5kgf)). These results equate to a rolling coefficient of friction of 0.014, and falls within the expected band of 0.01 to 0.02 based on previous tests.

Figure 59. Rolling friction tests with the magnetic trolley. The forces for rolling motion and vertical lift off were measured

The wheels were then removed, and the tests repeated to estimate the sliding coefficient of friction for metal to metal contact. In the absence of the air gap provided by the wheels, the device clamped more readily to the pipe. The force required to generate and sustain forward sliding motion increased to 100kgf, whilst that for direct pull-off increased to 230kgf. This corresponds to a sliding coefficient of friction of 0.43, again close to previously observed values.

Using these results, and the predicted non-contact pull-off forces for the magnetizer module allow an estimate of the contacting pull-off force to be made. This comes out at 600kgf, and a metal to metal sliding force of 260kgf, per shell. These values must be doubled to get the value for a module. These forces are considerably higher than for the non-contacting case with wheels, and emphasizes the point that in the event of the magnetizer grabbing to the pipe surface, the forces to free the device or move it are considerable.

PROPRIETARY INFORMATION FOLLOWS - APPENDIX F

Figure 60. (Appendix F)

Figure 61. Appendix F

Figure 62. Appendix F

Figure 63. Appendix F

Figure 64. Appendix F

The GE PII work in this phase has concentrated on developing a practical solution for the inspection module of the robotic system. Inspection and geometrical requirements have been

considered alongside each other, rather than separately, and this has resulted in the top level design of an integrated system.

A number of mechanisms have been explored. These have evolved into a practical design which we believe will allow a sensor platform(s) to be deployed against the pipe wall during times of inspection, and retracted or collapsed for plug valve and miter bend passing. These two extreme features, together with the requirement to navigate and inspect a range of diameters have imposed onerous constraints on the design.

The sensor platform has also been developed. Although the current emphasis has been on MFL, the platform could just as easily be used with any inspection technology which may be developed in the future. Magnetic methods invariably result in strong attractive forces, and the current development has been no exception. By performing experiments to determine the field sensitivity, and to confirm rolling friction, it has been possible to optimize the design to provide inspection to a GE PII 30/50 specification, whilst enabling us to bring those forces under control. By utilizing novel shunting mechanisms it will be possible to reduce the field and attractive power, making it easier to retract the sensor platform from the pipe wall, and also minimize the risk of accidental clamping onto other ferrous surfaces.

The data collection, storage and power modules will utilize current or future GE PII systems, and draw upon 30 years of experience. This includes electronics which can be mounted in pressure vessels or externally in the pressurized environment. The sensing electronics will also be based on current GE PII developments, providing high resolution mapping of the MFL distribution.

The work has provided top level solutions supported by some detail which has increased the confidence of success in going forward into a further phase. There is still a lot of work to be done in providing the detailed design, manufacture and testing of a working prototype system.

2.5.4 Integration Into RoboScan Platform

Figure 64 (Appendix F) details the integration of the MFL inspection sensor system into the RoboScan platform. The system is flanked by a centering mechanism (discussed later in report) and the center electronics module. The centering mechanism elevates the MFL sensor to the pipe centerline. Small rotary actuators on either end of the MFL sensor will be used to orient the sensor to the correct circumferential position. A hydraulic deployment mechanism (linear actuator at center of device) for engaging and disengaging the pipe wall is shown. The reservoir and hydraulic fluid pump will be packaged in the center module. Actuation of the centering, deployment, rotation, and shunting mechanisms will be performed through the RoboScan control system (discussed later in report).

Figure 64-A. Integration of MFL module into RoboScan platform. Appendix F

2.6 Ovality Sensor Module

The feasibility of incorporating a non-contacting pipeline ovality sensor system into the RoboScan platform was explored. At the outset of the study, it was determined that 2 options existed for an ovality sensor, the commercially available industrial single point sensor or the custom designed structured light sensor. The advantages, disadvantages, and issues of each approach are summarized below:

Option 1- industrial single point optical displacement sensor

- Advantages.
  - Minimizes development time and costs.
  - Established calibration procedures.
  - Minimal computer processing/data storage required.
- Disadvantages.
  - Forward speed restriction based on longitudinal resolution requirements.
  - Temperature/shock/vibration specifications must be considered.
- Issues.
    - Restricted to small sensors that fit within minimum package size.
    - Pressure housing must be provided.
    - Challenging mechanical design to incorporate sensor and scan mirror.

Option 2 – Custom designed structured light sensor.

- Advantages.
  - No moving parts.
  - High longitudinal resolution possible.
  - Custom design will adapt to package size constraints.
- Disadvantages.
  - Significant custom design required, therefore higher cost and longer development time.
  - Significant high-speed computer capacity required to process data.

- Issues.
    - Multiple cameras and line sources needed, mechanically configure and construct pressure vessel?
    - Calibration technique must be developed.

Based on information from the NGA member companies, dents greater than 2% of the nominal pipe diameter must be detected for the 12" to 24" pipe range. For the nominal design case of 18 inch pipe (+/- 1 pipe size), this translates to a depth resolution of 0.32 inches for the smallest pipe size of 16 inch. The choice was made to go with commercially available components (over a custom designed structured light sensor) due to the reduced development time and costs, established calibration procedures, and minimal computer processing/data storage required. A disadvantage to this type of system is its susceptibility to temperature, shock and vibration. Other design issues include the need to use small sensors that fit within a minimum package size, the need for pressure housings, and a somewhat challenging mechanical design that must incorporate the sensor and scan mirror.

To minimize development costs and time, a commercial off-the-shelf single point optical displacement sensor will be used as the core of the ovality sensor. A rotating mirror or prism will be used to scan the measurement point around the circumference of the pipe and data will be continuously collected as the robot moves forward. The ovality sensor module will be located in a center section of the robot placed away from the front or rear ends where bright lights for the video camera could interfere with the measurement. The demands on this device are considerable and only a few available sensors will satisfy all the requirements. In summary, the requirements include:

- The sensor must be small enough to fit within the space constraints of the platform.
- The sensor is not designed for high pressures and must therefore be contained in a pressure housing with an optical window for the laser beam.
- All optical triangulation sensors operate over a fixed range, for example the OMRON ZX-LD300 has a particularly wide sensing range from 100 mm to 500 mm (3.94 to 19.68 inches). Therefore, for a 12 to 24 inch pipe diameter range, the sensor must cover a 6 to 12 inch measurement range. Allowing distance for the scanning mechanism of 4 inches, the ZX-LD300 covers a maximum range of 15.68 inches and therefore the ovality sensor, if the ZX-LD300 is selected, must remain within 3 inches of the centerline of the pipe. These values will be tighter with some alternative commercial sensors.
- A high sample rate is required to achieve good coverage of the pipe surface during the 30 ft/minute forward scanning speed.
- Resolution of at least ½ of the required 0.25 inch ovality measurement resolution is required.
- Capability to measure a wide range of surface colors and finishes.
- Either an analog or a digital signal output with maintainable calibration.

The ovality sensor also requires:

- External amplifier for the displacement sensor.
- A/D converter or digital interface for the distance data.

- Driving circuits for the stepper motor with a means to detect a reference position each revolution.
- Computer to control stepper motor position and record the optical displacement, motor angle, time, and robot position in a data file.

A conceptual design for the ovality sensor is shown in Figure 65 (Appendix F).

Proprietary section follows (Appendix F).

Figure 65. Ovality Sensor Module (Appendix F)

2.7 Camera & Lighting

A state-of-the-art review of camera and lighting options for the robotic inspection platform was conducted. The camera system will be used to accomplish two important tasks, robot navigation through pipeline obstacles, and visual inspection of the pipe walls. A wide angle fisheye type lens mounted on a fixed camera was considered for accomplishing both tasks through a less complex system, but was deemed a compromise solution that may be inefficient for both these needs. Sidewall inspection will be limited in terms of the resolution achieved, and the wide-angle lens distortion may affect navigation, particularly as the future system moves towards autonomous control. The option of using a narrower lens with a single axis tilt mechanism (no pan axis) was deemed unacceptable because of the need to rotate the tractor to move the camera along the circumference of the pipe. Battery energy is at a premium, thus we could not justify the tradeoff. We believe that using a camera lens with no more than a 90 degree beam width together with either a pan and tilt or tilt and rotate system will provide effective inspection and navigation without compromise. These systems, even when placed in a suitable pressure housing, can be very compact. Further analysis of the camera options will be conducted in Phase II.

RoboScan vision/lighting requirements are as follows:

- Medium resolution camera fitted to the front and rear of the robot for basic navigation and sight.
- Sufficient lighting for basic navigation
- Higher resolution camera fitted to the robot for visual inspection of the pipe wall. This camera will be outfitted with pan and tilt capabilities.
- Sufficient lighting for detailed pipe wall inspection

For basic navigating, and orientation for obstacle negotiation, a cameral is required at each leading edge of the robot. Since the robot is bi-directional, cameras will be mounted at both ends of the outermost triads. These cameras will be fixed, have a large field of view, and will be used for recognizing upcoming obstacles, as well as spotting visual damage on the wall of the pipe. If a suspect area is identified on the pipe wall, then its approximate location may be recorded, and the robot will continue forward until that area is in the sight of the visual inspection camera located within the ovality sensor module (See Figure 65, Appendix F). This camera will have a

higher resolution than the basic navigational cameras, and will also have tilt and rotate capabilities.

Fixed HID lighting systems will be mounted front and back for the navigational cameras. The visual inspection camera on the ovality module will be fitted with a light ring mounted to the perimeter of the ovality module positioned in such a way as to not interfere with the laser light of the ovality sensor. The proposed camera systems are summarized as follows:

Visual inspection camera:
The visual inspection camera system is based around a compact high resolution color DSP, board level camera manufactured by Edmunds Industrial Optics. This camera reaches a resolution of 480 horizontal lines, which will be suitable for close up inspection of the pipe walls. It will be coupled to a Computar variable focus lens for optimum adjustability. The camera and its immediate electronics will be packaged into a pressure vessel that is mounted on a custom, 2-axis tilt/rotate mechanism.

Basic navigation camera:
The basic navigation camera system uses a Hitachi miniature board level camera and a custom electronic interface. This camera was chosen for its small size due to the space constraints on the triads. This camera is matched to a fixed focus lens by Edmunds Industrial Optics. These components will be packaged into a pressure vessel housing, and fixed onto each of the two outermost triads.

2.8 Battery Power System

System power was first calculated based on the assumptions from the earlier NYGAS study, resulting in a drive force of 2000 lb_f with MFL on, and 1200 lb_f with MFL off. These initial design values were based on the max flow conditions of 75 ft/s and 1000 psig. As mentioned earlier in this report, component selection for the drive systems of the wheel drive, wheel steering, and wheel clamping systems were based on this initial estimate, with the specifications for these components maintained to provide any unforeseen future needs for additional power. It was later decided, based on tether flow drag limitations, that the system will be designed for the nominal conditions of 350 psig and 20 ft/s. Under the nominal conditions, the flow drag forces will be insignificant, except for those infrequent times when passing through plug valve. Power consumption will chiefly be a function of sensor drag and module drag. As discussed below, these initial power estimates were reduced as PII advanced in their conceptual design for the MFL sensor system.

In order that we could better define the platform's power requirements, a template for a typical 2.5 mile mission was established based on NGA member input and the Phase I Needs Assessment, and includes the following attributes:

- (3) plug valves
- (3) back-to-back in-plane 1.5 D 90 degree elbows
- (1) back-to-back out-of-plane 1.5 D 90 degree elbows

- (1) mitered bend (in addition to launch)
- Total elevation change (approx 5 feet per back-back situation): 20 feet

Based on this typical "mission profile", the total energy required to operate the system was established. Initial estimates of power requirements for system power were made without the benefit of knowing how the MFL system would ultimately be designed. Questions about the MFL sensor drag, and the number of sweeps required for the MFL sensor to inspect the full pipe circumference still remained. The initial power assessment for a 2.5 mile mission is illustrated in Figure 66, Appendix F based on a single sensor sweep and a sensor drag of 800 lbs. At this early point in the program, the later accomplishments of PII to reduce significantly reduce sensor drag were not yet realized.

It is clearly demonstrated in the analysis that the sensor, with 800 lbs of drag, demands the majority of the power (65%). A key design criterion for the sensor is the reduction of drag. The estimate of 8 battery modules (Figure 67 Appendix F analysis) was based on an energy density of 2,500 W hr per battery module (which is approximately half-way between the capacities of the two battery module concepts discussed below).

Proprietary Section follows (Appendix F)

Figure 66. Initial power assessment (Appendix F)

Figure 67. Battery module configurations for oval module (Appendix F)

Figure 68. Battery module configurations for round module (Appendix F)

Figure 69. Revised power requirements (Appendix F)

Figure 70. Battery module shown passing through plug valve (Appendix F)

2.9 Location Sonde

An emergency location sonde will be integrated into the system. A low-frequency electromagnetic signal (20HZ) will be emitted and received above ground for emergency location. A potential candidate system, currently used in PII's pigging systems, is shown in Figure 71. The dimensions of the unit are approximately 50 mm (~2 in) O.D. and 235 mm (~9 in) long, and weights approximately 2.5 Kg (~2 lbs). The unit will fit inside the core of the winder spool.

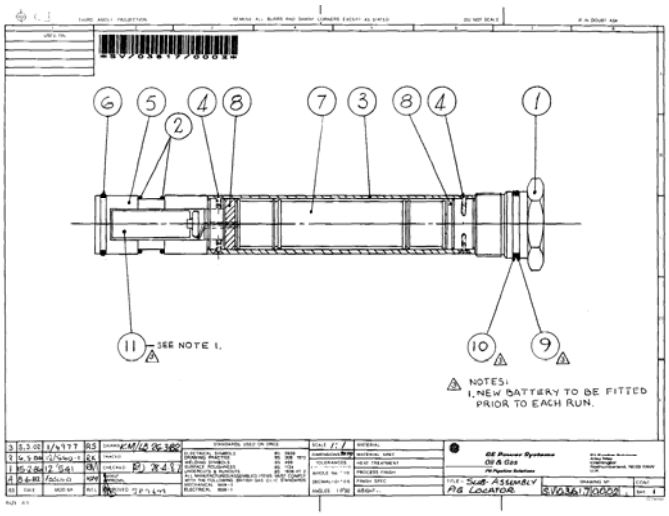

Figure 71: Emergency Location Sonde

2.10 Inter-Module Couplers

The inter-module couplings play a critical role in the RoboScan systems negotiation of the pipeline, keeping the train intact while transferring axial forces (tension and compression) and torsion, and performing supplemental control functions to get the platform through each obstacle. Electrical, sensor, and signal wires must be routed across the modules without risk of damage or impeding coupling function. Throughout the majority of the mission, the front and rear tractors will assume the same orientation in the pipe (typically 12:00 to 6:00) and work together to maintain a constant orientation and a forward inspection speed of 30 ft/min. Bend sensors are integrated into each bend link, and feed back degree of coupling bend so that the tractor drive control system can vary speed between the front and rear tractors to eliminate buckling. For example, if there is more resistance at the front of the train (for instance when entering a vertical climb), the rear tractor will tend to "compress" the train without any bend sensor feedback and cause buckling of the bend couplings. Front and rear tractor speed will be adjusted based on the degree of bend of each coupling in the train to maintain proper coupling orientation while maintaining the 30 ft/sec inspection speed.

In addition to the proper balance of flexibility and stiffness provided by the bend couplings, supplemental control is provided through other inter-module components for lifting the triads into a bend (curl), allowing relative twist between sections of the train (rotation), and lifting and centralization of the MFL modules for proper engagement of the pipe wall (centralization). When traversing obstacles, the front and rear tractors, in conjunction with the inter-module couples, will perform independent sequences of motion to move the train through the various twists and turns of the pipeline. Portions of the inspection platform must be able to twist (and sometimes lock and transmit torque) relative to the other sections of the train. All couplings will use the same bolt pattern for mounting to the RoboScan modules to maintain uniformity of design and facilitate modularity through a simple change-out process. The following types of inter-module couplings are used:

- Bend

- Curl
- Rotation
- Centralization

2.10.1 Bend

A concept for the bend coupling is shown in Figure 72, Appendix F. Modeled similar to a human vertebrae, it consists of a series of spool sections (vertebrae) bolted together with urethane springs that compress and expand in bending. As the coupling bends, the bottom urethane springs will be in compression while the top springs are in tension. The system will accommodate both tension and compression, and will have an integral bend sensor to monitor the degree of bend. Bend sensor output will be used by the control system to prevent buckling and assist (through interaction of front and rear tractor) the locomotion of modules through bends. For a given type of bend (1.5 D or miter) there will be a preferred orientation for moving a module through. The control system will regulate the relative speed between the front and rear triads so that the module moves through the bend in the most efficient manner. The core of the module is hollow to allow wire passing.

Figure 72. Bend coupling concept (Appendix F)

2.10.2 Curl

While the RoboScan must traverse a more complex pipe route than the original pipe mouse (i.e. back-back out-of-plane bends), the kinematics of the original pipe mouse have been maintained. One critical feature is the curling link (Figure 73, Appendix F). The tractor locomotion system (one on each end of the train) consists of 2 triads that work in tandem. When entering a bend, the front triad is oriented such that the front wheel "reaches" into the bend. Once properly aligned, the triad is "lifted" into the bend through torque applied by the curling link. The front triad will momentarily lose traction while being lifted by the curling link and pushed by the trailing triad. The concept shown in Figure 73 (Appendix F) provides torque through a commercially available clock-spring, which can rotate either gear (attachment points to triads) independent of the other.

Curling link torque was based on the following assumptions:

- Triad weight of 50 lb
- 22 inch offset from triad center of gravity to curling link attachment point
- 20 lb wheel preload desired to be induced by the curling link at the leading wheel (41 inch offset)

The resulting torque is approximately 160 ft-lbs ((22*50 + 20*41)/12). This is somewhat conservative in that once the triad makes the corner the CG offset reduces substantially. However, the torque delivered by the curling link also decreases as the spring unwinds (which occurs as the link rotates to help the triad turn the corner). The output of the link was designed for 90 degrees of rotation. At zero degrees of rotation (RoboScan in straight pipe), the resultant torque is 172 ft lb (200 inch spring at 5 turns). At 90 degrees when triad rounds the corner with

the remaining sections of the platform still in straight pipe, the resultant torque is 152 ft lb (200 inch spring at 4 turns). These values can be adjusted quite a bit depending on the number of spring turns required; the upper limit is 200 ft lb (which corresponds to 7 turns). The lower the torque the longer the spring life and the more packaging options available. The concept is drawn to the upper limit and is good for about 6400 bend cycles.

The spring may be locked out during deployment for ease of handling. The feasibility of a passive spring will be verified in Phase II. If the high degree of torque required is an operational liability in terms of ease of insertion into the pipeline, an active link may be incorporated through a motor/gearbox or linear actuator/crank arrangement. One other consideration is the estimated life of 6400 bend cycles. The passive system reduces complexity and size of the curling link, but its feasibility will ultimately be determined in Phase II.

Figure 73. Curling link (Appendix F)

2.10.3 Rotation

Rotation between sections of the RoboScan train and the capability to lock the rotary joint for torque transmission is a system requirement. A concept for such a joint is illustrated in Figure 74 (Appendix F). The rotary joint is designed as a completely sealed unit, and is comprised of two halves that rotate independent of each other on two sets of bearings. The normal state of operation is free rotation. To lock the joint, a miniature linear actuator located inside of the coupling is momentarily powered. The actuator moves a self aligning tapered spline into a spline cup. The spline and the spline cup, once coupled, lock up the joint until the actuator is re-energized, withdrawing the tapered spline from the spline cup.

Figure 74. Locking rotary joint (Appendix F)

2.10.4 Centering Module

The purpose of the centering module is to ensure that the forces exerted through the MFL sensor modules (tension, compression, torsion) by the front and rear tractors are exerted along the centerline of the pipe (Figures 75 and 76 – Appendix F). Maintaining the forces along the centerline of the MFL modules prevents any moments occurring at the attachment point which could cause misalignment of the magnetizer with respect to the pipe wall. The centering module works very similar to a tow truck. It uses a single rotary actuator and gearbox to rotate a ball screw (much like the clamping mechanism on the triads). As the ball screw rotates, it drives an internally threaded shaft (axially) that is pinned to a standard interface coupling plate. A second bar is pinned at that coupling, as well as at the base of the module for support. Driving the ball screw moves the threaded shaft along the ball screw, raising and lowering the coupling plate. A bend coupling is required between adjacent modules. The current design allows for the MFL module attachment plate to pivot about the transverse pin joint. This joint will allow relative

bending between modules for traversing bends, but requires that the plane of bend be oriented to the plane of the bend. This aspect of the design, along with the general approach used here to lift and center the MFL module, will be reevaluated in Phase II.

Figure 75. Centering module (Appendix F)

Figure 76. Centering module supporting MFL module (Appendix F)

2.11 Launch & Retrieval

With the length of the RoboScan platform at approximately 40 feet, the most feasible method for deploying the system is to install it in its launch tube at the pipeline maintenance facility and transport it by truck to the pipeline. Unlike conventional pigs, the RoboScan platform can be launched and retrieved in a variety of positions, facilitating a number of launch scenarios. The configuration of the launch tube and the launch alternatives are discussed below.

Launch Tube Features

The portable launching tube will be designed to withstand the pipeline pressure of the pipeline under test. A ball valve will be installed at the hot-tap saddle arrangement with appropriate flanging to accept the launch tube. The launch tube will be opened on one end (attachment to hot-tap) with a removable cover on the other end through which the tether (platform control and video/sensing data) and supplemental electrical and signal wires are fed through appropriate bulkhead connectors to the base station. These supplemental electrical and signal lines will support battery diagnostics and charging, and access to inspection data.

Two valves will mounted on the flanged cover, one for evacuating the launch tube and the other for pressurizing the tube with an inert gas (possibly nitrogen). The launch tube will also provide connection ports for battery charging and battery diagnostics which will be positioned within the tube to allow for automatic connection either through the motions of the platform (battery module engages a connector) or a mechanism built into the launch tube that connects battery power and signal wires. Whichever method is used (determined in later phases of project) the ability to charge the platform and retrieve data is an important design consideration in terms of reducing operating costs of the system. Another possible alternative for charging the batteries inside the launch tube is through an inductive coupling. A static coil assembly (no mechanism required) would be installed in a predefined positioned inside the pipe. The RoboScan platform would position the batteries adjacent to the static coil assembly where the batteries will be inductively coupled to the coil for charging. The feasibility of this technique, with the additional consideration of transmitting battery diagnostic data through induction, will be determined in later phases of the project.

Candidate Launch Tube Shapes

The simplest shape for the launching tube would be a straight length of tubing. This would be allow the simplest launching operation and result in the lowest weight and least expensive

launching tube. The only drawback is that it would require a fairly long vehicle (about 50 feet) to transport it from location to location. The next simplest shape would be a "U" shaped launching tube, which would reduce its total length to about 25 feet. The radius of the "U" would be at least equal to 1 ½ times the tubing diameter (Figure 77).

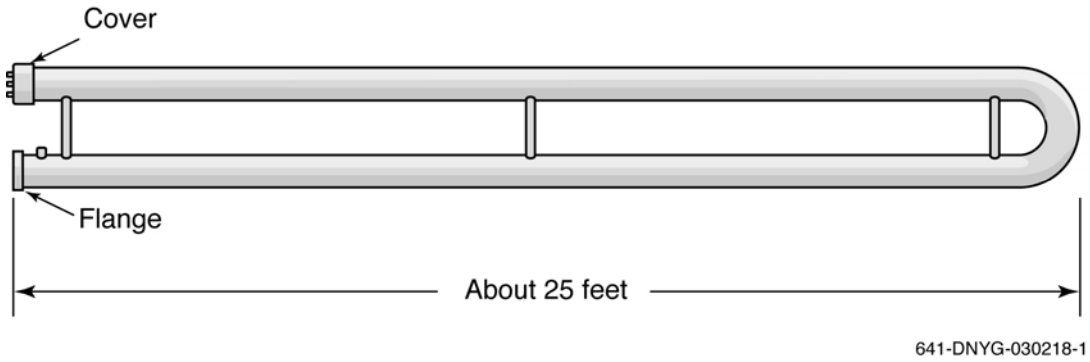

Figure 77. "U" shaped launch tube

A further increase in simplicity and compactness could be realized by fabricating the launch tube with two 180 degree curves, which would reduce the total length to about 17 feet (Figure 78). With three 180 degrees curves it is possible to further reduce the total length to about 12.5 feet, as shown in Figure 79.

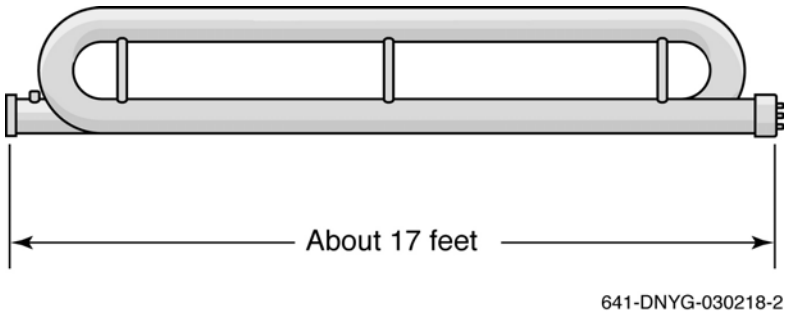

Figure 78. Launch tube with two 180 degrees curves

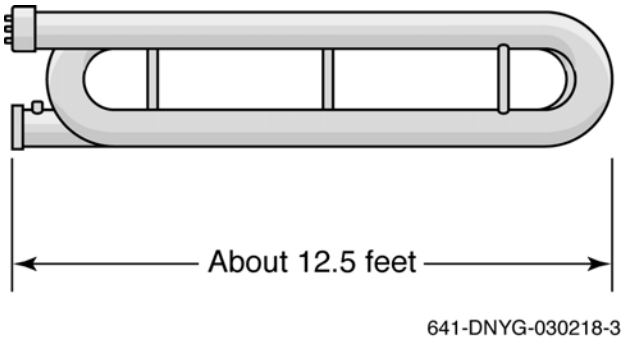

Figure 79. Launch tube with three 180 degrees curves

To save weight and cost, the launch tube should be sized based on the smallest diameter that the RoboScan platform can negotiate. One approach may be to use even smaller diameter than the platform is sized for, but increase the bend radii beyond 1.5 D to allow the modules to pass through unrestricted. The launching tube could be carried on a truck (or trailer) that also carries the purging hardware, chargers and control station. The launching tube would remain on the truck (or trailer) while connected to pipeline (See Figure 80). This would simplify the transportation of the Launching Tube/RoboScan system from one location to the other, as it would not be necessary to load and unload the system on the truck (or trailer), a burdensome operation, every time the system has to be moved.

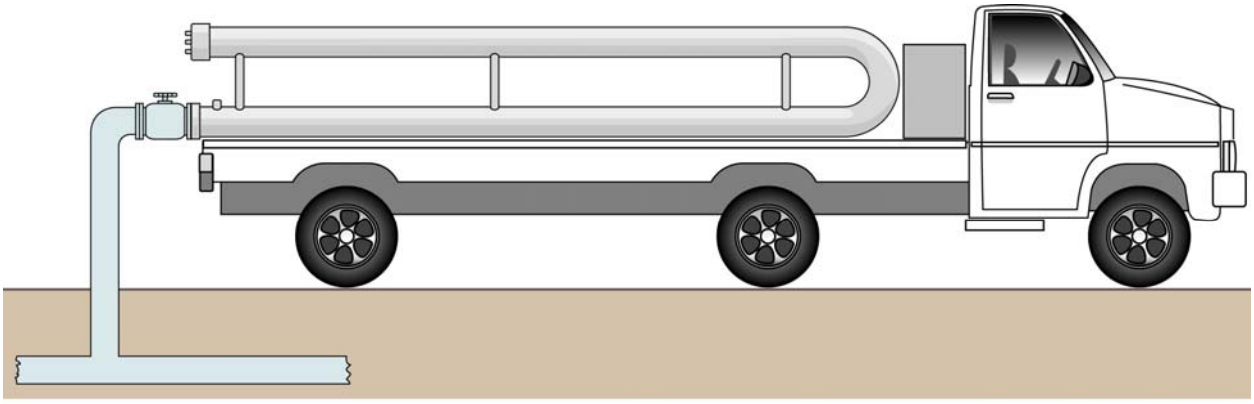

641-DNYG-030218-7

Figure 80. Truck-mounted launch tube

Launching Position

Since the RoboScan platform must be able to travel in both directions of the pipeline, a 90 degree entrance must be provided on the pipeline. A possible arrangement is shown in Figure 81. With this connection method, the launch tube is in the horizontal position, providing for simpler installation and handling vs. the vertical connection method shown in Figure 82.

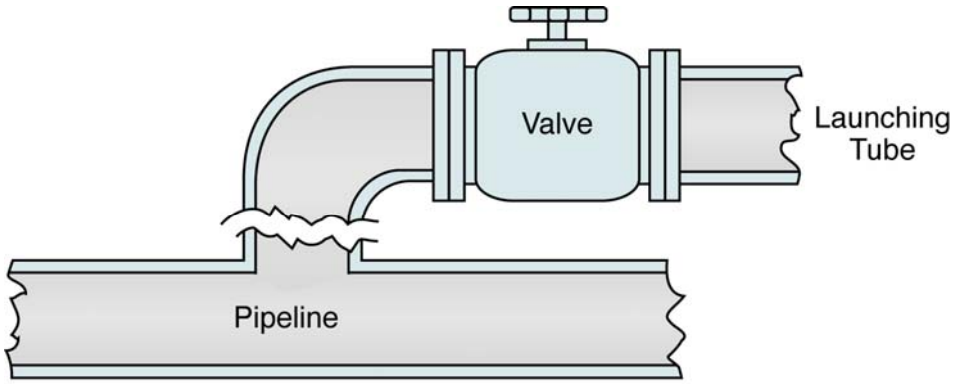

641-DNYG-030218-6

Figure 81. Pipeline entrance for travel in both directions

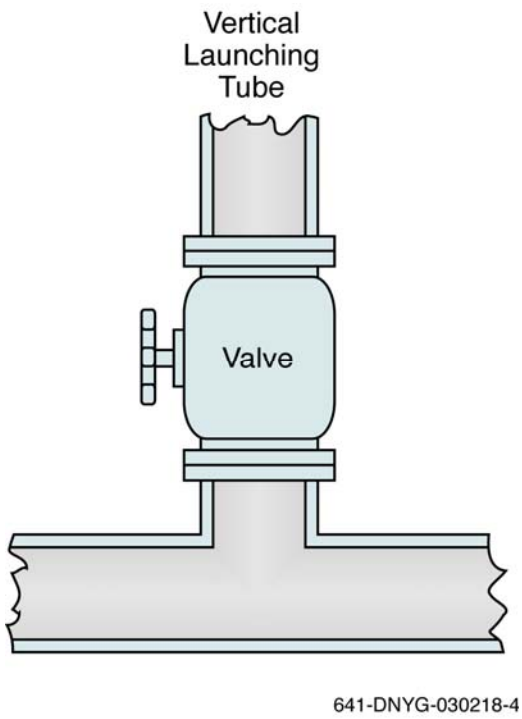

Figure 82. Pipeline entrance with launching tube positioned vertically

The proposed sequence of operations for launching is as follows:

- RoboScan platform, with its batteries charged, is placed in the launching tube.
- Launch tube is attached to the flange of ball valve on hot-tap saddle.
- Cover is bolted to far side of launch tube and all connections for power and signal wires secured.
- Evacuation valve is opened.
- An inert gas (possibly nitrogen) is pumped into launch tube through inlet valve mounted on flange. As the inert gas enters the tube, air is expelled through air evacuation valve.
- After all air has been purged, inert gas input and air evacuation valves are closed.
- Ball valve on hot-tap saddle is opened partially, to introduce the gas under pressure in the launching tube.

- After the gas pressure in the launch tube has stabilized, the ball valve on hot-tap saddle is opened fully and the RoboScan unit is driven into the pipeline.

- Once the RoboScan platform completes the first leg of its mission (for this study a length of 2.5 miles), the unit will return to the launch tube and recharge batteries (and download inspection data if desired).

- Once the batteries are charged, the platform will renter the pipe to inspect the second 2.5 mile leg of the pipeline.

- Upon completion of the mission, and the RoboScan platform is driven back into the launch tube, the hot-tap saddle valve is closed.

- A purging sequence is then initiated whereby the natural gas is vented from the pipeline and replaced with nitrogen. Specific details of this operation, including the nitrogen purge time required to fully out-gas all the natural gas, will be determined in later phases of the project.

2.12 Electrical & Control Subsystems

The RoboScan platform's electrical and controls system architectures may be divided into three primary components consisting of the Base Station, which is located above ground in the vicinity of the launch tube (possibly placed in adjacent truck or trailer), the RoboScan platform which is "resident" within the pipeline, and the Fiber Optic Communications system which allows the Base Station and RoboScan to communicate. Refer to Appendix D for a listing of the RoboScan's control sensors and Appendix E for the Power Interface Drawings. The control system block diagram is shown in Figure 83.

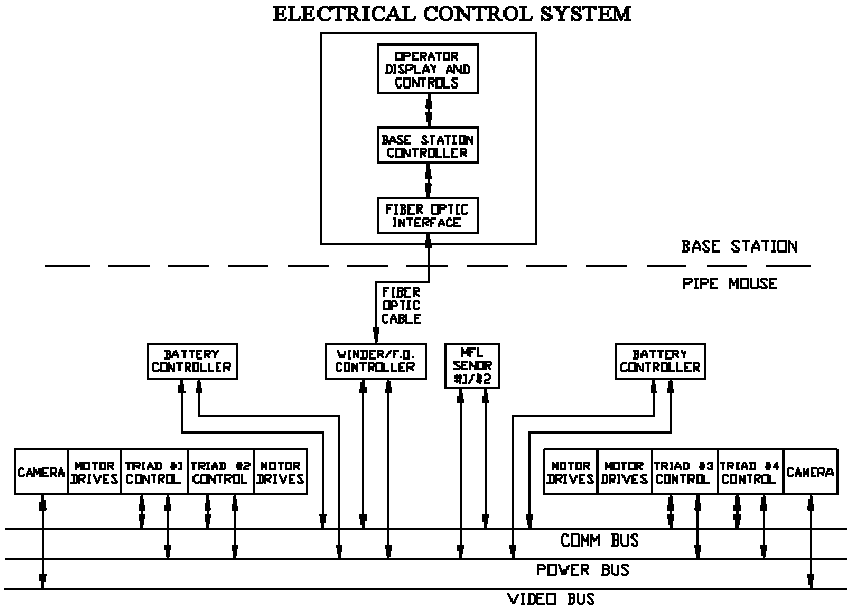

Figure 83. Control System block diagram

Base station

The Base Station will consist of the following subsystems:

1) User interface
2) Base Station Computer

The base station user interface will have a monitor for real time video feed from the RoboScan platform which will provide the operator with video for navigation, and a higher resolution image from the visual inspection for inspecting suspect areas (the data from the MFL sensors will be stored for later retrieval and processing). Initially, the system will be designed around a semi-autonomous philosophy where an operator will control the robot when traveling in straight pipe (vast majority of mission), and rely on autonomous control functions to take over control and get the platform through the pipeline obstacles. When an obstacle is encountered, the user will align the RoboScan in the proper orientation and input the appropriate operational mode whereby the system will automatically negotiate through the obstacle. The following control functions will be preprogrammed and available for the operator to initiate:

1) Plug valves
2) Mitered corners
3) Back-back out-of-plane bends

> *Note: in-plane back-back bends should not require an autonomous control function due to the fact that the couplings will be capable of "hyperextension" (bending beyond 90 degree limits of the Pipe Mouse), thus the system should be able to drive straight through the bend. Although not technically considered "autonomous control", the force feedback on the triad linkage will vary the size of the triad based on the cross-sectional shape of the pipeline it encounters, and will assist it in traversing simple changes in geometry such as back-back in-plane bends*.

The base station will have a computer for GUI (graphical user interface) and data storage. The computer will also take the input commands, serialize them and send them to the fiber optic transceiver.

Fiber Optic Communications

The Fiber Optic Communications system will consist of the following subsystems:

1) Base Station Fiber Optic Transceiver
2) RoboScan Fiber Optic Transceiver

Fiber optic transceivers will be located both in the base station and in the RoboScan winder car. Video and MFL sensor data will be sent from the RoboScan platform to the base station, while high level commands will be sent from the base station (user input) to the RoboScan platform. An Infineon Bi-directional Transceiver was chosen. Optical triplexer components of this type are being used today in the Fiber-to-the-Home (FTTH) industry. This industry has grown out of

the need to share bi-directional internet communications with cable television on a single fiber optic cable in the home. These systems feature high data rates and simple video interfaces to the fiber optic cable. The features of the Infineon High Power Triport-BIDI Optical Triplexer, shown below in Figure 84, are as follows:

• Integrated WDM filters for Tx/Rx1/Rx2 operation at 1310/1490/1555 nm.
• 1310 nm FP laser diode transmitter suitable for data rates up to 1.25 Gbit/s.
• 1490 nm PIN diode digital receiver with integrated 622 Mbit/s, 3.3 V TIA.
• 1555 nm PIN diode analog video receiver.
• –40°C to +85°C operating temperature range.
• Single-mode fiber pigtail with different connector options.
• Class 3B laser product.
• Hermetically sealed Tx and Rx sub-components for high reliability.

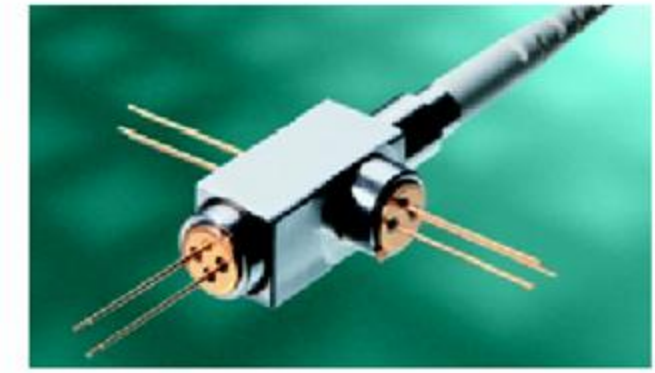

Figure 84. Infineon High Power Triport-BIDI Optical Triplexer

The simultaneous transfer of information between the base station and RoboScan winder transceivers will be transmitted through the fiber optic tether. The jacketed single-mode fiber will be stored in the winder module and paid out (and retracted) while maintaining a very low tension (1 to 2 lb) on the fiber at all times. System functionality is illustrated in the block diagram of Figure 85.

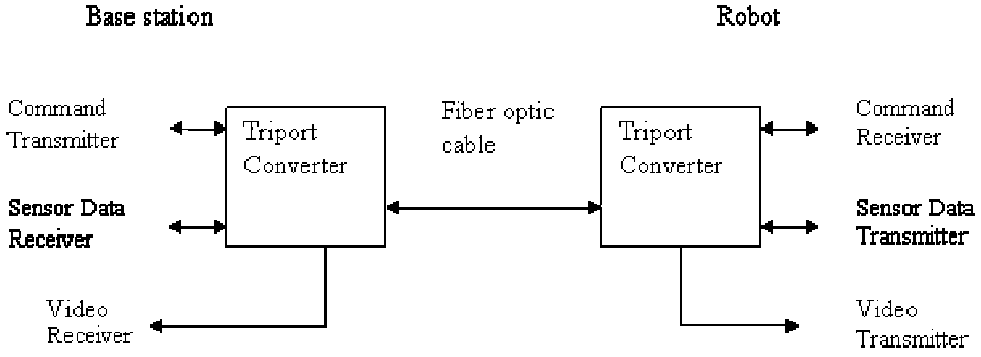

Figure 85. Block diagram of base station to RoboScan communication system

Future Integration of Wireless Communication

While the emphasis of this study was on a tethered communication system, a wireless system could be integrated into the RoboScan system by replacing the Base Station Fiber Optic Transceiver and RoboScan Fiber Optic Transceiver with the appropriate wireless transceivers. At this time, Foster-Miller's position on wireless technology is that the physical limitations imposed by the steel pipeline would require an infrastructure that is not economically feasible to the pipeline operator due to the limitations in signal travel distance (thus more antennas required). If the technology improves to the point where implementation of a wireless system is practical, integration of the wireless communication hardware into the RoboScan system could be easily accommodated. Signal distance limitations of a wireless communication system in a steel unpiggable pipeline may be summarized as follows:

- Gas pipes are made of steel and the low conductivity of steel will increase the attenuation of the waveguide compared to typical aluminum or copper.
- Bends in waveguides are sources of high attenuation and are designed with as high a radius as possible to maximize signal throughput. Sharp bends in the pipelines may be frequent and have high levels of signal attenuation..
- For most pipes, multiple electromagnetic modes will travel at different velocities. This causes the phenomena known as multipath where "echoes" of the transmission arrive at different times, thus limiting transmission distance.
- Signals will reflect at bends possibly echoing back and forth between two bends increasing multipath distortion.
- Any roughness, flanges, weld joints, or other deviations from a smooth pipe will also act to cause attenuation and limit the signal's range.
- The pipe interior must be free of any dielectric coatings or water, which will also increase attenuation.

RoboScan

The RoboScan electrical and controls system will consist of the following components:

1) Winder processor
2) Battery processors (2)
3) Triad processor (4)
4) MFL sensor processor (1)
5) Robot bus

Winder module

The winder module is primarily a communications device that is used to convert the fiber optic data between the base station and the RoboScan local control/data bus into meaningful signals, and control the payout and take-up of the fiber optic tether. The local control/data bus connects all of the onboard processors. The payout and take-up of the fiber optic tether is accomplished through a mechanical accumulator with a constant tension spring. The spring is designed to keep

a slight tension on the fiber at all times to facilitate a smooth winding onto the winder spool. The accumulator allows for fast response without the need for a large servo motor on the spool. A position sensor on the accumulator will control the servo motor to keep the accumulator in a nominal (mid-range) position so it can rapidly payout or take-up the tether as required.

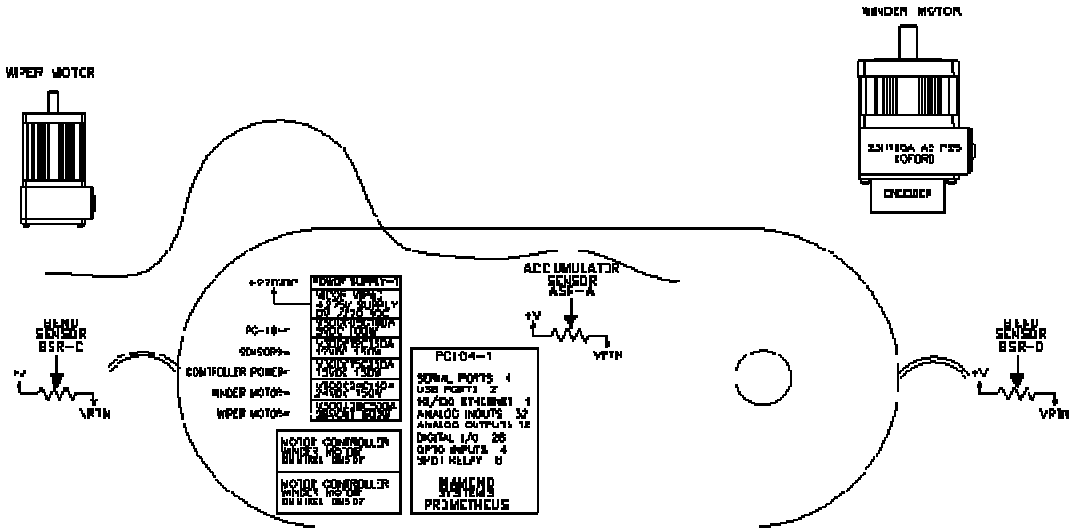

Figure 86. Winder control module schematic

Battery Module

The battery module control system consists of a processor that is responsible for all battery maintenance functions and communication with the local buss. During normal operation the battery will transmit the state of charge, temperature, and the rate of system energy consumption. By sensing the battery voltage and current, the processor can locally calculate state of charge. Onboard intelligence will use this information to calculate remaining battery life, and warn the operator, well before an emergency situation arises, if battery capacity is not sufficient to complete the mission. The platform would then be returned to the launch tube for recharge and an evaluation of system diagnostics. During recharge, the processor will control battery charging and record the number of charge cycles (to be used in a battery life calculation). It is anticipated that the processing requirements will be limited, thus allowing for a small and inexpensive embedded microcontroller. System cost will be reduced, and more importantly, available volume for battery packaging will be increased.

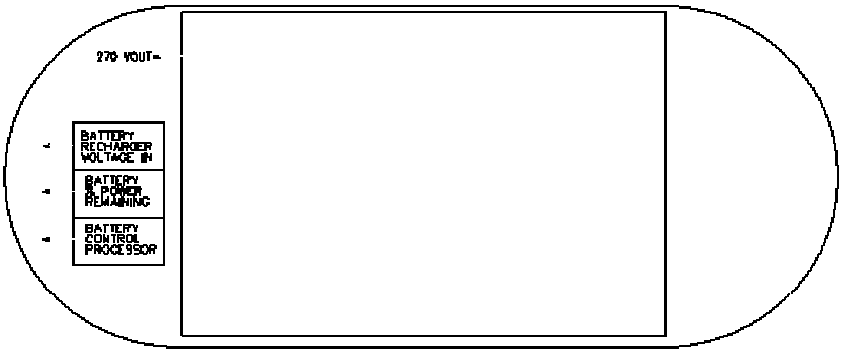

Figure 87. Battery control module schematic

Triad module

Each of the two tractors has a control module between the 2 triads. Within the control module are a duplicate set of electronics, each to control one of the triads. Each has a PC104 computer, various power supplies and all motor drivers necessary to control one triad (see Figures 88 & 89). The module was designed in this way to maintain close proximity with the triads, reducing the length of wiring required, and the number of inter-module joints that must be passed over. All wiring for the sensors and motors passes between the module and the triads. The processor is programmed to take high level commands from the local buss and close the motion control loops for each motor. The control loops are performed in the following ways:

Clamping force

A high level command from the base station is received as a reference. The clamp force sensor output is read and the clamping motors are actuated to generate the desired force. Clamp angle sensors monitor the clamping angles between each leg of the triad.

Steer angle

A high level command from the base station is received as a reference. The position sensor output on each wheel is read. The wheel is steering motor is actuated to achieve the desired angle. The steering control also has an automatic mode that maintains a desired roll angle based on the gyro/ roll sensor.

Drive speed

A high level command from the base station is received as a reference, and a torque loop is closed by the triad processor to maintain drive speed. There will be many scenarios where the system will override the drive command and control the speed based on the obstacles encountered.

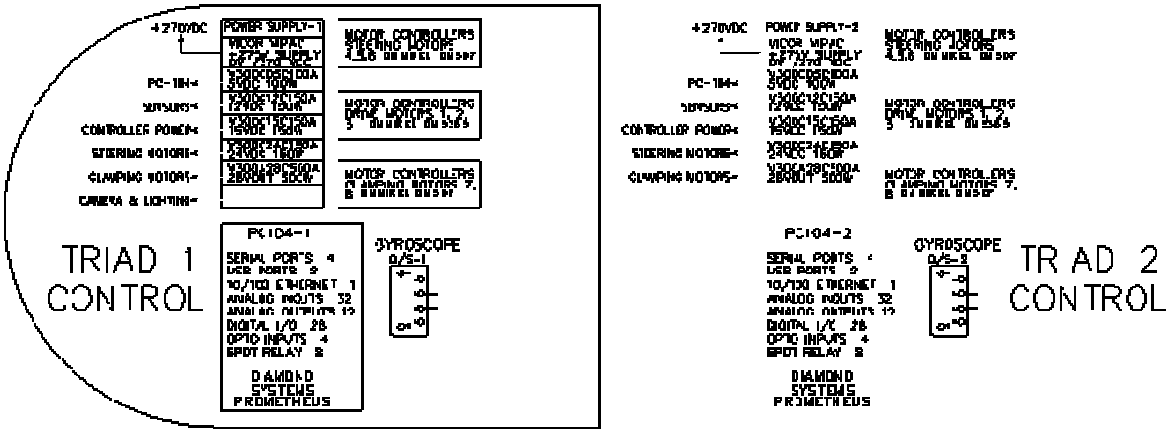

Figure 88. Triad control module schematic

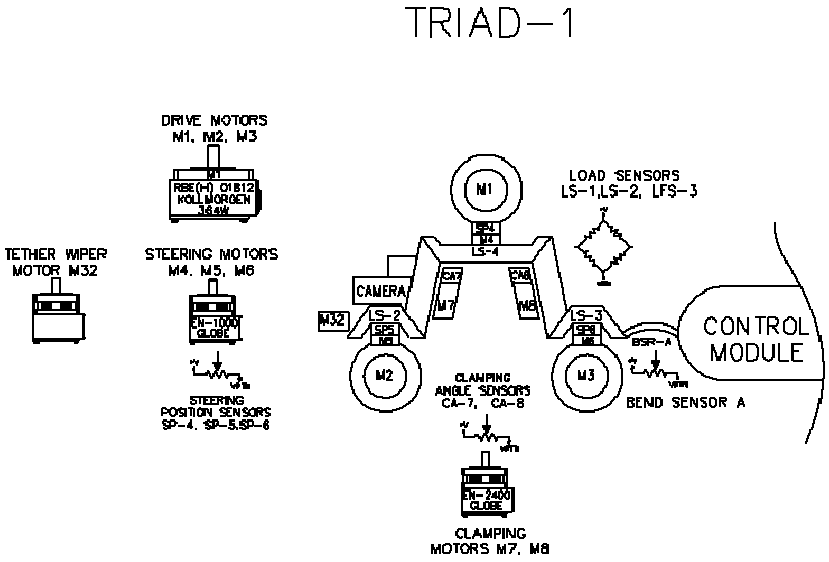

Figure 89. Triad motors and sensors

MFL module

Components of the MFL control module are located in two electronics modules, with a portion of the components in the electronics module between the 2 MFL sensor modules, and the balance in a module outboard of the MFL sensors. MFL sensors motion (centering, deployment, orientation, and shunting) is controlled through a PC104 along with required power supplies (see Figure 90). The processor also collects stores and sends back data to the base station.

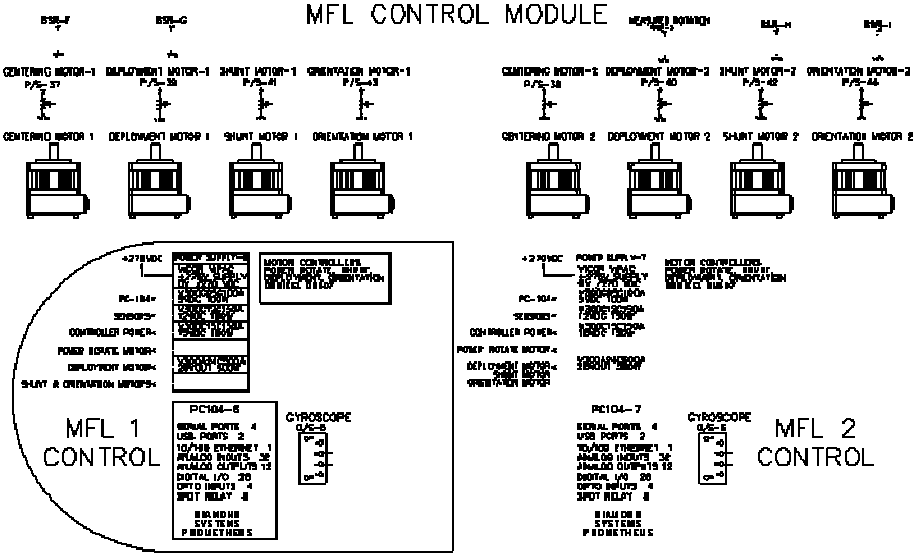

Figure 90. MFL control module

The MFL inspection system electronics will consist current or future GE PII electronics, repackaged if necessary to meet the volume constraints imposed by the plug valve and mitered bend requirements. This includes electronic sub-systems which can be mounted in the pressurized gas environment of the pipeline. PII's experience with potting and encapsulated "external" electronics for hostile environments will be utilized when the time comes to design the system for a pipeline environment.

The electronic sensors that will be mounted on the MFL inspection platform will utilize Hall effect sensors within a molded polyurethane carrier. The technology is similar to that currently in use within GE PII. There will be 144 sensors over the two magnetizing modules and the data, which will be digitized to 12 bits, will be multiplexed before storage. Assuming a total mission length of 8km, it is estimated that a storage capacity of around 10Gb, will be required to support the collection of primary inspection data.

The final decision, on whether the actuation for the deployment and shunt mechanisms should be electrical or mechanical has not yet been made. This awaits further work in a later phase. The decision will be based on determining the most efficient means of generating the mechanical forces for platform and shunt deployment, and providing maximum power within a minimum space envelope.

Robot bus

The robot bus, consisting of the communications bus, power bus, and video bus integrates the functions of all subsystems. Commands for coordinating the control functions within all modules of the RoboScan are sent through the communications bus. Power is distributed through the power bus. Video signals from the fore and aft cameras, and center inspection camera are also relayed between all modules through the video bus.

System Health Management

A prognostic/diagnostic system for monitoring system health and warning of impending failure will be designed into the RoboScan system. In the early stages of development (Phase II), the infrastructure (sensors, data storage) will be implemented. As the system is tested and a better understanding of potential failure modes is achieved, the "intelligence" for monitoring, diagnosing, and reconfiguring the control system to "work around" a malfunction in the interest of getting back to the launch tube can be implemented. Foster-Miller has substantial prior experience in machinery diagnostic/prognostic areas and can apply this know-how to reduce maintenance for the RoboScan platform.

Early warning of degradation or impending failure of critical mission related components is critical to the operation of complex systems such as the RoboScan. It is not an option to operate in a "run-to-failure" mode. Machinery condition prognostics, early warning and tracking of degradation, and optimized scheduling of limited maintenance resources represents the only approach that will work.

Going forward with the development of a RoboScan inspection platform requires that automated machinery diagnostics be incorporated into the system design. Foster-Miller will address this need through a Health Monitoring And Prognostics (HealthMAP) system that will provide both fault detection and machine performance degradation information for the operator. Signals that sense out-of-limit conditions (over temp, over voltage, etc.) or sense only when equipment has failed do not address the need for early warning of impending failure. The detection and tracking of automated equipment performance degradation provides the Prognostics ingredient that is crucial to meeting the expected reliability of the RoboScan while supporting operational needs.

The HealthMAP system is intended to accomplish two basic functions:

- Monitor the functionality of each subsystem and determine the health of major components by direct test as well as measurements during operation (determine degradation and impending failure, not just failure).

- Archive all raw and processed diagnostic data for diagnostic verification, and generation of Maintenance Work Orders.

To accomplish the Prognostic and Degradation Monitoring functions, HealthMAP relies on the subsystems to provide:

- Monitoring of tests to each major component subsystem, and performance of tests that verify subsystem readiness and indicate degraded component performance (not just failure).

- Performance measurements during operation for degradation detection and trending.

The incorporation of HealthMAP functions into the design of the RoboScan subsystems requires careful planning as implementation might affect the design of the subsystem. The following concepts will be used to guide the design of the HealthMAP system and individual subsystems.

- HealthMAP should be non-intrusive. This means that signals measured should be isolated and that test programs should be internally contained and exercised as part of the normal software flow during operation.

- HealthMAP should add the minimum number and complexity of sensors required to accomplish its task to any subsystem.

- HealthMAP design architecture is an "overlay" to the automated system. This means that the HealthMAP system has its own bus and is functionally, electrically, and ground-wise isolated (optically preferred) from all subsystems.

- A failure in HealthMAP hardware or software must not cause a subsystem fault nor give indication that a subsystem fault exists.

- HealthMAP system itself must have a built in validation and test routine.

2.13 System Control

2.13.1 Modes of Operation

The RoboScan robot was designed as a semi-autonomous robot, with a controls architecture that would readily allow a future migration to fully autonomous control. One of the key concepts behind the operation of the RoboScan robot is the curling link. This link exerts a constant torque on each of the triads, in a downward direction. This principle is known as 'preferential curl'. The preferential curl concept permits the robot to automatically steer itself into and through corners with minimal operator interaction. Upon the encounter of a bend, the operator simply rotates the robot such that the direction of preferential curl is in line with the direction of the bend. Continued forward motion in conjunction with the preferential curl will guide the robot into the bend, and allow it to continue onward.

In additional to preferential curl, another key concept behind the functionality of the robot is the triad clamping feature. Each of the triads have the capability to draw their outer wheels together, effectively shortening the wheelbase. Doing this will increase the total height of the triad; if the

robot is constrained within a fixed diameter pipe, then the triads will push on the pipe walls trying to grow in height. Throughout the majority of the inspection, the robot will use this principle to exert a constant force on the walls of the pipe. Force sensors are used to measure the exerted force on the pipe walls so that a closed loop control system for triad clamping may be implemented. This clamping force ensures that the robot is stable within the pipe, and provides enough force so that there is sufficient traction for the drive wheels.

Mitered Bends

Mitered bends also utilize the preferential curl concept. Due to the non-sweeping nature of a 90° mitered bend, their negotiation is more complex than a gentle bend (see Figure 91). Preferential curl assists the leading triads entering the bend, however passing through the bend is an exercise in timing and control. Three main operations must be performed in concert in order for the robot to successfully pass through a mitered bend. As the robot enters a mitered bend, the curling links will introduce the leading triad into the corner. As the lead wheel of the triad leaves the pipe wall, and begins to 'reach into the bend', clamping force drops to zero. The triad then begins to contract, increasing its height, searching for the pipe wall. At this point, if forward motion is too slow, the triad will continue to contract, and will become jammed in the corner.

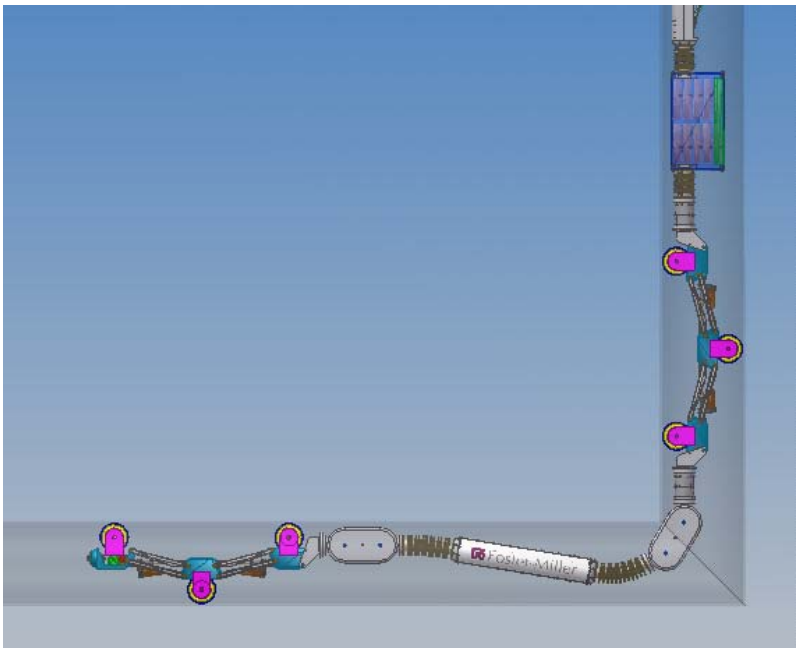

Figure 91. RoboScan traversing mitered bend

The forward motion of the robot needs to be timed such that the triad is directed out of the bend before it grows prohibitively tall. In addition to the complex controls requirements, the geometric and kinematics design will require a reasonable amount of consideration. Passing through the mitered bend tends to position the triads such that fairly tight coupling angles will need to be accommodated. The modularity of the bending couplings will allow us to tune the length and extent of bend so that it may successfully pass through the bend. This maneuver will

require a large degree of lab testing and evaluation to succeed, but once the timing and controls are sorted, the maneuver should be a passive one.

Back-to-Back Bends

One of the more difficult obstacles to negotiate is the back-to-back out-of-plane bends (see Figure 92). The robot operator will be required to position the robot and make control maneuvers throughout the entire duration of the obstacle. This obstacle requires the triad to pass halfway through the set of bends before rotating tangentially, aligning itself for the subsequent bend. Each triad will have to travel into the bend to a set position before re-aligning themselves. In addition to preferential curl and the closed loop triad clamping control, this move demands precise degrees of freedom, and careful coupling design. Rotating the triad in a bend and constantly updating the effective height of the triad tends to produce awkward coupling angles, and these angles must be accommodated for in general coupling design.

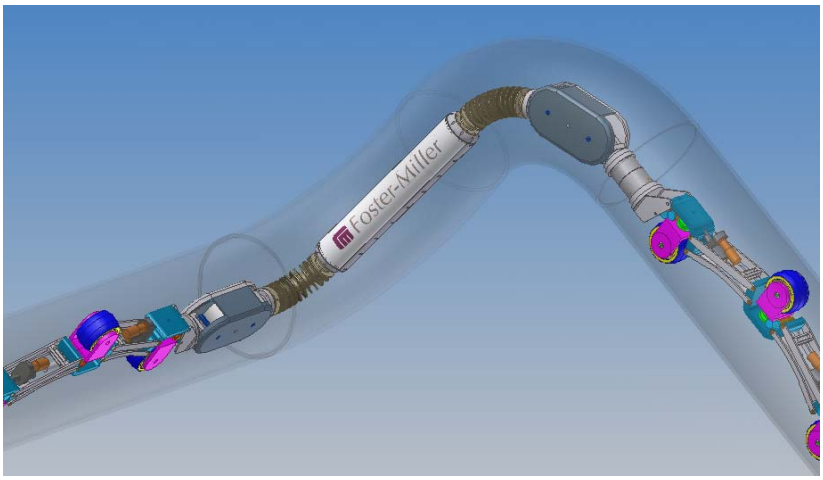

Figure 92. RoboScan traversing back-back out-of-plane bend

When compared to back to back out-of-plane bends, the in-plane counterpart is an easy obstacle to negotiate. In order to pass through in-plane back to back bends, RoboScan must overcome its own preferential curl. Rather than requiring each triad to rotate 180° half way through the obstacle, we have designed the robot to pass straight through the back to back bends without re-aligning. In order to do this, the robot will be working against the torque exerted by the curling link. The triad will enter the first bend curling in the preferred direction. Upon entering the second bend, the robot will be required to hyper-extend to pass through. Excluding the curling link, all couplings on the robot are omni-directional- this eliminates the need for any aligning for this obstacle. The curling links were designed such that they may roll back against the direction of preferential curl sufficiently to pass through the obstacle.

Plug Valves

Plug valve passing will require that the triads be aligned in the 6:00 to 12:00 position prior to entering the valve. The cross-sectional area of the triad and train modules has been sized for passing through the Nordstrom 16" plug valve (drawing no. C-50710). The triad drive wheels have sufficient height (6 in diameter) and power to pass over the lower lip of the plug valve. All modules are symmetric in shape (sausage) except for the battery module, which was designed with a tall oval cross-section (still within the constraints of the Module Volume Study) to take advantage of the additional volume available. The battery module must be properly aligned by the adjacent triad (2 batteries at either end of train). Prior to entering the plug valve, the battery will be rotated into position by the adjacent triad, with the triad and the battery both approaching the plug valve in the 6:00 to 12:00 position.

2.13.2 Obstacle Detection

This section discusses several options for detecting and identifying obstructions in the pipeline and resolving their orientation with sufficient resolution to align the robot for passage. This feature will be required for autonomous control of the RoboScan, a control function that is expected to be implemented in future platforms. An overview of the system architecture of the RoboScan platform in terms of the numerous features required to facilitate both supervised and autonomous inspection through obstacle detection and ID is also presented.

Obstructions that must be recognized and negotiated

A number of obstruction have been identified the robot must recognize and perform different maneuvers to negotiate:

- **Plug Valves –** should be readily identified by a simple video camera system. The angle of the pass through can be clearly visualized and the robot can turn to the necessary angle for passage.
- **Bends –** are somewhat more difficult to classify. The center of an empty pipe will always appear black because there is no surface to reflect light back to the video camera. The upcoming pipe wall at a bend or corner will be visible clearly identify an approaching obstruction. With proper lighting a shadow should be visible along one side that can identify the direction of the bend.
- **Mitered Corners –** as in the case of the bends, the obstruction of a mitered corner will be visible to a video system and shadows can identify the direction of the turn. The additional challenge will be distinguishing a mitered corner from a smooth bend so that the appropriate navigation mode can be used. Video image analysis is the first choice for this task, but more powerful sensing techniques are described below that can be applied if necessary.
- **Back to Back Bends --** both in plane bends and out of plane bends must be identified. Out of plane bends require a more complex steering technique to guide the robot through. Options for sensing multiple bends are described and proposed testing on subscale or full scale pipe segments will be used to evaluate the effectiveness of the proposed sensing modalities.

Sensing Techniques

There are several potential sensing techniques that can be used in autonomous control of the robot. The various techniques must be evaluated through experimental trials on actual pipes. Because the goal of these trials will be to evaluate the appearance of different obstructions such as mitered corners and multiple bends, many of these tests may be performed on reduced scale pipes for efficiency and economy. The techniques will be listed in order of recommended investigation. Once a technique has demonstrated through testing that it has the capability of dealing with all the obstruction that will be encountered in a pipeline, evaluation may be halted without further testing of the more complex and costly techniques.

Video Cameras and Image Interpretation

The robot will have video cameras and lights mounted on both ends for manual guidance and internal inspection. Therefore, the first option to explore is the feasibility of adding image capture and interpretation capability to the onboard computer to identify the different obstructions and their orientations. Foster-Miller has developed algorithms for biomedical applications that seek paths through body cavities and this expertise will be applied to this problem. The appearance of the expected obstructions must be characterized and the patterns of the light and shadows used for classifications. The classification problem may be complicated by the surface condition of the pipe walls, variations in color and texture can significantly complicate visual identification.

Structured Light

The differences in curvature between mitered corner and bends may be difficult to identify under the illumination of the video lights. The use of a structured light source may aid in the identification of surface shapes. For example, when a single line of light is projected at an appropriate angle on a curved surface, the line of light will appear curved as well. When viewed by the video system this curvature may provide sufficient discrimination to identify obstructions and their orientation Structured light may take the form of single or multiple stripes, cross hairs, grids, or concentric circles. Small compact laser sources are available. The projection source may be offset from the location of the camera to enhance the effectiveness of the technique.

Related techniques used to identify surface contours such as shadow moiré may be applicable here as well. In one applicable version of moiré interferometry, a uniform pattern of light and dark stripes is projected on the target while the video camera views the scene through a grid with a similar pattern of stripes. This produces a pattern of fringes that can be processed to identify and measure the surface contours. These types of moiré fringes may be observed on many everyday circumstances, such as striped patterns when viewed through the scan lines of a television set.

Mechanical Feelers

If the complexity of image analysis is found to be an infeasible for navigating the robot through all pipe obstructions, mechanical feelers may be incorporated into the system. These may take

the form of one or more rods with wheels at the tip rolling along the pipe walls ahead of the robot to sense angle changes. An encoder at the robot end of the rod would monitor the angle. Options would include rotating the forward tractor to measure wall angles changes around the pipe circumference once a change in the curvature is sensed, or rotate the sensor locally. While this technique is clearly immune to changes in wall color and texture, it will be limited to sensing structural chances only a short distance in front of the robot. It could be used as a supplement to the vision based system rather than a complete replacement.

Laser and Ultrasonic Distance Sensors

There are several types of optical sensors that can measure the distance to a surface, typically using either triangulation, pulse time of flight, or continuous wave phase shift. Ultrasonic based distance sensors are also available using time of flight but the wider beam spread of at least seven degrees yields a more limited spatial resolution than found in the optical devices. Time of flight and phase shift devices measure the distance to a surface from a straight-line path from the single point sensor. Triangulation sensors are simple and use low cost off the shelf components but a known baseline distance between the transmitter and receiver is required to produce an accurate measurement. Creating the necessary baseline might complicate the process of including a triangulation device on the already somewhat complex pipe robot. One promising option would be to use the existing video camera together with a structured light projector to build a multipoint triangulation sensor. Foster-Miller has developed a structured light-based triangulation system that produced high-resolution profiles of small object surfaces.

The distance sensor can be applied in a scan pattern to measure any upcoming contours of an obstruction. The requires the inclusion of a scan mechanism in the optical system The sensor would normally point straight down the pipe and a scan of the contours need only be initiated after an obstruction is detected. These scans would produce a precise map of the obstruction contours within the line of sight of the robot, which would provide sufficient information for navigation and orientation.

Scanned distance sensors would provide a powerful tool capable of identifying any structure within the line of sight. However, they would complicate the design of the robot tractor and increased the hardware cost. Therefore, their use will only be explored if the use of simpler vision sensors proves to be inadequate.

Extended Camera

All options described so far only detect the portions of obstruction within line of sight of the front of the robot. This does not permit the detection of compound bends until the robot has traveled far enough through the first bend to view the second bend. The capability of extending a camera on a flexible shaft would allow the robot to look around corners and line up earlier to negotiate a path through back-to-back obstructions. A camera with the capability of extending in front of the robot and turning to look through different angles would also provide an enhanced view of single obstructions, potentially improving identification and navigation. The extended camera would also provide potential benefits allowing close inspection of the walls of the pipe.

Very small low cost video cameras are currently available as well as compact white light LED illumination sources. Foster-Miller has been involved in the development of video camera borescopes and some of these concepts could potentially be adapted to this application. The added complexity of an extended camera makes the incorporation of this technique advisable only if navigation development demonstrates a need for early identification of compound bends or additional imaging capability is need to identify all incarnations of single obstructions when obscured by difficult pipe surface conditions.

Pipe Mapping – Application to Autonomous Control

Detailed mapping of the pipeline obstructions provides significant advantages to the processes of recognition and navigation. If a map can be created of the locations and types of obstructions, the capability demands on the sensor system and associated computers are greatly reduced. The robot will know what type of obstruction it will next arrive at and the sensors do not need to be able to autonomously discriminate between bends and mitered corners or identify multiple bends. The video sensor system is simply required to identify the correct orientation of the obstruction. Once the orientation is determined the robot can be driven to the correct orientation for passage.

One approach to generating the pipe map could be to navigate the first pass of the pipe under operator control. The distance to each obstruction and the type of obstruction would be recorded creating the map. When an experienced operator is watching the video images, with a human's vastly superior image processing capability, identification of the types of obstructions will be readily accomplished. A simple structured light source could be included if its use simplifies the task of visual identification. Compound bends will be identified as the robot progresses through them and, if required, the operator can back up to readjust orientation for smooth passage. The robot should include a roll sensor to measure its orientation angle when traversing the obstruction and the ability to measure the angles on one triad to determine the size of the obstruction. The angle of both bends in the compound should also be measured and recorded. The angle and size information will be included in the digital map.

The position of each obstruction would be measured using the distance traveled by the robot. While there may be some inaccuracy in the measured position due to wheel slippage during transit, small errors in distances will not be important, identification of the obstruction type and approximate distances between obstructions will provide sufficient data for subsequent autonomous navigation. In addition, errors in distance measurements can be minimized by instrumenting two or more wheels on the robot to detect individual wheel slippage and correct the errors.

After a single manual pass through the pipeline, a complete map will have been generated. Now under autonomous control the robot can proceed back through the pipe. The map will identify the first obstacle to be encountered and the measured distance. The robot can readily identify the obstacle using the video system once it comes into visual range. Differences in distance traveled from the map distance may exist but they do not effect navigation. The robot's position estimate will be set to match the obstacles location based on the digital map, and the distance between

obstacles will be used for navigation purposes, rather than the total distance traveled, to prevent the accumulation of errors in the measured distance.

The video image will provide sufficient information for the robot to identify the correct orientation angle needed to negotiate the obstruction. The map provides the exact type of obstruction, its dimensions, and orientation/size for the next element of a compound bend. The robot will be steered through the appropriate motions to negotiate the obstacle, then travel will resume to the next obstruction.

2.13.3 Supervised and Autonomous Inspection

The proposed system architecture of the RoboScan platform incorporates numerous features to facilitate both supervised and autonomous inspection. As the RoboScan platform concept has matured the need and inclusion of sensors and control surfaces became apparent and have been included. The first generation RoboScan platform is geared towards supervised (tele-operated) control via a fiber-optic cable with autonomous control planned for later inclusion.

Kinematical analysis of the RoboScan platform indicate that the platform will be able to maneuver through typical pipe configurations discussed previously in this report. FMI's analysis of the RoboScan and previous experience with the Pipe Mouse indicates that even mild improvements in kinematics performance will greatly simplify operation and controller development. To that end, the mechanical design has sought to ensure control motions are as simple as possible, yet autonomous control will still require significant work.

The control system may be decomposed into various layers, each which performs a specific function and relies upon its lower layers. This control layering is as follows:

- Autonomous Level – This top layer seeks to run the vehicle without any human intervention. This is the ultimate goal of the RoboScan, but relies heavily on the lower layers for performing control. This layer requires several additional components including an identification system to determine upcoming pipe configuration (see previous discussion) and a navigation system to ensure that the RoboScan reaches an exit (onboard power management and system diagnostics).
- Command Level – This layer's sole purpose is to provide an interface between either the autonomous layer or an operator, who may be tele-operating the RoboScan. This layer will translate high-level commands into actions which the subordinate coordination layer can act upon, such as move forward, reverse, rotate, traverse a plug valve, etc.
- Coordination Level – This layer accepts high level commands and translates them into actionable items that various sub-systems (such as the Triads) can act upon; it coordinates the actions of the underlying layers to produce meaningful results. By necessity, this layer must aggregate data from its underlying layers to determine the vehicle's exact orientation and configuration. It must combine configuration knowledge with environmental interaction information (e.g. wheel contact forces) to determine such things as slip between Triads, etc..

- Triad Control – This layer abstracts an individual Triad's multiple actuators to enable the system to be treated it as one locomotive unit. This layer must coordinate multiple actuators to ensure that the Triad is moving properly and in the correct orientation.
- Low Level Controller/Measurements – This layer cover numerous stand alone actuators and sensors as well as the individual components of each Triad.

The low level control and measurement is achieved through COTS devices with minimal customization. Commercially available devices are used to regulate the speed of Triad's wheels, to measure contact forces, to determine the bend between sections, etc. This level presents neither significant challenge nor technical risk.

The Triad's controller is responsible for coordinating each of the Triad's wheels orientation and motion. It must also monitor contact forces to ensure that the wheels are not slipping and that Triad is moving as expected. Performing these actions represent some technical risk, which is mitigated by FMI's considerable experience from other Triad-based systems such as Pipe-Mouse.

The Coordination Level presents some new challenges to the FMI team but is also mitigated by FMI's previous experience with Pipe-Mouse. The fundamental new questions at this level are what Triad motions and sensing are required to navigate various pipe configurations such as back-to-back, out-of-plane bends. Algorithms for handling single bends and performing basic locomotion can be extracted from FMI's earlier experiences with Pipe-Mouse.

The Command Layer does present new challenges to the FMI team. The Pipe-Mouse system required an exceptionally well-trained operator and suffered from the computational limitations of the day. More than a decade later, many of the intricacies of performing motion can be automated. At this point, the real key to success will be developing a simple enough operator interface so that anyone can handle the system with only minimal training. The interface also needs to be exceptionally clear, so that the next stage of autonomous control can happen easily.

The Autonomous Control Layer presents new challenges, but can be approached in a piece-meal manner mitigating both technical and programmatic risk. The current state of the art for autonomous vehicles include commercially available free swimming deep-sea robots, oil rig inspection robots and vacuum cleaners. These platforms use behavior-based control methodologies, which have been refined over the past two decades by various pioneers in computer science.

These behavior-based controllers rely heavily upon the vehicle control algorithms, (such as those being proposed for the Command and Coordination layers of RoboScan) to perform basic locomotion. Using these locomotion algorithms as a building block, behavior-based controllers add a layer of sophistication which seeks to replace the operator.

The operator is replaced by numerous simple behaviors, which are single goals such as obstruction avoidance, pipe inspection or battery preservation. All the behaviors run concurrently and may issue locomotion commands such as turn right, turn left, etc. Collectively the behaviors will issue numerous commands, each based on the behavior's own goal and its inputs. When conflicting commands are issued from the behaviors, the system will prioritize the behaviors, *a*

priori, and accept only the command issued from the highest priority behavior. With a suitably rich set of behaviors, the robot is able to accomplish mission goals (also programmed as behaviors) while reacting to unpredictable environments. Unlike deep-sea robots or autonomous vacuum cleaners, the RoboScan's constraints more easily defined. Schools of fish or house-hold pets will not be attacking the RoboScan. In fact, the RoboScan's path can be determined well in advance (through pipe maps) and back-tracking should almost always be a viable option.

A piece-meal development plan for both tethered and autonomous control becomes evident from reviewing the control layers described earlier. Naturally, the lowest layers would be completed in short order and would be quickly followed with algorithms for controlling the motion of an individual Triad. The next step of building the Coordination Layer would be natural and followed with the Command Layer. In developing the Command Layer, operator experiences will help define the relevant behaviors required of an autonomous controller. The advantage of this design methodology would be that the tethered system would be available early and could act as the “training wheel” version of the autonomous RoboScan, where an operator can intervene until the autonomous system is wrung out.

3.0 CONCLUSIONS AND RECOMMENDATIONS

Foster-Miller, in partnership with GE/PII Pipeline Solutions has completed an overall assessment, and has developed a preliminary specification and design for a robotic inspection tool for unpiggable gas pipelines. This development effort was performed with the overall philosophy that ultimately all transmission and distribution pipelines should be capable of 100 percent inspection. The first step in achieving the ultimate goal of developing an unpiggable pipeline inspection platform, capable of providing equivalent information to that gathered by smart pigs, was met with the concept design produced in this project. The results of this initial phase of the RoboScan inspection platform development demonstrated that the following performance targets could be met with further development:

- Capable of bringing a full suite of NDE sensors into transmission and distribution networks.
- Self-powered and capable of traveling long distances from the entry point.
- Negotiate mitered (zero degrees) elbows and tees as well as back to back out-of-plane bends.
- Navigate in both the horizontal and vertical planes in both directions.
- Not dependent on pressure drop to "push" the robot.
- Passable through partially ported valves such as plug valves.
- Automatically adaptable, up to a factor of two, to changes in pipe diameter.

The RoboScan system was based on the requirement for a platform capable of inspecting a nominal pipe size of 18 inch. The “portability” of the system, or the range of pipe sizes that a given system will operate in (16 inch to 20 inch in this case), was limited by two conditions, with each condition affecting a different part of the system. The first of these design-limiting conditions, the presence of plug valves in the pipeline (which were based on the Nordstrom 16 inch plug valve, drawing no. C-50710), limited the range of pipe sizes that the MFL module could inspect due to the following considerations:

- The magnetizer, shunting mechanism, sensors, and deployment mechanism must be sized for a valve opening that reduces available width by approximately 70 percent and available height by approximately 20 percent.
- The amount of magnetizer that can pass the valve (and sized based on the smallest pipeline inspected) must be of sufficient size to inspect the pipeline with a “reasonable” number of passes (a segmented module requires some number of passes through the pipeline to achieve full circumferential inspection).

With the decision to develop the single, plug passing axial field MFL design, it was clear that it would be impossible to inspect the whole pipe in a single pass. The initial concept was to use two diametrically opposed magnetizer platforms or shells. A tradeoff between the number of modules and the number of passes was required (increasing the number of MFL modules reduced the number of passes but increased train length). It was also realized that if the pipe could be inspected on the outward and return legs of the mission it would have a positive effect on the system design in terms of efficient use of power. Detailed modeling confirmed that it was possible to design and operate a pair of MFL modules that will inspect the whole pipe by collecting data on the outward and return journeys. The drag from two modules will be greater than for a single module, utilizing battery capacity for the tractors to overcome the additional

drag. However, using a pair of modules overcomes the need for multiple passes with a single module.

The second design-limiting factor was the presence of back-back out-of-plane bends in the pipeline, which affected the portability of the tractor. Discovered during mockup testing, the tractor must be able to rotate 180 degrees after passing the first bend so as to align for proper entry into the second bend. If the wheel base of the tractor is too long for a given bend, the triad will not be able to rotate the full 180 degrees. Based on the mockup testing, in 16 inch pipe, the longest possible link length to achieve bend passing will net a 24 inch triad height (smallest wheel base where triad remains stabile). Preliminary indications are that with optimization, a range of 16 inch -24 inch may be possible with a single platform

Battery capacity was reduced due to the need to pass plug valves (less volume available). The choices of battery module profile were limited to a "sausage shape (passes the lower portion of the plug valve) or an oval "asymmetric" module shape (utilizes most of the valve opening area). In deciding on a shape, bend passing capabilities also had to be considered. The asymmetric shape was chosen since it could pack more battery cells, reducing the total number of battery modules (for the prescribed 5 mile mission) by approximately 50 percent if a sausage profile was used. The asymmetric module will result in more control complexity on the platform as the battery module must be correctly oriented by the leading tractor (the symmetric sausage passes in any orientation). Each module, whether battery, communication, tractor, or tether will be designed with a focus on modularity to facilitate simple exchange of modules in the field.

The current status of the design effort for each major subsystem of the RoboScan platform is presented below, along with a summary of the requirements for the next phase of development.

Tractor/Triad Kinematics and Control

The three motorized control axis of the triad (the wheel drive system, steering drive, and wheel clamping actuator system) were developed based on the power requirements to traverse and inspect 16 inch to 20 inch unpiggable pipeline. Closely modeled after the Pipe Mouse design (same kinematics operation but with much greater load requirements), the systems have the benefit of many years of Pipe Mouse development. The tractor wheel drive system was designed based on the worst-case loading situation presented by the pipeline environment (steady-state plus peak loads) along with the power required to pull the two magnetizer modules. Drive components were packaged within the hub of the 6 inch wheel resulting in a space-efficient system that fits the width constraints of the smallest plug valve (16 inch). The wheel steering drive system, consisting of a worm and gear coupled to a compact gear motor through a set of spur gears, was developed based on the worst-case loading requirement of turning the middle triad wheel (which experiences twice the radial load of the 2 outside wheels) under maximum loading condition without forward movement under peak drive load conditions (vertical climb). The required steering torque will be much lower under conditions when the wheel is rolling. The wheel clamping actuator mechanism consists of a machine screw jack type actuator that is driven by a gear motor that is coupled to the screw through a set of spur gears. A machine screw form was chosen in order to prevent back-driving so as to minimize power consumption. A conservative design approach was used that was based on the worst case wheel clamping force

that is required under peak driving conditions (vertical climb) while the four bar linkage in the position with the least mechanical advantage (roughly a 2:1 mechanical disadvantage).

Prior to entering detailed design in a Phase II development effort, it is critical that the kinematics and control requirements of the RoboScan platform be fully understood and verified with extensive mockup tests (small and full-scale) and computer simulations. These tests and simulations will permit design engineers to evaluate the kinematics and operation of both the tractors and sensor modules as they pass through the difficult geometric constraints, and the function, degrees of freedom, compliance, wire passing capability, etc. of the inter-module couplings. While we believe that the concepts presented are feasible, some aspects of these designs must be further evaluated. Specific tasks/issues to be addressed include:

- Bend coupling requirements – the platform must be able to transmit tensile and compressive forces from interaction between front and rear tractors without buckling while having sufficient flexibility to bend around corners without requiring excessive force. Couplings must be "tuned" to meet these requirements while accommodating pass-through of power and control wires. Bend sensors must be integrated into all couplings to determine degree of buckling (system will control through interaction of front and rear tractors).
- Evaluate interaction of modules and couplings when negotiating obstacles – determine the location of connection points, shapes (potential catch points), and the affect of coupling stiffness on module motion, etc.
- Control sensor requirements optimization – determine if bend sensors and platform orientation data (gyro) are sufficient for proper control.
- Curling links - will passive curling links suffice, or will the relatively high output torque impede deployment (manual positioning into launch tube). Determine if "full-time" curl reduces performance. Option will be to implement active control to be deployed only when needed.
- Rotary couplings – evaluate splined coupling engagement technique in terms of reliability.
- Centering couplings (MFL module) – evaluate other methods, possibly integrated with MFL deployment function of elevating and supporting modules. Evaluate design options for reducing length. Verify bend passing capabilities and need for supplemental bend coupling.
- Module friction reduction– strategically place wheels or wear surfaces (once kinematics are better understood) on modules to reduce drag and improve energy requirements.
- Coupling kinematics – overall evaluation of requirements to determine if simpler techniques/control functions exist.
- MFL obstacle negotiation capabilities - verify how shunting will be employed (in corners and through valves), and degree of magnetic drag reduction achieved. Reevaluate deployment, centering, and rotation functions and determine if they can be simplified.
- Verify structural design – once kinematics are fully understood, structural requirements must be determined based on the forces produced. Components (structure, bearings, wheels, triad compliance system, etc.) must be designed, and if necessary, the impact on kinematics reevaluated based on any change in size/shape/mass of component.

- Electronics packaging/potting – use GE/PII's expertise to determine what components can be potted and which need to be packaged in pressure vessels. Although a "pipe ready" design is not a requirement for the next phase, proper "volumes" must be simulated to verify proper kinematical operation of the prototype unit.
- Venting requirements – determine requirements for venting (in launch tube prior to removal) and how component design/packaging may be impacted. Although pipeline tests are not a part of Phase II program, critical issues relative to the safe venting of components after use in the pipeline should be identified.

MFL Inspection Module

A practical solution for the inspection module of the RoboScan platform utilizing a segmented MFL module and deployment mechanism was developed based on operational and geometrical requirements. A number of mechanisms were explored, evolving into a practical design that we believe will allow a sensor platform(s) to be deployed against the pipe wall during times of inspection, and retracted or collapsed for plug valve and miter bend passing. Performing these two modes of sensor operation, together with the need to navigate and inspect a range of diameters, presented the greatest design challenges.

The sensor platform consists of two segmented modules (90 degrees out of phase) that will inspect half the pipe circumference going away from the launch tube, and the remaining half during the return to the launch tube. Although the current emphasis has been on MFL inspection technology, the platform could just as easily be used with any inspection technology that is currently available or developed in the future. Magnetic methods invariably result in strong attractive forces, and the current segmented sensor development has been no exception. By performing experiments to determine the field sensitivity, and to confirm rolling friction, it has been possible to optimize the design to provide inspection to a GE PII 30/50 specification. By utilizing novel shunting mechanisms, it will be possible to reduce the field and attractive power, making it easier to retract the sensor platform from the pipe wall, and also minimize the risk of accidental clamping onto other ferrous surfaces.

The data collection, storage and power modules will utilize current or future GE PII systems, and draw upon 30 years of experience. This includes electronics that can be mounted in pressure vessels or externally in the pressurized environment. The sensing electronics will also be based on current GE PII developments, providing high resolution mapping of the MFL distribution.

Tether Optimization

A commercially available single-mode fiber optic cable (tether) that will provide the communication link between RoboScan and the base station has been identified. An analysis of the fluid dynamics of the tether when exposed to pipeline conditions was performed, along with simple lab tests to verify the analysis and test the tether under high wear/stress conditions. The situation of the tether being pulled tight around a zero degree bend (mitered corner) has been identified as the limiting factor when specifying a tether for a particular pipeline flow condition, ultimately reducing signal loss to unworkable levels and possibly leading to the failure of the tether. Based on this initial assessment, it appears that signal loss will drive the design of a tether for a given set of pipeline conditions, not the tensile strength of the fiber. Full scale pipeline testing, under actual flow velocity and pressure conditions (simulated with air), is recommended

to verify these preliminary results. Tether stress levels as a function of flow velocity and pressure will need to be verified, along with the effect of flutter on attenuation and jacket wear. Design requirements for the tether umbilical system will be updated based on these tests in the next phase of development. The degree of pipeline debris will have to be ascertained so that the requirements for a tether cleaning system to keep dirt/debris out of the winder module may be generated.

Battery Power System

A power analysis was conducted based on a 2.5 mile mission (inspect out and inspect back for 360 degrees of coverage) that takes into account the resulting drag of the sensor modules, and the route through a "typical" pipeline. Using commercially available Lithium-ion technology, four battery modules of secondary (rechargeable) cells would be required to complete a mission. Discussions were conducted with a battery manufacturer who claimed that a Lithium-polymer battery could be developed with twice the power density, thus reducing the battery modules from four to two. Of the two choices of module shape (dictated by plug valve geometry), the asymmetric shape (over the symmetrical sausage shape) was chosen based on greater battery cell packing density. If not the for the plug valve, the modules (whether battery or any other supporting system) could utilize the full diameter of the pipe, providing more volume (battery energy) in a much shorter package.

Connection ports for in-situ battery charging and battery diagnostics will be provided in the launch tube. Automatic connection will be achieved either through the motions of the platform (battery module engages a connector) or a mechanism built into the launch tube that connects battery power and signal wires.

Winder design

A winder module, based on the earlier Pipe Mouse winder design, was developed. The system includes a mandrel upon which the fiber optic tether is wound, and a take-up and payout mechanism that manages the tether as the RoboScan system moves through the pipe. The housing consists of a two-piece shell that is supported by a series of bulkheads along the length of the module. Current thinking is to keep the system open to the pressurized gas environment, while individually sealing any electrical/electronic components that are susceptible to damage. A purging sequence for the complete RoboScan system (within the launch tube and prior to removal from the pipeline) will be defined in the next phase of the project. The need for a totally sealed system will be evaluated in the next phase of development, and will depend on the time required to purge the winder car, and any difficulties that arise in protecting electronics as separate modules.

Camera/Lighting

A review of commercially available camera/lighting options was conducted. During the next phase of the project it is recommended that the validity of this information be reevaluated and updated as the technology is changing and rapidly improving.

Ovality Sensor

A concept for an ovality sensor was presented that utilizes commercially available components integrated into a custom-designed system. A cost-benefit analysis should be conducted in the next phase of development to compare this non-contacting ovality sensor with a contacting system that utilizes mechanical calipers. Although traditional systems are not designed to pass plug valves, one possible option is to integrate mechanical sensors into the MFL deployment mechanism.

Emergency Location Sonde

An emergency location sonde will be integrated into the system. A low-frequency electromagnetic signal (20HZ) will be emitted and received above ground for emergency location. A potential candidate system, currently used in PII's pigging systems, will be considered for the next phase of the design.

Launch and Retrieval

Launch and retrieval will be achieved through a pipeline mounted, portable launch tube that will allow the inspection robot to travel in and out of the pipeline through operator control (fiber optic tether). The launch tube will be designed to withstand the pressure of the pipeline under test. An isolation valve will be installed at the hot-tap saddle arrangement with appropriate flanging to accept the launch tube. The launch tube will be opened on one end (attachment to hot-tap) with a removable cover on the other end through which the tether (platform control and video/sensing data) and supplemental electrical and signal wires are fed through appropriate bulkhead connectors to the base station. These supplemental electrical and signal lines will support battery diagnostics and charging, and access to inspection data.

Autonomous Control

Although the command and control system focused on the use of a fiber optic tether for real-time communication between the operator and the robot, the proposed system architecture of the RoboScan platform incorporates numerous features that will facilitate both supervised and autonomous inspection. Throughout the development of the RoboScan platform, the need and inclusion of sensors and control surfaces became apparent and have been integrated into the control system design. The first generation RoboScan platform is geared towards supervised (tele-operated) control via a fiber-optic cable with autonomous control planned for later inclusion.

Based on the research efforts completed (to date) by Foster-Miller and GE/PII, the team members have the confidence to bring the RoboScan design concept into a detailed design phase based on a thorough understanding of the design challenges discussed above, and believe that the fully-developed system will achieve these anticipated benefits:

- Ability to inspect otherwise inaccessible pipelines (transmission and distribution).
- Cost savings from not having to remove pipeline obstacles for conventional pigs.
- Inspection cost lower ($/mile) than direct assessment or hydro testing.

- A more versatile platform capable of performing a variety of inspection services.

REFERENCES

W. Leary, R. Torbin, and G. Vradis, *Robotic Pipeline Inspection System*, Natural Gas Technologies II, Phoenix, AZ, February 8-11, 2004.

W. Leary, R. Torbin, and G. Vradis, *Robotic Inspection System for Unpiggable Pipelines*, IPC 2004 International Pipeline Conference, Calgary, Alberta, Canada, October 4 - 8, 2004.

Appendix A Tractor Power Analysis – Proprietary (See Appendix F)

Appendix B Tether Attenuation Test Data – Oscillation and Tension

1.0 Fiber Tested

1.1.1 Fiber #1 – Opticonx Type, OFN-FT4 Single Mode, P/N 167033-001, 30 Meters, 2.9mm Jacket OD (.114in)

1.1.2 Fiber #2 – Opticonx Type, OFNR 1 Single Mode, P/N 161033-001, 30 Meters, 1.6mm Jacket OD (.063in)

1.1.3 Vestamid, Nylon .66@1550nm, P/N SR12059, 30 Meters, 900um Jacket OD, (.035in)

1.1.4 Stocker Yale Fiber, Bend Insensitive Fiber, BIF-1310-L2, 30 Meters, 245 um OD (.009 in)

1.1.5 Stocker Yale Fiber, Bend Insensitive Fiber, BIF-RC-1310-L2, 30 Meters, 130um OD, (.005 in)

1.1.6 Stocker Yale Fiber, Bend Insensitive Fiber,BIF-1310-L2, 30 Meters, 900um Jacket OD, (.035in)

2.0 Communication - Vibration Loss

2.1.1 Material: Fiber #2 – Opticonx Type, OFNR 1 Single Mode, P/N 161033-001
Pipe Length: 8' total = 6' straight plus 2 elbows and insert
Source: 1310nm laser
Test Date: 4/29/03
Notes:
1. Static cable loss measured with no airflow
2. Loose and Taught cable measured at max airflow and static pressure of ?? In/water

	-dB	Strum effect
Static	-12.5	-
Loose cable	-12.5	Moderate
Taught cable	-12.8	Heavy

2.1.2 Material: Stocker Yale Fiber, Bend Insensitive Fiber, BIF-1310-L2, 30 Meters
Pipe Length: 8' total = 6' straight plus 2 elbows and insert
Source: 1310nm laser
Test Date: 4/29/03
Notes:
1. Static cable loss measured with no airflow
2. Loose and Taught cable measured at max airflow and static pressure of ?? In/water

	-dB	Strum effect
Static	-12.5	-
Loose cable	-12.5	Heavy
Taught cable	-12.5	Slight

2.1.3 Material: Stocker Yale Fiber, Bend Insensitive Fiber, BIF-RC-1310-L2, 30 Meters
Pipe Length: 8' total = 6' straight plus 2 elbows and insert
Source: 1310nm laser
Test Date: 4/29/03
Notes:
1. Fiber is too small for splice. No comms.

2.1.4 Material: Vestamid, Nylon .66@1550nm, P/N SR12059, 30 Meters
Pipe Length: 8' total = 6' straight plus 2 elbows and insert
Source: 1310nm laser
Test Date: 4/29/03
Notes:
1. Static cable loss measured with no airflow
2. Loose and Taught cable measured at max airflow and static pressure of ?? In/water

	-dB	Strum effect
Static	-20.8	-
Loose cable	-20.4	Moderate
Taught cable	-20.4	Slight

2.1.5 Material: Fiber #1 – Opticonx Type, OFN-FT4 Single Mode, P/N 167033-001, 30 Meters
Pipe Length: 8' total = 6' straight plus 2 elbows and insert
Source: 1310nm laser
Test Date: 4/29/03
Notes:
1. Static cable loss measured with no airflow
2. Loose and Taught cable measured at max airflow and static pressure of ?? In/water

	-dB	Strum effect
Static	-13.9	-
Loose cable	-13.9	Slight
Taught cable	-13.9	Slight

2.2 Communication - Bend Loss - Measured as dB loss vs force across 2 – 90 degree elbows (short radius).

2.2.1 Material: Fiber #2 – Opticonx Type, OFNR 1 Single Mode, P/N 161033-001
Pipe Length: 8’ total = 6’ straight plus 2 elbows and insert
Source: 1310nm laser
Test Date: 4/29/03
Notes:
1. Force is measured in pounds of pull (load)
2. No airflow.

Force (lbs.)	-dB loss
Static	-12.5
1	-13
2	-13.8
3	-15.2
4	-17
5	-23.8

2.2.2 Material: Stocker Yale Fiber, Bend Insensitive Fiber, BIF-1310-L2, 30 Meters
Pipe Length: 8’ total = 6’ straight plus 2 elbows and insert
Source: 1310nm laser
Test Date: 4/29/03
Notes:
1. Force is measured in pounds of pull (load)
2. No airflow.
3. “Slip” indicates fiber slipped in test rig. No readings are taken if fiber cannot be clinched without causing microbend losses.

Force (lbs.)	-dB loss
Static	-12.5
1	-13.9
2	-15.7
3	Slip
4	Slip
5	Slip

2.2.3 Material: Stocker Yale Fiber, Bend Insensitive Fiber, BIF-RC-1310-L2, 30 Meters
Pipe Length: 8' total = 6' straight plus 2 elbows and insert
Source: 1310nm laser
Test Date: 4/29/03
Notes:
1. Fiber cannot be tested. Too small for splice

2.2.4 Material: Vestamid, Nylon .66@1550nm, P/N SR12059, 30 Meters
Pipe Length: 8' total = 6' straight plus 2 elbows and insert
Source: 1310nm laser
Test Date: 4/29/03
Notes:
1. Force is measured in pounds of pull (load)
2. No airflow.

Force (lbs.)	-dB loss
Static	-20.8
1	-20.9
2	-22
3	Snapped fiber

2.2.5 Material: Fiber #1 – Opticonx Type, OFN-FT4 Single Mode, P/N 167033-001, 30 Meters
Pipe Length: 8' total = 6' straight plus 2 elbows and insert
Source: 1310nm laser
Test Date: 4/29/03
Notes:
1. Force is measured in pounds of pull (load)
2. No airflow.

Force (lbs.)	-dB loss
Static	-13.9
1	-13.9
2	-13.9
3	-13.9
4	-13.9
5	-14
6	-14.2
7	-14.4

Appendix C Tether Attenuation Test Data – Mitered Corner

Date	Time	Reading (dBm)	Status		
2/12/2004	0900	-13.9	Test start.		
2/12/2004	1015	-13.7	adjusted tension at upper end		
2/12/2004	1100	-13.6	ok		
2/12/2004	1215	-13.5	ok		
2/12/2004	1320	-13.3	reset laser source, reseated fiber connection at source		
2/12/2004	1415	-13.5	ok		
2/12/2004	1500	-13.8	adjusted tension at upper end		
2/12/2004	1615	-13.7	ok		
2/12/2004	1700	-13.7	shut down for day		
				Hours for day	8
2/13/2004	0800	-13.6	start up		
2/13/2004	0900	-13.6	ok		
2/13/2004	1000	-13.6	ok		
2/13/2004	1100	-13.8	ok		
2/13/2004	1205	-13.8	ok		
2/13/2004	1315	-13.7	ok		
2/13/2004	1400	-13.4	ok		
2/13/2004	1500	-13.4	shut down for day		
				Hours for day	7
2/16/2004	0800	-13.2	Test start, reset source and fiber connections, adjusted fiber tension upper		
2/16/2004	0900	-13.2	ok		
2/16/2004	1030	-13.2	ok		
2/16/2004	1100	-13.3	adjusted fiber tension		
2/16/2004	1200	-13.3	ok		
2/16/2004	1310	-13.3	ok		
2/16/2004	1400	-13.3	ok		
2/16/2004	1515	-13.3	ok		
2/16/2004	1615	-13.3	shut down for day		
				Hours for day	8
2/17/2004	0800	-13.2	Test start		
2/17/2004	0900	-13.3	ok		
2/17/2004	1000	-13.3	ok		
2/17/2004	1130	-13.3	ok		
2/17/2004	1230	-13.2	ok		
2/17/2004	1330	-13.2	reset source		
2/17/2004	1450	-13.3	ok		
2/17/2004	1615	-13.3	shut down for day		
				Hours for day	8
2/18/2004	0800	-13.3	Start test		
2/18/2004	0900	-13.4	ok		
2/18/2004	1000	-13.4	ok		
2/18/2004	1045	-13.4	ok		
2/18/2004	1145	-13.4	ok		
2/18/2004	1245	-13.4	ok		
2/18/2004	1345	-13.3	ok		
2/18/2004	1450	-13.4	ok		
2/18/2004	1610	-13.4	ok		
2/18/2004	1705	-13.4	shut down, test complete		
				Hours for day	9
	Avg reading (dBm)			**Test Hours total**	**40**
	-13.43				

Appendix D Control Sensors

TRIAD MOTOR I/O & POWER SUPPLY(S)			VOLTAGE	PC-104 I/O TYPE AIN	AOUT	DIG	SER
DRIVE MOTOR	MOTOR POWER SUPPLY$_{DC}$		270				
CONTROLLER /DRIVE	CONTROL POWER SUPPLY$_{DC}$		15				
OM 9375	COMMAND VOLTAGE	SPEED CONTROL			3		
	DIRECTION	FORWARD/BACK				3	
	SPEED					3	
	ENABLE	MOTOR DRIVE KILL				3	
	CURRENT SENSE	MONITOR MOTOR CURRENT		3			
STEERING MOTOR	MOTOR POWER SUPPLY$_{DC}$		24				
CONTROLLER /DRIVE	CONTROL POWER SUPPLY$_{DC}$		15				
OM 507	COMMAND VOLTAGE	SPEED CONTROL			3		
	DIRECTION	FORWARD/BACK				3	
	ENABLE	MOTOR DRIVE KILL				3	
	CURRENT SENSE	MONITOR MOTOR CURRENT		3			
STEERING MOTOR POSITION SENSOR	STEERING MOTOR POSITION			3			
CLAMPING MOTOR	MOTOR POWER SUPPLY$_{DC}$		27				
CONTROLLER /DRIVE	CONTROL POWER SUPPLY$_{DC}$		15				
OM 507	COMMAND VOLTAGE	SPEED CONTROL			2		
	DIRECTION	FORWARD/BACK				2	
	ENABLE	MOTOR DRIVE KILL				2	
	CURRENT SENSE	MONITOR MOTOR CURRENT		2			
CLAMP MOTOR ANGLE SENSOR	MONITOR LEG ANGLE OF TRIAD			2			
FORCE SENSOR	MEASURE FORCE OF DRIVE WHEELS	(AS THE CLAMP ANGLE > FORCE >)		2			
BEND SENSORS	MONITOR ANGLE BETWEEN MODULES			3			
ROTATION MEASURED	ROTARY POSITION BETWEEN TRIADS			1			
Gyroscope	TRIAD Pitch, Yaw and Attitude			3			1
		TRIAD PC-104 Required Total		22	8	19	1
Diamond Prometheus w/ MM-48-AT Available Total				32	12	28	4

TETHER MOTOR I/O & POWER SUPPLY(S)			VOLTAGE	PC-104 I/O TYPE AIN	AOUT	DIG	SER
TETHER ACCUMULATOR MOTOR	MOTOR POWER SUPPLY$_{DC}$		24				
CONTROLLER /DRIVE	CONTROL POWER SUPPLY$_{DC}$		15				
OM 507	COMMAND VOLTAGE				1		1
	DIRECTION					1	1
	ENABLE					1	1
	CURRENT SENSE			1			1
TETHER WIPER MOTOR	MOTOR POWER SUPPLY$_{DC}$		24				
CONTROLLER /DRIVE	CONTROL POWER SUPPLY$_{DC}$		15				
OM 507	COMMAND VOLTAGE				1		1
	DIRECTION					1	1
	ENABLE					1	1
	CURRENT SENSE			1			1
TETHER SENSORS							
Accumulator Dancer				1			1
		Tether PC-104 Required Total	**TOTAL**	**3**	**2**	**4**	**9**

OVALITY SENSOR	MONITOR ROUNDNESS OF PIPE	(Self Contained Processor)					
	CAMERA(3)			**3**			
MFL MOTOR I/O & POWER SUPPLY(S) (X2)		PC-104 for each MFL Sensor Module	**VOLTAGE**	**PC-104 I/O TYPE**			
				AIN	**AOUT**	**DIG**	**SER**
CENTERING MOTOR POSITION	MOTOR POWER SUPPLY$_{DC}$		24				
CONTROLLER /DRIVE	CONTROL POWER SUPPLY$_{DC}$		15				
OM 507	COMMAND VOLTAGE				1		
	DIRECTION					1	
	ENABLE					1	
	CURRENT SENSE			1			
CENTERING MOTOR POSITION SENSOR	CENTERING MOTOR POSITION			1			
ORIENTATION MOTOR POSITION	MOTOR POWER SUPPLY$_{DC}$		24				
CONTROLLER /DRIVE	CONTROL POWER SUPPLY$_{DC}$		15				
OM 507	COMMAND VOLTAGE				1		
	DIRECTION					1	
	ENABLE					1	
	CURRENT SENSE			1			
ORIENTATION MOTOR POSITION SENSOR	ORIENTATION MOTOR POSITION			1			
DEPLOYMENT MOTOR POSITION	MOTOR POWER SUPPLY$_{DC}$		24				
CONTROLLER /DRIVE	CONTROL POWER SUPPLY$_{DC}$		15		1		
OM 507	COMMAND VOLTAGE					1	
	DIRECTION					1	
	ENABLE						
	CURRENT SENSE			1			
DEPLOYMENT MOTOR POSITION SENSOR	DEPLOYMENT MOTOR POSITION			1			
SHUNT MOTOR POSITION	MOTOR POWER SUPPLY$_{DC}$		24		1		
CONTROLLER /DRIVE	CONTROL POWER SUPPLY$_{DC}$		15			1	
OM 507	COMMAND VOLTAGE					1	
	DIRECTION						
	ENABLE						
	CURRENT SENSE			1			1
SHUNT MOTOR POSITION SENSOR	SHUNT MOTOR POSITION			1			
Gyroscope	Monitor MFL Pitch, Yaw and Attitude						
		MFL(2) PC-104 Required Total	**TOTAL**	**8**	**4**	**8**	**1**

Appendix E
Electrical Power Interconnect Diagrams Proprietary (See Appendix F)
